Nasa CR-65225

STUDY OF PROPELLANT VALVE LEAKAGE IN A VACUUM

Phase I Report

7 June 1965 to 24 November 1965

For

Manned Spacecraft Center
National Aeronautics and Space Administration

Contract No. NAS9-4494
Control No. PR No. 433-7065

ATLANTIC RESEARCH
CORPORATION

ATLANTIC RESEARCH CORPORATION
ALEXANDRIA, VIRGINIA

STUDY OF PROPELLANT VALVE LEAKAGE IN A VACUUM

Phase I Report

7 June 1965 to 24 November 1965

by

Ralph D. Gift
John A. Simmons
Joseph P. Copeland
Jack M. Spurlock

for

Manned Spacecraft Center
National Aeronautics and Space Administration

Contract No. NAS9-4494

Control No. PR No. 433-7065

Atlantic Research Corporation
Alexandria, Virginia
15 December 1965

This report was prepared by the Atlantic Research Corporation under Contract No. NAS9-4494, entitled "Study of Propellant Valve Leakage in a Vacuum," for the NASA Manned Spacecraft Center. The work was administered under the technical direction of the Propulsion Design Section of the Propulsion and Power Division, Manned Spacecraft Center, with Mr. B. B. Sprague serving as project manager.

PHASE I REPORT

TABLE OF CONTENTS

FIGURES

1.0 SUMMARY

The purpose of this program, which began June 7, 1965, is to investigate propellant leakage through propellant valves, similar to those used in the Apollo Service Module propulsion system, and the possibilities of resultant freezing and blockage of propellant flow systems when the propellants become exposed to a vacuum environment.

The program is divided into three Phases. Phases I and II consist of studying and defining the phenomena associated with the various leakage and freezing situations, using N_2O_4 in Phase I and Aerozine-50 in Phase II. Phase III studies will evaluate effects of propellant freezing on hypergolic ignition and examine techniques to resolve associated problems.

Phase I tests have been completed and this report delineates the accomplishments achieved during this phase of the program. A total set of 85 tests has been conducted using N_2O_4 as the test medium. Also, a theoretical analysis was made to predict the limiting N_2O_4 leak-rates for freezing in the propellant manifold and injector of the Apollo SPS engine. The lower limit leak rate of N_2O_4 for the Apollo SPS engine (the point below which the sublimation rate exceeds the leak rate) is predicted to be approximately 180 cc/hr. Leak rates below this value cannot result in an accumulation of frozen N_2O_4 and therefore present no flow blockage problem. The maximum leak-rate of N_2O_4 for which freezing can occur in the manifold and injector of the Apollo SPS engine is predicted to be 450,000 cc/hr. Although leak rates above 450,000 cc/hr will not result in flow blockage, a serious hazard would be created because of propellant accumulation in the combustion chamber prior to ignition.

The experimental results and conclusions drawn from visual observation, studying the motion pictures taken of each test and analyzing the recorded data, approximate very closely the theoretically predicted results. Measurements made before and at the end of each test, in which freezing occurred, showed that the torque required to open the leak valve was unaffected even when the N_2O_4 froze in the vicinity of the leak valve

ball or stem.

Flow delays, due to propellant freezing between the leak-valve and injector plate, were observed on 41 of the 85 tests conducted. The delays ranged from 10 milliseconds to eight minutes.

2.0 INTRODUCTION

Several cases of propellant freezing have occurred during static testing of the Apollo Service Module (SPS) engine. While no adverse effects apparently were noted during these tests, additional data are required to determine the extent to which propellant freezing can create a serious problem. The purpose of this program is to determine the conditions under which propellant leakage through propellant valves will produce freezing and interfere with or prevent engine ignition in space.

This report delineates the accomplishments achieved during Phase I (which has been completed) of a three-phase program. The overall program began June 7, 1965 and will be completed June 7, 1966. Phases I and II consist of experimental and theoretical studies to define the phenomena associated with the various leakage and freezing situations, using N_2O_4 in Phase I and Aerozine-50 in Phase II. Phase III studies will evaluate effects of propellant freezing on hypergolic ignition and examine remedial techniques to resolve associated problems.

Although these three phases are predominantly experimental efforts, a theoretical analysis is also a part of the overall program. The theoretical analysis and experimental data will allow extrapolation of the characteristics of the freezing phenomena from the conditions of the simulated flow system being tested to those of the Apollo SPS engine.

The exposure of liquids to vacuum involves a great variety of phenomena, most of which result directly or indirectly from the suddenly imposed supersaturation (Reference 1). Volatile liquids exposed either in bulk or by leakage usually boil, and the growth and bursting of bubbles break the liquid up into a cloud of vapor and droplets. Surface forces and other disturbances created by the flow of the liquid also contribute significantly to the breakup. Simultaneous with breakup and dispersal, evaporation occurs from all free surfaces of the liquid. The rate of evaporation depends primarily on the temperature of the surface, or consequently the equilibrium vapor pressure of the surface. Vapor-phase

resistance to evaporation is slight unless the ambient pressure is greater than about 10 per cent of the equilibrium vapor pressure. Because of the associated removal of the latent heat of vaporization, evaporation causes cooling of the liquid. For the case of liquid N_2O_4 this value is 356 cal/cm^2-sec. In a space environment, the rate of evaporative cooling is very great, and usually exceeds the rate of heating from outside sources, even when the vapor pressure of the liquid at the surface is a small fraction of a mmHg. Consequently, small drops of a liquid whose triple point pressure is greater than one mmHg cool, freeze, and sub-cool, all within a second or less after exposure to a space environment. The triple point pressure of N_2O_4 is 140 mmHg, such that the difference between this value and the vacuum conditions of space produces a very large driving force for evaporative cooling and freezing of N_2O_4.

Section 3.0 of this report presents a theoretical analysis of the freezing phenomena. The theoretical predictions were in good agreement with the experimental results. Limiting N_2O_4 leak-rates for freezing in the propellant manifold and injector of the Apollo SPS engine have been determined and are tabulated.

The experimental studies are described in Section 4.0. A detailed description of the test equipment and test procedure is presented. Data, results and analysis are also discussed in Section 4.0.

Other major sections of this report include Remedial Techniques, Section 5.0; Program Status (including future work), Section 6.0; and Appendix A which includes the detailed body of data gathered in the experimental program.

3.0 THEORETICAL ANALYSIS

3.1 PRELIMINARY CONSIDERATIONS

A brief discussion of the evaporative cooling and freezing process, and the associated phenomena, was presented in Section 1.0 of this report. In previous work, sponsored by NASA Marshall Space Flight Center (Contract NAS 8-11044), Atlantic Research investigators experimentally and theoretically studied the behavior of various liquid propellants in a vacuum environment.[1] The analysis of the results obtained during that investigation identified the principal parameters upon which the extent of freezing effects depends. In general, the rate of flow of the liquid into the vacuum environment, the geometry of the flow system, the triple-point vapor pressure of the liquid (for a single-component liquid such as N_2O_4), the initial temperature and area of the liquid surface that is exposed to the vacuum, and the rate of heat exchange between the fluid and the surrounding system, all are key factors in the evaporative cooling and freezing process.

On the basis of this previous experience, it was predicted early in the present program[2] that for any specified propellant delivery and injector system, the extent of evaporative freezing effects would be a function essentially of liquid leak rate alone (i.e., propellant properties, system geometry, thermal conditions, etc., will have been specified). Further, it was predicted that potentially deleterious freezing effects, resulting from significant accumulation of frozen propellant in the valve and/or flow passages of the system, would occur within some range of leak rates. This leak-rate range would be bounded by a "minimum" leak rate below which significant accumulation of frozen propellant could not occur, and a "maximum" leak rate above which significant freezing of propellant behind the downstream face of the injector could not occur. The factors and conditions associated with each of these two limiting cases are discussed below.

At particularly high propellant leak rates, liquid rapidly flows through the valve and lines and the passages of the injector assembly, such

that the liquid is effectively exposed to the vacuum environment only in the passages between the valve and injector, or as it emerges from the ports in the injector. At the locations where the liquid actually is exposed to the vacuum, evaporation and attendant cooling of the liquid rapidly occur. In the lines and injector the rate of evaporation, and hence cooling and freezing, is limited by the area of the injector ports through which the vapor must flow. Consequently, if the leak rate is too great, the limited rate of evaporation and vapor flow is insufficient to cool and freeze the leaking propellant. Moreover, at high leak rates, liquid may be expelled through the injector ports, which further reduces the area for vapor flow. Under these conditions, freezing of the liquid cannot occur in the flow passages.

However, if the leak rate is gradually lowered, a level is reached at which the flow of vapor through the injector ports is just sufficient to permit evaporation at the rate necessary to cool all of the leaking liquid and produce extensive freezing in the passages. Furthermore, if the leakage situation also is such that no solid or liquid is expelled through the ports, then the vapor flow through the ports is at a maximum rate. These conditions define the "maximum" leak rate that is discussed in this analysis.

At very low propellant leak rates, liquid slowly passes through the valve, such that the principal exposure of the liquid to the vacuum environment occurs in a region very near the valve seal. Under the influence of the vacuum exposure, the liquid will vaporize rapidly; and if the geometric configuration of the flow system permits rapid removal of the vapor out of the system, the pressure rise in that region will be small; therefore, the liquid will continually be exposed to a sufficiently low pressure that rapid vaporization will be sustained. If the leak rate is somewhat greater than the rate at which vaporization can occur, the unvaporized liquid will be cooled rapidly to its triple-point temperature (for a single-component fluid such as N_2O_4) and freezing will occur. This process results in the accumulation of frozen propellant in the vicinity of the valve, and can lead to plugging of the flow system in that region.

However, if the vaporization rate is the same as the leak rate, it is obvious that a steady-state process will occur such that all the liquid that leaks through the valve will be rapidly vaporized, and no net accumulation of frozen propellant will occur. At this leak rate level, or below, plugging of the valve or flow system as a result of accumulated frozen propellant will not be a problem. It should be realized, however, that this lower limit, or "minimum" leak rate, is very dependent upon the propellant vaporization rate that can occur in the region of the flow system where the effective vacuum exposure occurs. This vaporization rate strongly depends upon the environmental conditions which govern heat exchange between the propellant flow system and the external surroundings. For example, for a system in which there is a large thermal flux from the surroundings into the propellant valve and lines (as from a source of thermal radiation located near the flow system), the propellant vaporization rate might be significantly large, and the tolerable leak-rate value would be greater than for a case in which the thermal flux from the surroundings was much smaller. Therefore, extreme caution must be exercised in calculating and using values of the "minimum" or tolerable leak rate as a valve specification; and geometric as well as environmental heat-transfer conditions that are used as a basis for such calculations must be carefully or conservatively estimated for each new flow-system configuration.

The assumptions and procedures used in the derivation of predictive models for the maximum and minimum leak-rate criteria, together with the calculated results obtained with these models for the experimental N_2O_4 flow system used in this phase of the program, are discussed in Sections 3.2 and 3.3, which follow.

3.2 PREDICTION OF MAXIMUM LEAK-RATE CRITERIA

An analytical model was derived for the prediction of the maximum, steady leak-rate, through a propellant flow-control valve, for which significant evaporative freezing effects can be produced. As discussed in Section 3.1, above, this "maximum" level of leak rate is defined as the value above which accumulation of frozen propellant cannot occur in the flow passages

upstream from the injector discharge ports. As explained above, the condition that characterizes this limiting rate is that evaporation of propellant in the flow passages is just sufficient to cool and freeze the propellant which is introduced into the flow passages by the valve leakage. The analysis is based on heat and mass balances for the leaking propellant, assumes choke-flow of vapor through the injector port, and utilizes the usual Hertz-Knudsen evaporation-rate expression.

The analytical system consists of all the propellant (solid, liquid and vapor) which is contained in the flow passages between the leaking valve and the injector discharge ports at any instant of time, t. The system is further defined by the following assumptions:

(1) The liquid propellant enters the system at a constant leak rate, $\dot{M}_o$, and has a temperature, T_o, at entry;

(2) Vapor (only) leaves the system at conditions of choke flow through the injector ports which, together, have a total cross-sectional area, A_h; this is one of the theoretical conditions for the "maximum" leak rate, discussed above in Section 3.1;

(3) The temperature throughout all phases of the propellant in the system is uniform at the value T;

(4) Heat from the external parts which bound the system (valve, flow passages, injector plate, etc.) is absorbed by the system at the rate q_e, a function of the temperatures of the surroundings and the system.

Based on these assumptions, mass balances can be written for the condensed phases and the vapor phase, and an energy balance can be written for the system (neglecting the small kinetic energy of the leaking liquid). The Hertz-Knudsen evaporation-rate expression is used in the mass balance for the condensed phases, and the relationship $pL/\sqrt{T}$ is used in the mass balance for the vapor to represent choke-flow of the vapor through the injector ports, where:

$$L \equiv A_h (\gamma \bar{M}/R)^{1/2} (2/\gamma+1)^{(\gamma+1)/2(\gamma-1)} ,$$

p is the total pressure in the system, γ is the ratio of the specific heats for the vapor, $\bar{M}$ is the molecular weight of the fluid, and R is the gas constant.

When the mass balances are combined with the energy balance for the system, the following expression is obtained:

$$(m_v c_v + m_c c_c)\frac{dT}{dt} = \lambda_v K \frac{p_\sigma - p}{\sqrt{T}} + \dot{M}_o (e_l^o - e_c) + q_e$$

$$- \frac{Lp}{\sqrt{T}} \left(\frac{p}{\rho_v} + \frac{U^2}{2} \right) + \dot{M}_o \frac{p}{\rho_l} - \frac{d(m_v U^2/2)}{dt} , \qquad (1)$$

where m_v is mass of vapor in system, m_c is mass of condensed phases, λ_v is the energy of vaporization, p_σ is the saturation vapor pressure, ρ_v is the density of the vapor, ρ_l is liquid density, U is the vapor velocity, e is internal energy, c is specific heat at constant volume (it is assumed that e for all phases is a function only of temperature, such that $de = cdT$); further, $K = A_e \alpha (\bar{M}/2\pi R)^{1/2}$, where A_e is the total surface area of the condensed phase over which evaporation occurs, and α is the evaporation coefficient. Equation (1) can be reduced on the basis of the following factors:

(1) The time-rate-of-change of the mass of vapor in the system (dm_v/dt) is negligible compared with the total efflux rate of vapor from the system; this is reasonable since the volume of vapor in the system is displaced continually by that portion of the liquid leaking into the system which does not vaporize (obviously, this amounts to a rate that is smaller than the liquid leak rates, which is already small by definition);

(2) The term $\dot{M}_o p/\rho_l$ in Equation (1) is negligibly small;

(3) The expression $\Delta H_v = \lambda_v + p/\rho_v$ is very nearly correct for phase conditions much removed from the critical temperature;

(4) The quantities e_c, p_σ, and q_e are functions of the temperature of the system, whereas the remaining quantities, except for m_v and m_c, are constants;

(5) Because of evaporative cooling in the system, the sign of dT/dt is negative; accordingly, the maximum leak rate for which the system can remain at any given temperature (as is the condition during the freezing process) is prescribed by the steady-state condition dT/dt = 0, at that temperature.

Factor (1) above gives rise to expressions for p and U which permit their elimination from Equation (1). This result, combined with the effects of Factors (2) through (5), yields an expression for the maximum leak-rate for which freezing can occur in the flow passages upstream of the injector plate. This expression is:

$$\dot{M}_{o\,max}\left[c_c(T_o - T_p) + \lambda_f\right] = \frac{KLp_\sigma}{(K+L)\sqrt{T_p}}\left[\Delta H_v + \frac{\alpha^2 RT_p}{4\pi \bar{M}}\left(\frac{L}{K}\right)^2\right] - q_e \,, \qquad (2)$$

where T_p is the triple-point temperature and λ_f is the energy of fusion. Physically, Equation (2) shows that the maximum leak-rate for freezing in the flow passages is established when evaporative cooling just balances the sensible heat of the leaking liquid and the heat flow from external sources.

Further analysis of Equation (2) showed that for the condition $A_e \geq A_h$ (that is, when the evaporation area of the condensed phases in the flow passages is greater than or equal to the total area of the injector ports), the term $(\alpha^2 RT_p/4\pi \bar{M})(L/K)^2$, in Equation (2), is negligible compared with ΔH_v. In the actual case, the condition $A_e \geq A_h$ may reasonably be expected to be fulfilled if there has been any appreciable accumulation of propellant within the flow passages. Accordingly, Equation (2) can be used, to a high degree of accuracy, in the simplified form:

$$\dot{M}_{o\,max} = \frac{\dfrac{KLp_\sigma\ \Delta H_v}{(K+L)\sqrt{T_p}} - q_e}{c_1(T_o - T_p) + \lambda_f} \,. \qquad (3)$$

Since for $A_e \geq A_h$ it can be shown that KL/(K+L) is directly proportional to

A_h, then $\dot{M}_{o\ max}$ is also directly proportional to the area of the injector ports. In addition, $\dot{M}_{o\ max}$ decreases with increasing initial temperature of the propellant at entry into the flow passages.

Equation (3) was used to compute predicted values of the "maximum" leak-rate of nitrogen tetroxide, assuming various initial propellant temperatures and values of total area of the injector ports. The term q_e was assumed to be negligible, as in fact it would be, in any reasonable environment, compared with the extremely large magnitude of the evaporative heat flux (represented by the first term in the numerator on the right side of Equation (3)). The results of the calculations are presented in Table 3-1. Maximum leak rates were calculated for three values of total injector-port area and initial temperatures of the propellants. The two smaller values of injector-port area correspond to the injectors that were studied experimentally in this phase of the program. The largest area corresponds to the actual N_2O_4 injector-port area for the SPS engine of the Apollo Service Module.

The computed "maximum" leak rates for N_2O_4 agree quite well with the experimental values for the smaller areas, and establish considerable confidence for the predicted value of the "maximum" leak rate of N_2O_4 for the Apollo SPS engine.

3.3 PREDICTION OF MINIMUM LEAK-RATE CRITERIA

An analytical model was also derived for the prediction of the minimum, steady leak-rate, through a propellant flow-control valve, at or below which significant net accumulation of frozen propellant cannot occur in the vicinity of the valve seal or in the flow passages between the valve and injector. Again, the analysis is based on heat and mass balances for the leaking propellant. However, the principal case of interest this time is the steady-state condition for which all the leaking liquid immediately vaporizes such that no accumulation of condensed phases will occur. This, of course, defines the minimum leak-rate condition. Thus, since steady-state leaking and vaporization is occurring at the inlet boundary of the system,

TABLE 3-1

PREDICTED MAXIMUM LEAK-RATES FOR FREEZING: NITROGEN TETROXIDE

ΔH_v (sublimation) = 111.85 cal/gm, T_p = 11.8°F, p_σ(triple point) = 139.8 mmHg

γ = 1.12, $f(\gamma)$ = 0.639

INJECTOR-PORT AREA, A_h (in^2)	INITIAL PROPELLANT TEMPERATURE, T_o (°F)	LEAK-RATE, $\dot{M}_o$ (cc/sec)		EVAPORATIVE HEAT FLOW (watts)	
		$A_e = A_h$	$A_e \gg A_h$	$A_e = A_h$	$A_e \gg A_h$
0.00504	40	0.170	0.440	44.9	116
	80	0.143	0.370	44.9	116
	130	0.120	0.310	44.9	116
0.0463	40	1.58	4.06	414	1070
	80	1.33	3.42	414	1070
	130	1.11	2.86	414	1070
1.42^2	40	48.6	126.5	12800	33200
	80	-	-	12800	33200
	130	34.2	89.1	12800	33200

a. Total area for the oxidizer injector-port for the SPS engine.

for the system:

$$\frac{dT}{dt} = 0 \qquad \text{and} \qquad \frac{dm_c}{dt} = 0 \ ;$$

that is, no change in temperature and no change in the mass of condensed phase in the system occurs with time.

From relationships for mass and energy balances, similar to those employed in the derivations in Section 3.2, the following expression was established:

$$\dot{M}_{o\ min} = \frac{h_e\ (T_o - T_s)}{\left[\Delta H_v - (e_1^o - (e_c)_s)\right]} \ , \qquad (4)$$

where $\dot{M}_o$ is the propellant leak rate at steady state, T_o is the temperature of the propellant at entry into the system, T_s is the steady-state temperature in the system, e is internal energy, $(e_c)_s$ denotes internal energy of the condensed phase at T_s, ΔH_v is the heat of vaporization, and h_e is a thermal flux coefficient of the type used in heat balances which have the form $q = h\Delta T$.

Actually, the numerator of Equation (4) could as easily have q_e substituted for $h_e\ (T_o - T_s)$, where q_e is the total heat flux to the propellant in the system from surrounding sources. Thus, it can be seen that predicted values of $\dot{M}_{o\ min}$ are extremely dependent upon the thermal conditions of the environment, which must be specified very carefully.

Examination of Equation (4) reveals that all variables are written as functions only of T_s. But before $\dot{M}_{o\ min}$ can be calculated by means of Equation (4), a value of T_s must first be obtained. This leads to a trial-and-error solution procedure involving Equation (4) and another expression which is valid only when $dm_c/dt = 0$:

$$\dot{M}_{o\ min} = \frac{KL}{(K+L)} \frac{P_\sigma}{\sqrt{T_s}} \ , \qquad (5)$$

in which K, L and p_σ have the same significance discussed in Section 3.2. All variables in Equation (5) also are functions only of T_s. Therefore, the calculation procedure involves the assumption of a trial value for T_s which is used in Equation (4) to obtain a value of $\dot{M}_{o\ min}$. Then, these values of T_s and $\dot{M}_{o\ min}$ are used in Equation (5), which must yield an equality if T_s is the proper value. This procedure is repeated and aided by graphical means until the proper value of T_s, and therefore $\dot{M}_{o\ min}$, are computed.

This calculation procedure was used to compute a predicted value of the "minimum" leak rate (or maximum allowable leak rate) for the N_2O_4 valve on the Apollo SPS engine. A very conservative case was used, involving as low an environmental thermal flux value, q_e, as could reasonably be expected to occur under normal circumstances. For this case, the maximum allowable value of leak rate was estimated to be about 180 cc/hr (or 0.07 gm/sec) of N_2O_4. As is discussed in later sections of this report, experimental results indicated that this predicted value also represents rather well the minimum leak-rate limit for freezing observed in tests with the small-scale test system used in this phase of the program.

4.0 EXPERIMENTAL STUDIES

4.1 DISCUSSION

The objective of the experimental program is to investigate propellant leakage through propellant valves, similar to those used in the Apollo propulsion system, and the possibilities of resultant freezing and blockage of propellant flow systems when the propellants become exposed to a vacuum environment. Effects of such freezing on hypergolic ignition and remedial action to resolve associated problems are also a part of the over-all program objectives. The test program is divided into three phases. The following is a brief outline of the program by phase.

Phase I - Evaluate effects of leaks through a propellant valve using nitrogen tetroxide as the test medium

Phase II - Evaluate effects of leaks through a propellant valve using Aerozine-50 (50% UDMH/50% hydrazine) as the test medium

Phase III - Evaluate effects of propellant freezing on ignition of the hypergolic propellants nitrogen tetroxide and Aerozine-50, and investigate remedial techniques to resolve associated problems.

Phase I tests have been completed, and this report delineates the accomplishments achieved during this phase of the program. A total set of eighty-five tests has been conducted using nitrogen tetroxide as the test medium. The effects of six variables on leakage phenomena were investigated:

1. Leakage rate
2. Duration of leak
3. Propellant temperature
4. Initial temperature of valve
5. Line size
6. Injector orifice area.

The most important results can be summarized as follows:

1. Measurements made before and at the end of each test, where freezing occurred, showed that the torque required to open the leak-valve was unaffected even when the N_2O_4 froze in the vicinity of the leak-valve ball or stem;

2. Propellant leakage, through the propellant valve, can result in evaporative freezing in the cavity between the valve and injector face;

3. Flow delays caused by blockage of frozen N_2O_4 from milliseconds to minutes were experienced and the longest delay recorded was eight minutes;

4. Leak rate and injector port area had far more effect on the freezing phenomena than any of the other variables investigated;

5. The maximum leak rate for propellant freezing in the injector manifold increases in direct proportion to the total area of the injector ports, and has a slight inverse dependency on the initial temperature of the liquid (see Table 3-1);

6. There is a minimum leak-rate, below which there is no accumulation of frozen propellant within the manifold; the limit depends strongly on the heat flux to the manifold from outside sources, such as the engine itself surrounding full tanks, etc. For the SPS engine, 0.05 cc/sec was estimated for this minimum rate. In the experiments, the observed minimum rate was approximately 0.1 cc/sec.

4.2 TEST APPARATUS

4.2.1 High Altitude Facility

The major tool used in performing the experiments of this program is the Atlantic Research Corporation high altitude tunnel facility. Figure 4-1 depicts this facility and some of its pertinent characteristics.

The test section consists of a cylindrical stainless steel

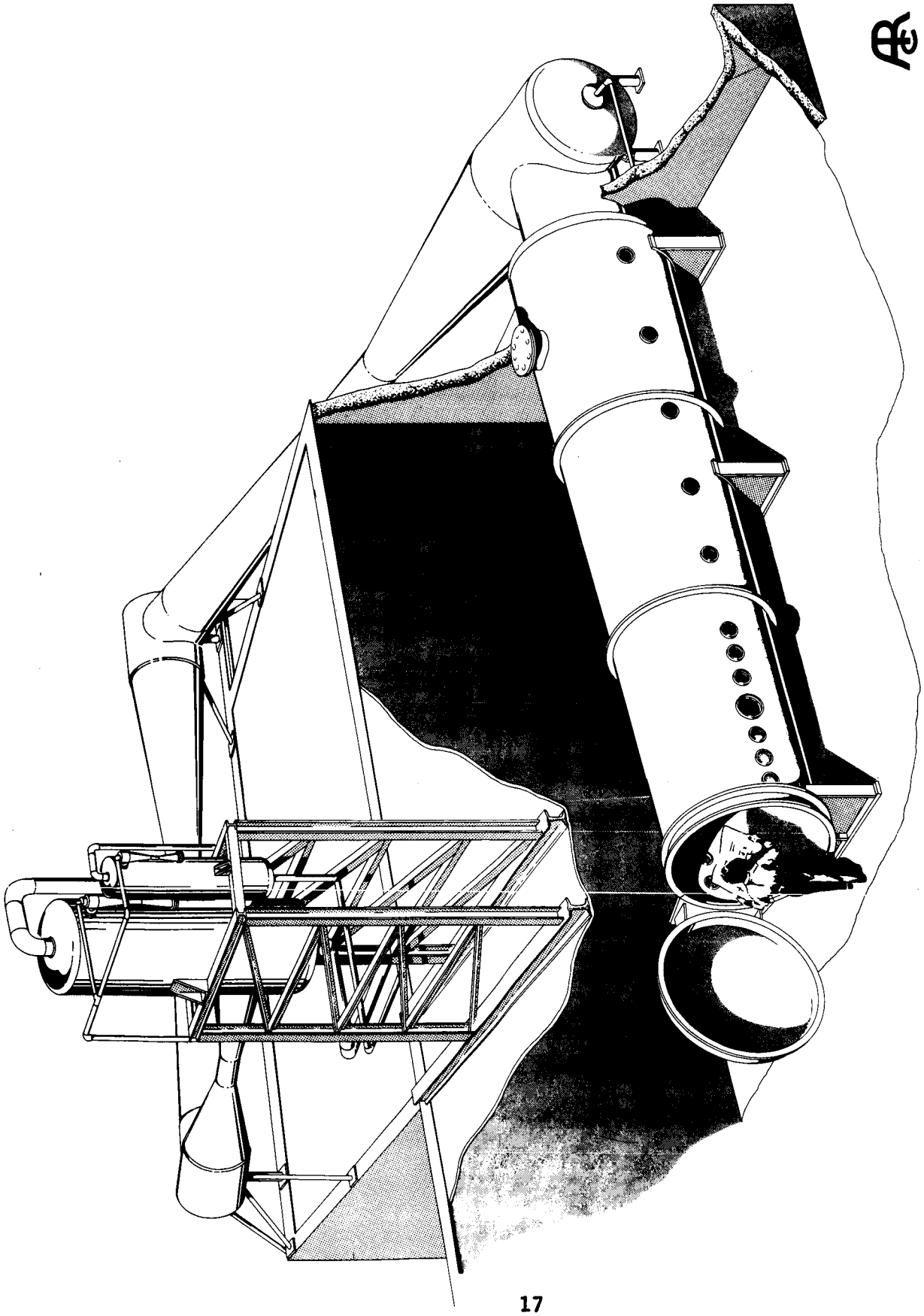

Figure 4-1. High Altitude Research Tunnel.

tunnel, 6 feet in diameter and 25 feet long, which is exhausted by a 5-stage steam ejector system. The tunnel is housed in a building adjacent to the Atlantic Research Corporation principal laboratories located in Alexandria, Virginia. Figure 4-2 is a photograph of the facility including the cooling towers for the condenser water.

The facility has a design pumping capacity of 71,000 liters of air per second at a pressure of 60 microns of mercury and a no-load, minimum pressure capability of 20 microns of mercury, which simulates an altitude of approximately 245,000 feet. The ejectors use 9,000 pounds of steam per hour, and the two condensers require 1200 gallons of cooling water per minute. Direct-contact type condensers are located between the third and fourth stages and between the fourth and fifth stages. The condensers are used to reduce the overall steam consumption of the unit. The steam is supplied by a gas-fired, automatic boiler with a rated output of 10.35 MBTU/hr. A preheater using steam as the heat source is used to preheat the boiler feed water to approximately 190°F. The boiler, including the electrical control panel, is shown in Figure 4-3. The tunnel control panel and some of the instrumentation used for the program are depicted in Figure 4-4. The vacuum tunnel is shown in Figure 4-5.

4.2.2 Flow System

The flow system for the Phase I test apparatus is shown in Figures 4-6 through 4-10. All metal components in contact with either liquid or gaseous propellant were fabricated of stainless steel. Gaskets and seals were made of teflon.

Liquid nitrogen tetroxide was contained in the propellant tank attached to one end of a balance beam (the operation of this balance is discussed in Section 4.2.3). Flow was achieved by applying nitrogen pressure to the vapor space at the top of the propellant tank, thereby forcing the propellant into a feed line which ran through the tunnel wall to the leak-

AR35048

Figure 4-2. High Altitude Research Facility.

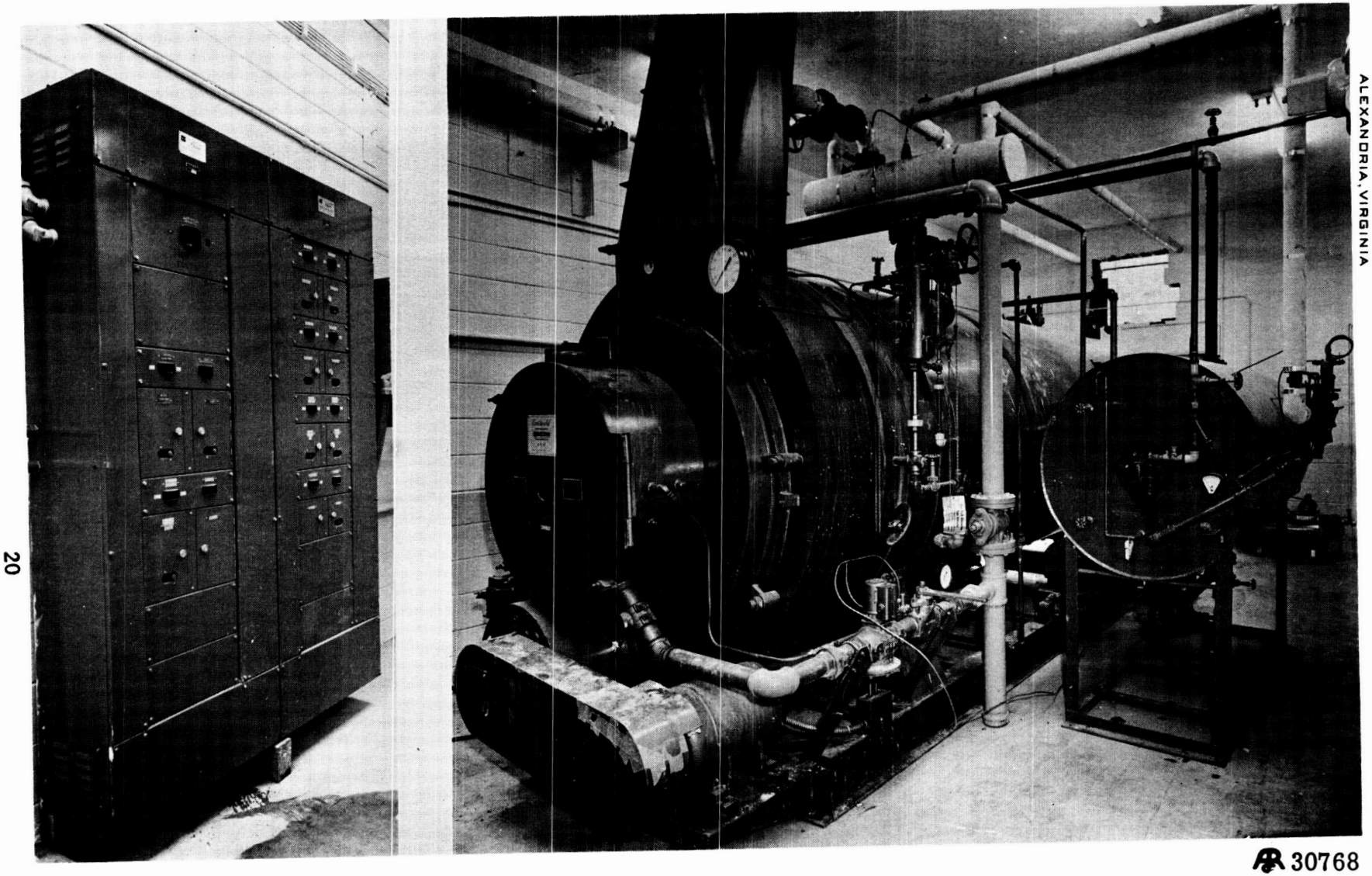

Figure 4-3. Boiler for High Altitude Research Tunnel.

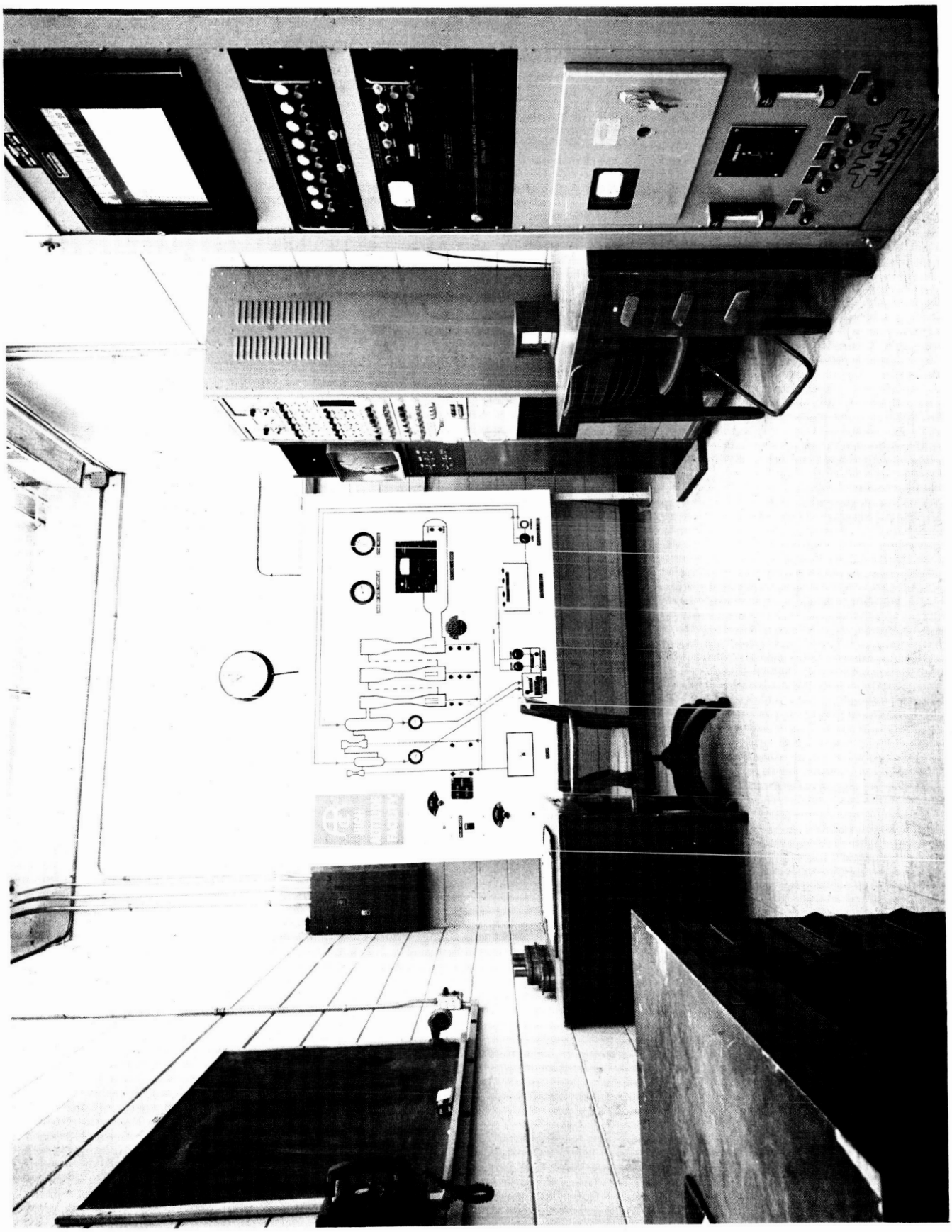

9869-3 | AR7682

Figure 4-4. Control Panel and Instrumentation for High Altitude Research Tunnel.

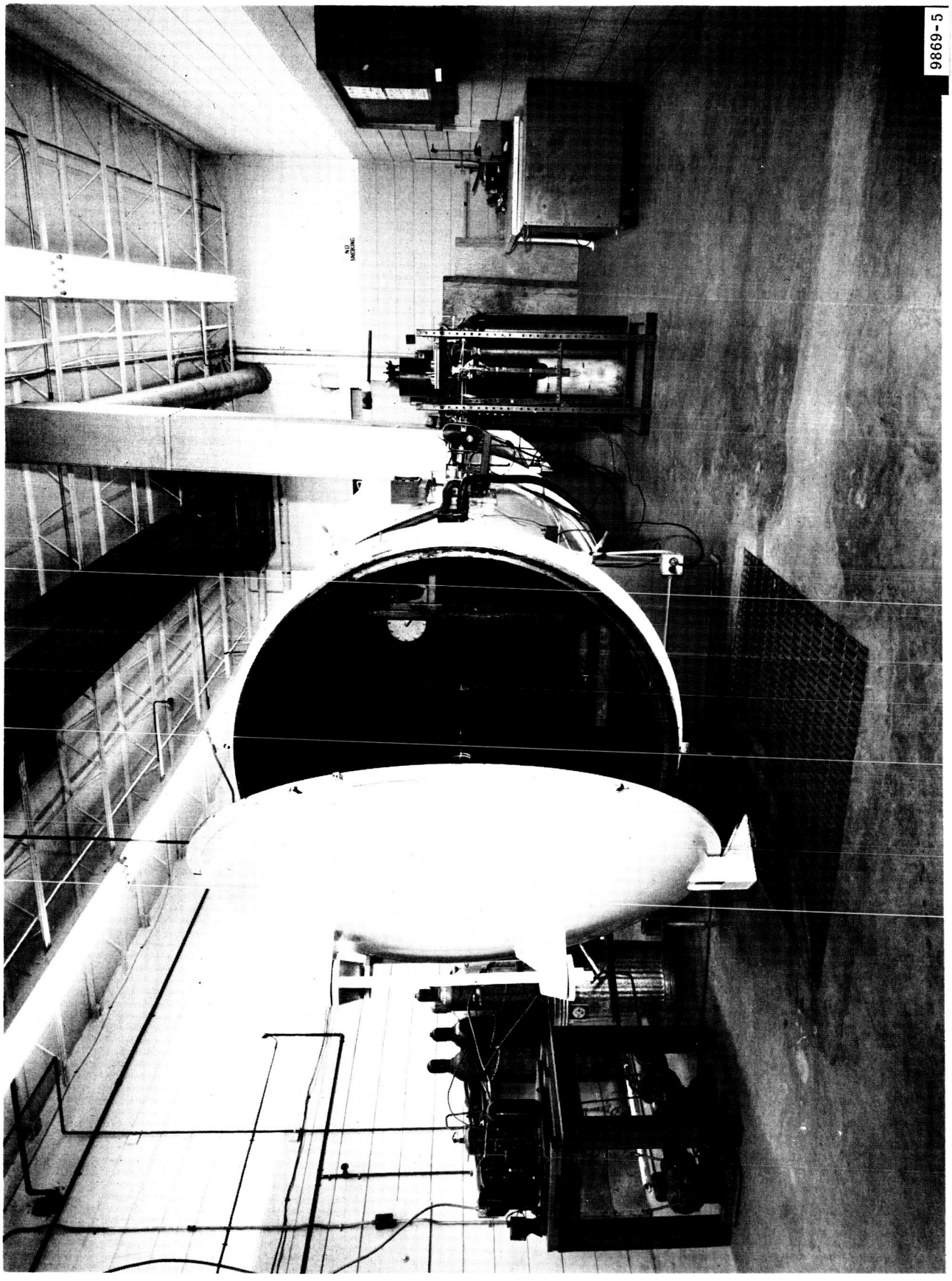

Figure 4-5. Vacuum Tunnel of the High Altitude Research Facility.

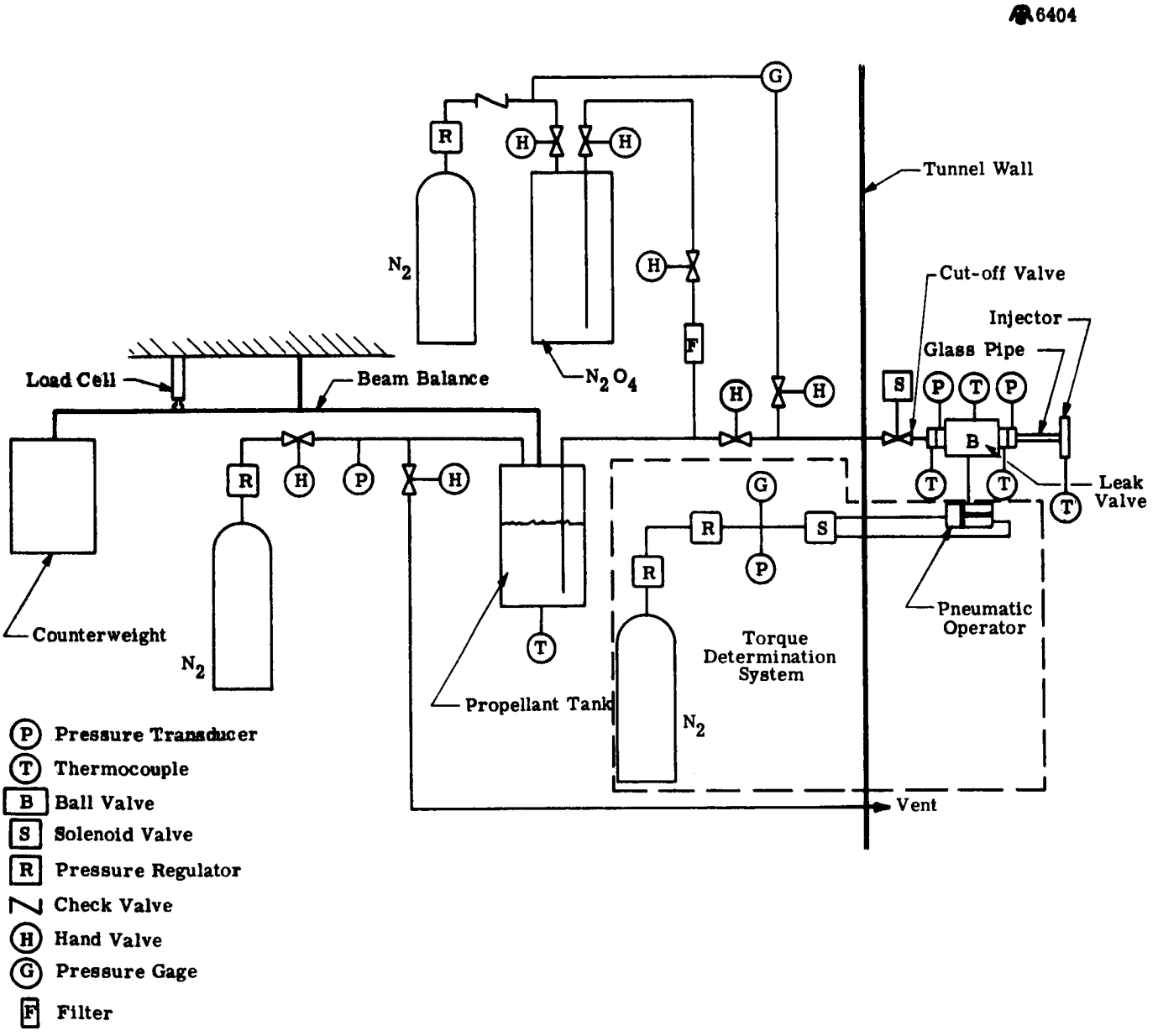

Figure 4-6. Schematic Diagram of Propellant Flow System for Phase I Tests.

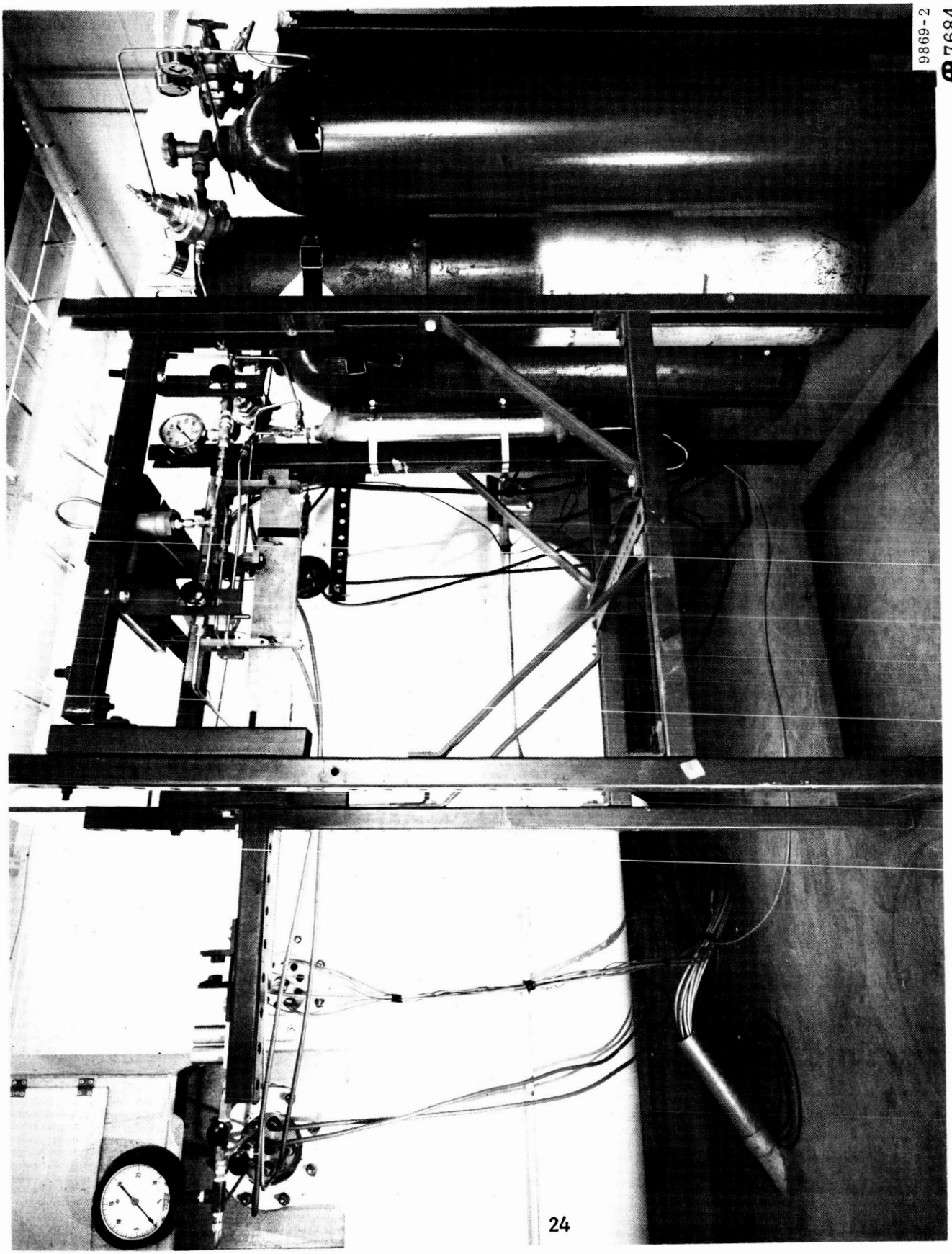

Figure 4-7. Flow System for N_2O_4 Tests Showing Pivot Balance System.

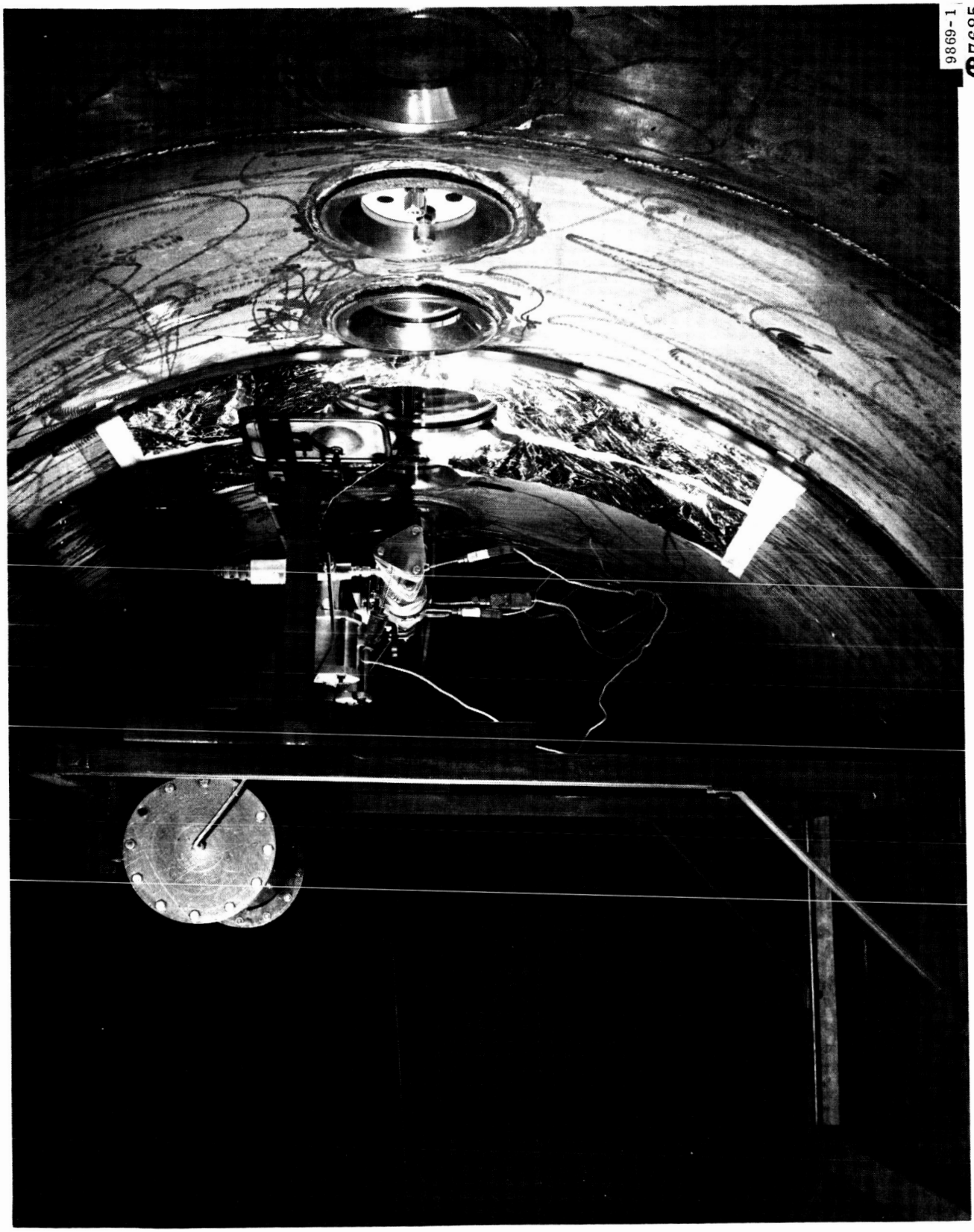

Figure 4-8. Flow System for N_2O_4 Tests (Inside Tunnel).

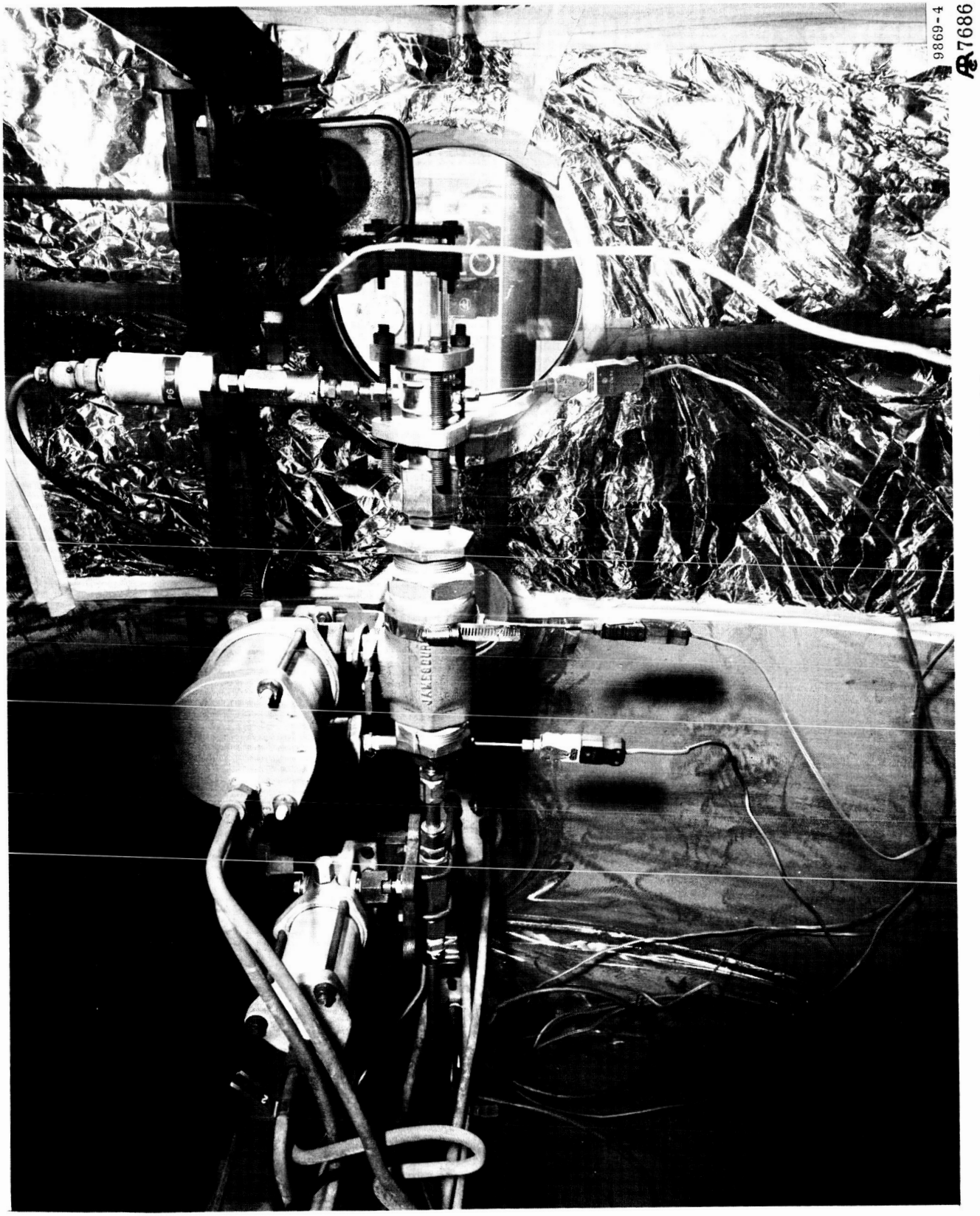

Figure 4-9. Two-Inch Leak Valve Located Inside of Vacuum Tunnel.

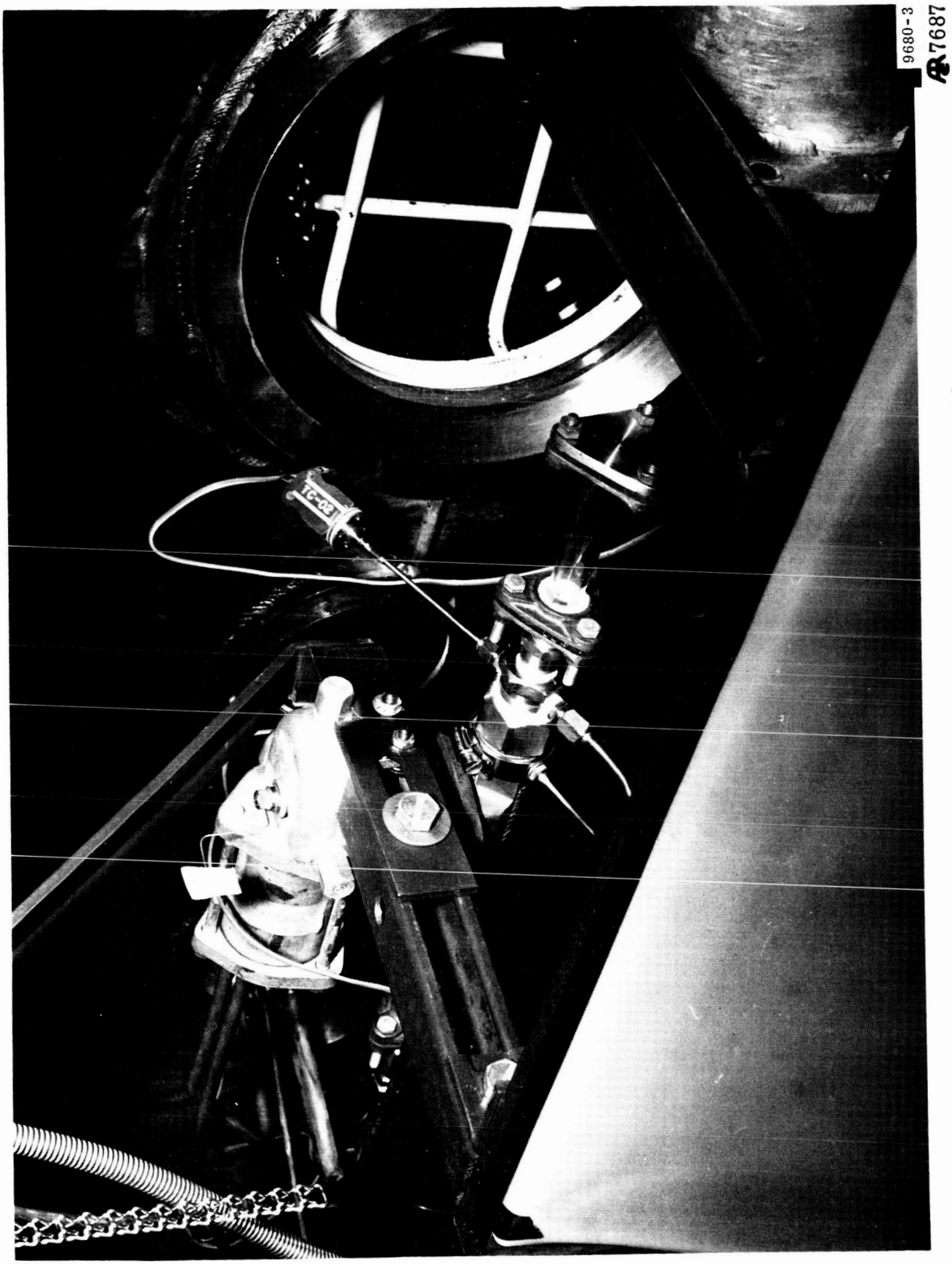

Figure 4-10. One-Inch Leak Valve Located Inside of Vacuum Tunnel.

valve. A ball-type leak valve was used which is similar to the propellant valves that are employed on the Apollo SPS engine.

Two other ball valves were installed in the feed line-- a hand-operated valve located outside the tunnel and a remotely-controlled valve which was installed inside the tunnel just upstream from the leak valve. The reason for the use of these valves is discussed later.

A schematic drawing of the leak valve is given in Figure 4-11. Three alterations were made to this ball valve to induce leakage:

1. The upstream seal was bypassed by drilling a 1/8 inch diameter hole into and perpendicular to the ball cavity. The ball was installed in the valve in a manner such that the relief hole faced upstream when the ball was in the closed position;

2. The downstream seal was scored;

3. The pressure on the downstream seal was varied by adjusting the associated body cap; flow was varied from run to run by changing the adjustment of this cap with the aid of a thickness gauge, as shown in Figure 4-11.

A glass pipe four inches long was connected to the outlet of the leak valve to permit observation of any freezing phenomena which might occur. To the end of this pipe was attached an injector plate that was counterbored in the center such that it was 1/16-inch thick in the area of the hole pattern. As shown in Figure 4-12, a thermocouple was inserted in the side of the plate in a manner such that the junction was located very near the injector holes.

Capability for filling the propellant tank was provided by means of a fill line which ran from a storage tank to the feed line. The vapor pressure of the nitrogen tetroxide in the storage tank was sufficient to cause flow when the propellant tank was vented. A 20 micron filter was installed in the fill line to remove any particulate matter which might have clogged the leak valve.

Figure 4-13 is the flow diagram for the coolant system. The leak-valve temperature was maintained by a mantle surrounding the valve body, as shown in Figure 4-14. This mantle consisted of several small-

7484

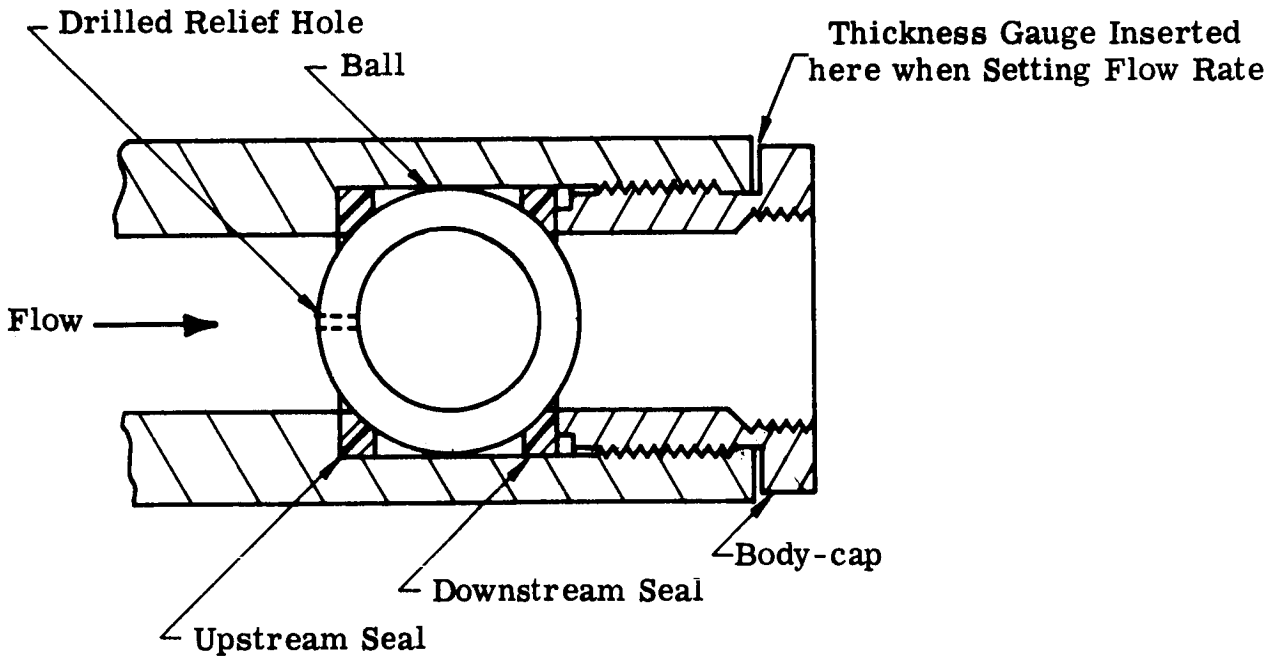

Figure 4-11 Schematic Cross Section of Test Valve.

9874
AR7688

Figure 4-12. Injector Plate Configurations used in the N_2O_4 Tests.

AR7483

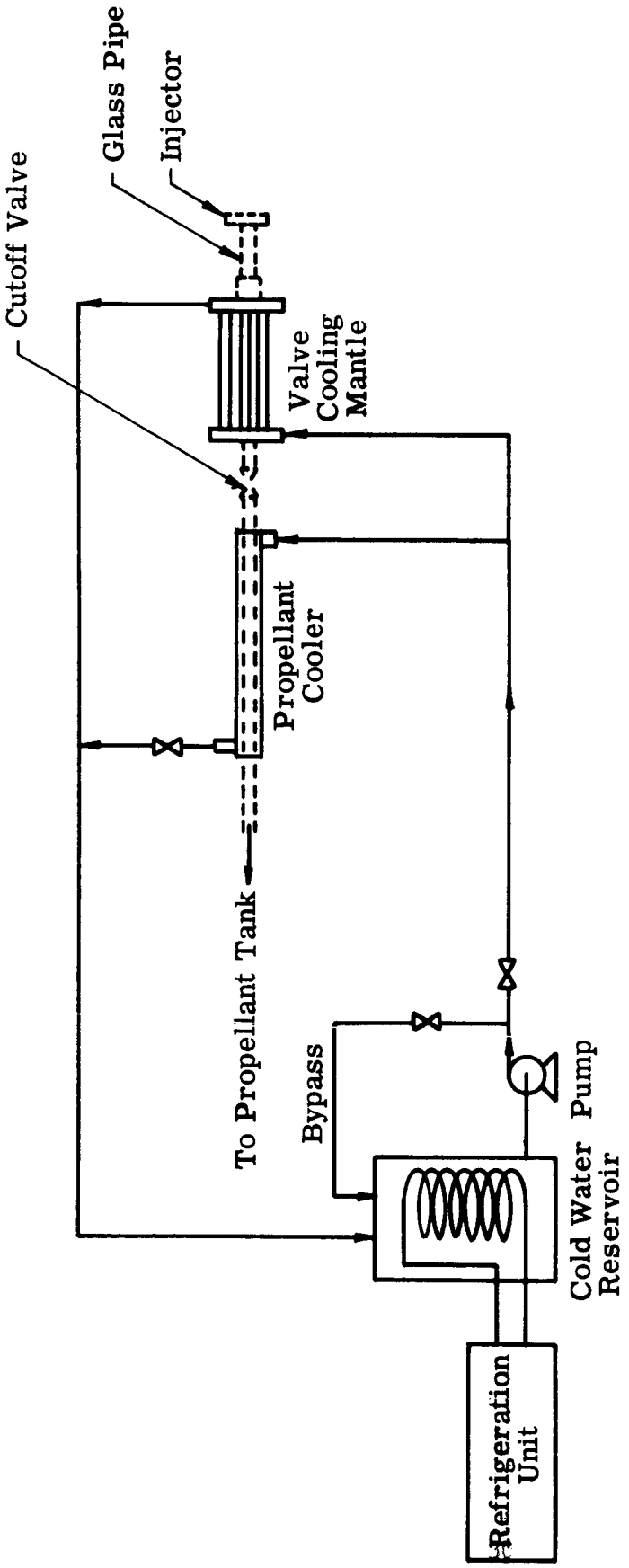

Figure 4-13 Coolant Flow Sheet.

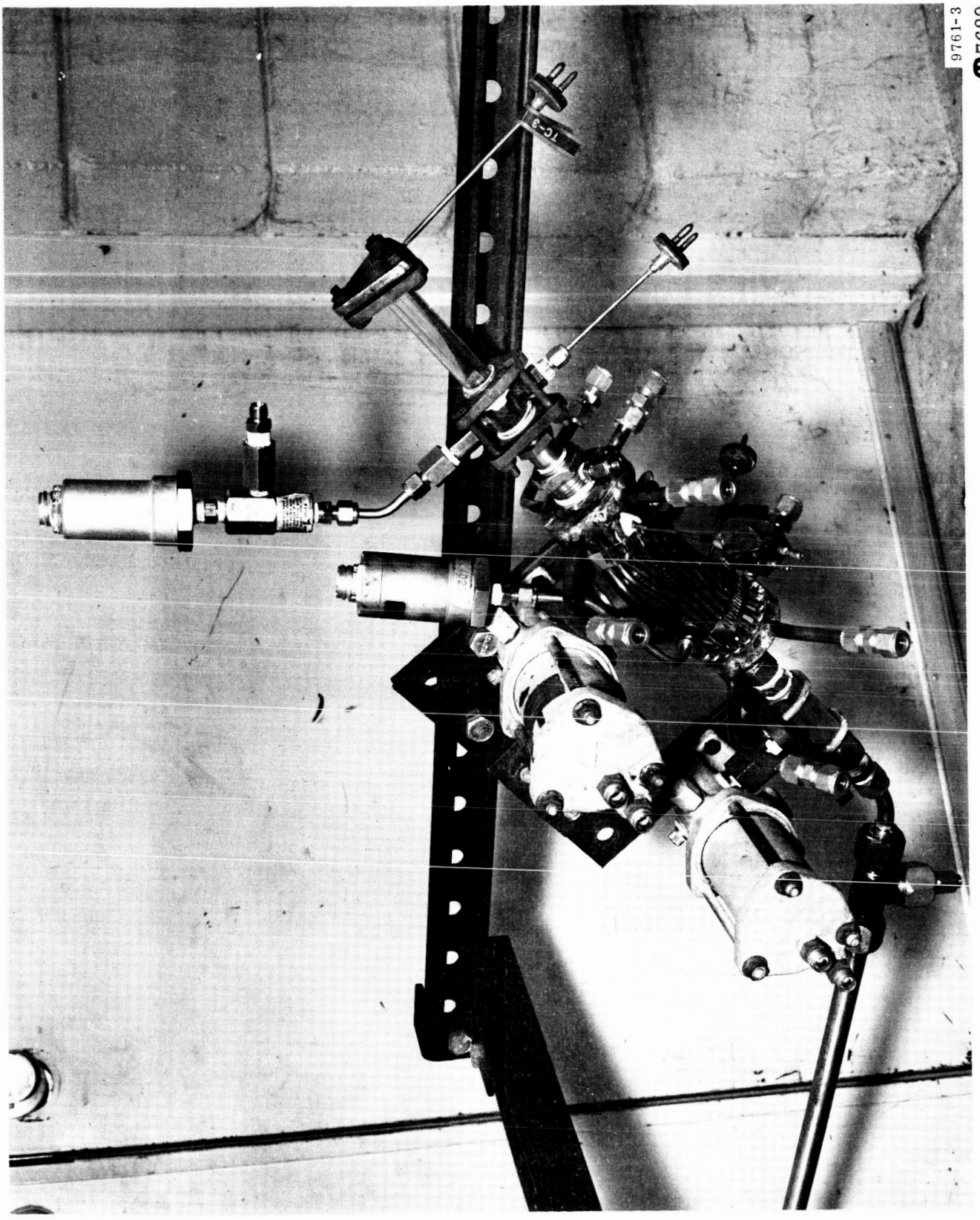

Figure 4-14. One-Inch Leak Valve with Cooling Mantle and Concentric Liquid Heat Exchanger.

diameter copper tubes which were securely clamped onto the valve body. The tube ends were silver-soldered into manifolds located at each end of the valve.

The temperature of the propellant entering the leak valve was controlled by a heat exchanger installed in the feed-line upstream from the cut-off valve. The cut-off valve, identified in Figure 4-6, is the main control valve used to initiate and terminate a run. Test procedure details are presented in Section 4.3. For tests conducted with cooled propellant, a concentric-tube heat exchanger was used in which the coolant passed through the annulus. For tests conducted with heated propellant, the concentric-tube heat exchanger was replaced with a section of tubing that was wrapped with an electrical heating tape.

The leak valve was opened and closed by a pneumatic operator which was activated by compressed nitrogen. This device was calibrated before the leak tests were performed so that the torque required to open the valve was known as a function of the gas pressure applied to the operator.

Since motion pictures of the phenomena occurring in the glass pipe and injector plate were desired, these components were mounted in front of a viewing window in the tunnel wall. After some early difficulties in relating the movies to the recorded data, a pocket watch was photographed together with the glass pipe and injector plate (from run number 25 on), and a flag was affixed to the leak valve operator such that it swung into the viewing field of the camera when the valve was opened. The relative positions of the photographic and test apparatus are shown in Figure 4-15. Note that primary illumination was obtained by back lighting and that fron lighting was achieved by taping aluminum-foil reflectors to the tunnel wall.

The initial flow configuration contained a glass pipe, four inches long, upstream from the leak valve, which allowed visual observation of the liquid flow. It was found that by evacuating the line downstream of the hand operated ball valve before a test was started, the line always completely filled with liquid up to the leak valve when the cut-off valve was opened to start a test. The glass pipe, having served its purpose, was then removed and the cut-off valve was moved as close to the leak-

AR7485

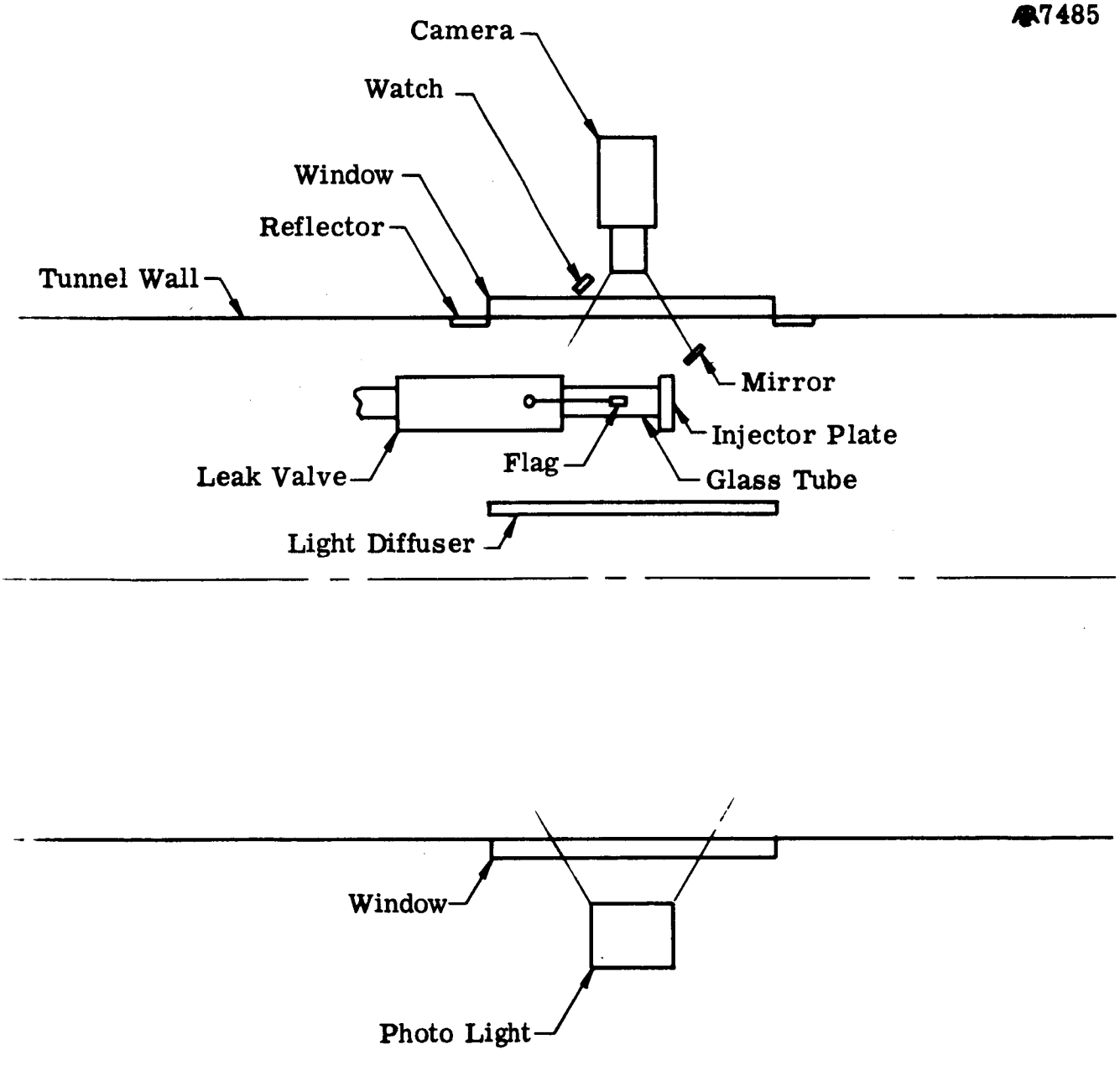

Figure 4-15 Photographic Setup.

valve as was conveniently possible. The reason for this was to minimize the volume upstream of the leak-valve that had to be filled with liquid at the beginning of each test. This arrangement also allowed a more rapid shut-down after a test was terminated.

4.2.3 Instrumentation

All of the pertinent run data were recorded by a multichannel recording oscillograph. Table 4-1 summarizes the pressure and temperature variables which were measured, indicates the type of sensing elements used, and gives the sensor locations in the test apparatus. In addition to these parameters, the change in weight of the propellant tank charge was recorded by means of a variable-reluctance-type force transducer that was mounted on the balance. Run-time was obtained from timing marks imposed on the oscillograph trace.

The sensing thermocouples were connected to reference thermocouples which were maintained at 150°F. Their signals were conditioned by bridge circuits which allowed pre-run balance and electrical calibration. Because of the corrosive nature of the propellant, stainless-steel-sheathed thermocouples were used throughout the system.

Pressures were measured by means of unbonded strain gage pressure transducers. These were connected to conditioning circuits which provided the excitation voltage for the strain gage bridge and allowed pre-run balancing and electrical calibration.

Propellant loss was measured by a specially constructed beam balance shown in Figure 4-7. The bean is suspended from a carriage by a strip of stainless steel shim stock which serves as the beam fulcrum. The propellant tank was securely fastened to one end of the beam and was counterbalanced by a weight clamped to the opposite end.

A force transducer, wired to a carrier-demodulator, was affixed to the balance carriage such that the transducer button touched the beam when the beam was in a horizontal position. When the tank was

Table 4-1

Pressure and Temperature Measurements

Variable	Sensor	Location of Sensor[1]
Tank pressure	Strain-gage pressure transducer, 0 - 250 psig	Tank pressurizing line
Tank temperature	Iron-Constantan thermocouple	Bottom of propellant tank
Upstream pressure	Strain-gage pressure transducer, 0-250 psig	Upstream end of leak valve
Upstream temperature	Copper-Constantan thermocouple	Upstream end of leak valve
Valve temperature	Copper-Constantan thermocouple	Leak valve surface on downstream end
Downstream pressure	Strain-gage pressure transducer, 0-5 psia	Instrumentation ring located between leak valve and glass tube
Downstream temperature	Copper-Constantan thermocouple	Instrumentation ring
Injector temperature	Copper-Constantan thermocouple	Soldered into channel in injector plate
Operator pressure	Strain-gage pressure transducer, 0-75 psig	Opening pressure line to leak-valve operator
Tunnel pressure[2]	Alphatron Vacuum gage	Tunnel wall near door

[1] See Figure 4-6

[2] not recorded by oscillograph

fully loaded, enough small counterweights were placed on the beam to position the transducer trace at maximum deflection. The size of these weights and their location on the beam were chosen such that when the trace approached zero deflection, due to propellant flow out of the tank, the removal of one of these weights would restore the trace to a nearly full-scale position.

The balance was calibrated by pouring measured quantities of water into the tank and recording the resulting galvanometer deflections. By repeating the process with various amounts of water initially in the tank, it was shown that the calibration did not change significantly with a change in liquid level. The result of this procedure was a constant calibration factor of the dimensional form: grams of weight change per inch of deflection. The magnitude of the factor was determined by the span adjustment in the demodulator circuit and the location of the load cell on the balance beam relative to the balance pivot point. Since the data obtained from the balance were in the form of propellant weight versus time, it was necessary to differentiate these data to obtain flow rates. By dividing the change in weight by the time interval over which the change occurred, the average mass rate for the interval was obtained. Multiplication of these mass rates by the specific volume of the liquid at the upstream temperature yielded the average volumetric flow rate of the propellant entering the test valve. These rate data were plotted against time at the mid-point of the intervals over which they were calculated. Since the accuracy of the resulting curve depends on the size of the time intervals, the data were reduced over very small increments in the regions where large changes in slope of the tranducer trace were evident.

4.3 TEST PROCEDURE

Before tunnel pump-down, the test valve was pre-set for a particular flow rate by adjusting the tightness of the body cap. Because of the construction of the valve and the cold-flow property of the teflon

seal, this adjustment would yield a flow rate that was only approximately equal to the one desired.

During the tunnel evacuation, the propellant tank was charged by opening the fill line and venting the tank into the tunnel. All the while, the remote cut-off and leak valve had been open so that the feed line was evacuated between the injector plate and the hand valve located outside the tunnel. When pump-down was complete, the line was filled by closing the cut-off and opening the hand valve. Then the propellant tank was pressurized with regulated nitrogen pressure, and the force transducer trace was brought to full deflection by placing counterweights on the balance beam. At this point, the flow system was prepared for the leak test.

Two final pre-run operations were performed. The temperature and pressure instruments were balanced and electrically calibrated. The initial opening torque requirement of the leak valve was determined by slowly increasing the operator pressure until the valve opened. This valve was reclosed before the test was run.

A leak test was initiated by opening the cut-off valve but with the leak valve remaining closed. The oscillograph chart drive was operated during the entire run, and motion pictures were taken of any freezing or unusual flow phenomena observed in the glass pipe and injector. Whenever the force transducer trace approached zero, the balance was reset by removing one of the small counterweights from the beam.

The run was terminated when (1) the leak rate became zero as indicated by the force tranducer trace and visual inspection of the glass pipe, (2) the phenomena observed in the glass pipe and injector were unchanging, or (3) the phenomena were cyclic. When either of these occurrences became evident, the leak valve was opened according to the procedure for measuring torque discussed previously and was kept open until full flow was achieved. After this the run was terminated by closing the cut-off valve.

The variables studied in this research are:

1. Valve size: one and two inch
2. Downstream line size: one-half and one inch inside diameter
3. Valve temperature: nominal 40°F and ambient
4. Upstream propellant temperature: nominal 40°F, ambient, and 135°F
5. Injector hole area: 0.00503 sq. in. and 0.0465 sq. in. with the 1/2-inch tube, and 0.00503 sq. in. and 0.0530 sq. in. with the one-inch tube.

Data were taken over a wide range of flow rates for each variable or combination of variables. The range extended from a leak rate of about 0.007 cc/sec, which resulted in no accumulation of frozen N_2O_4 in the valve, up to a rate that was sufficiently high that no freezing occurred upstream of the injector face.

4.4 DATA RESULTS AND ANALYSIS

The experimental effort consisted of eighty-five tests which were conducted with N_2O_4 to investigate propellant leakage through a propellant valve and into a vacuum environment. The tests were performed with the test equipment and procedures described in the preceding sections of this report.

The results and conclusions drawn from visual observation, studying the motion pictures taken of each test, and analyzing the recorded data, approximate very closely the theoretical predictions discussed in Section 3.0.

Measurements made before and at the end of each test, in which freezing occurred, showed that the torque required to open the leak valve was unaffected even when the N_2O_4 froze in the vicinity of the leak valve ball or stem. These results were expected since N_2O_4 contracts as it freezes (the opposite of water which expands). This was true for both the one-inch and two-inch ball valves.

Evaporative freezing of N_2O_4 that has leaked by the propellant valve does occur, and frozen N_2O_4 does accumulate between the ball valve and injector plate during certain freezing modes. For a given injector geometry the type of freezing mode obtained during a test is primarily a function of the leak-rate.

In order to simulate as closely as possible an actual leak condition, the leaks were created by adjusting or defacing the teflon seals in the ball valve. During a run the liquid pressure applied to the upstream side of the ball caused the teflon to cold-flow and reduce the leak cavity; therefore, a characteristic of most of the runs is that the leak rate constantly decreased during a run. Consequently, more than one type of freezing mode can be obtained during a run.

Five different types of liquid freezing modes were experienced. One type consisted of freezing and plugging of the injector ports while the glass pipe was completely filled with liquid. This type of plug usually occurs at about the maximum leak rate for which freezing can be obtained for the injector port area being used (see Section 3.0). In the case of the injector containing four 0.040-inch diameter ports this value was 0.42 cc/sec. The life of this type of plug is very short, usually less than two minutes, since there is only a small amount of N_2O_4 to be sublimed. After the plug breaks, the freezing phenomenon repeats and continues in a cyclic manner.

A second type of freezing mode consists of a plug formation in the glass tube, as shown in Figure 4-16. This freezing mode usually occurs at a leak rate slightly lower than that required to produce the first freezing mode described above. In the initial stage, Figure 4-16 (a), liquid sloshes in the glass pipe due to boiling of the liquid and causes intermittent flow through theorifices of the injector plate. A frozen plug forms in the lowest orifice(s). The plug then sublimes away, and freezing progresses into the liquid in the pipe, Figure 4-16(b). Meanwhile, the liquid level in the pipe has risen, and because of continued sloshing, the higher injector orifices become plugged. Then,

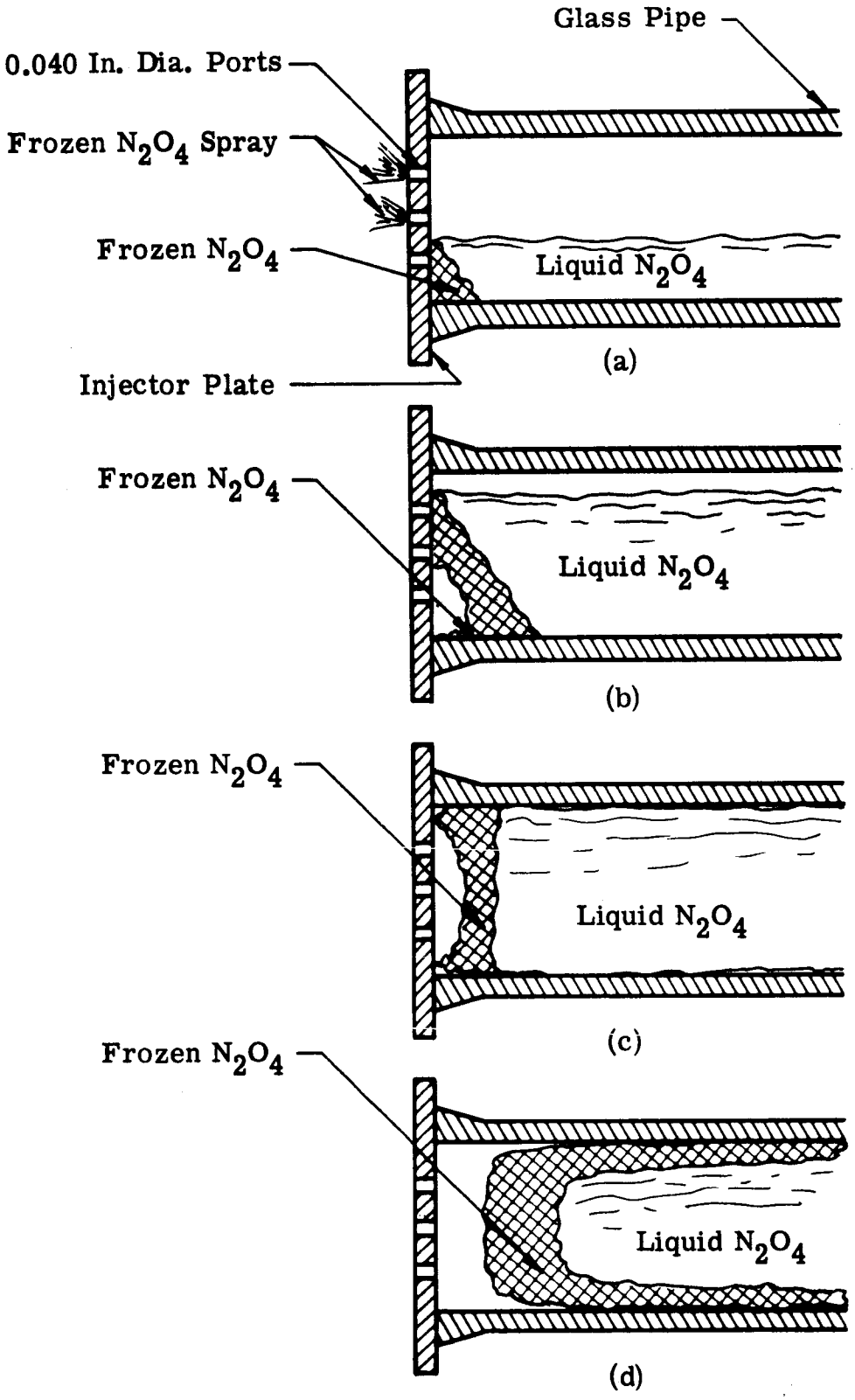

Figure 4-16. Stages in Plug Growth.

as shown in Figure 4-16(c), plugs in the higher orifices also sublime away, and the freezing continues to progress into the pipe. The liquid now completely fills the pipe diameter, and the plug assumes a shape similar to that shown in Figure 4-16(d). Pressure on the liquid continues to rise as leakage continues. Tiny amounts of liquid cyclically escape between the pipe walls and the plug, only to freeze when exposed to the vacuum of the cavity between the injector orifices and the plug.

The cavity between the plug and the rear face of the injector plate is essential for maintenance of the plug. This is because evaporation from the total orifice area is too small to maintain a large frozen mass by evaporative cooling. On the other hand, the orifice area is sufficiently great to handle the vapor flow from a large surface of frozen material such as that of the plug.

During one of the cycles, when the liquid is leaking past the plug and its adhesion to the glass pipe wall is least, the high pressure in the liquid causes the plug to occlude one or more of the orifices, resulting in a reduced rate of evaporation and causing a substantial portion of the plug to melt. However, the plug usually survives, and no liquid is lost through the injector. Evaporation restores the cavity and growth of the plug resumes; but before it obtains its original size, slippage and remelting reoccurs. This cycle repeats several times, and at the same time the pressure in the liquid continues to rise. Eventually, as a result of the gradual reduction of the plug size and the increasing liquid pressure, one of the plug slippages is catastrophic. The plug is forced to the rear face of the injector, sealing-off the orifices, and the liquid melts through the plug and flows out of the injector orifices before evaporation can restore the cavity. Nearly all the liquid is expelled from the pipe, and the whole plugging cycle begins again. Each complete cycle of this type may last several minutes.

The third type of freezing mode usually occurs when the system has been precooled from a previous run and when the leak rate is slightly slower than requird for the second freezing mode just described. Liquid

entering the glass pipe freezes almost immediately, and the pipe is never filled. By the time the solid N_2O_4 in the pipe sublimes, the leak rate has decreased sufficiently to prevent liquid from being seen in the glass pipe for the remainder of the run. In some cases, runs were continued for over two hours. At the end of the run, when the leak valve is opened, particles of frozen N_2O_4 were observed to be entrained in the liquid deluge which filled the glass tube, thus indicating that freezing had indeed occurred in the vicinity of the valve ball. The particles varied in size and shape from approximately one to eight mm in cross-section.

The fourth freezing mode is very similar to the third mode except that the leak rate is low enough to allow the liquid to freeze in the region between the glass pipe and the valve ball; therefore, no visual evidence of a leak can be seen until after the leak valve is opened and the particles of solid N_2O_4 are observed as in the third mode.

The fifth freezing mode occurs at a leak rate below which no solid N_2O_4 will accumulate (see Section 3.0). This requires the sublimation rate to be equal to or higher than the leak rate. The absence of solid particles in the liquid deluge obtained when the leak valve is opened can be used to distinguish the fifth from the fourth freezing mode. An analysis of the 16 mm color motion picutres and the oscillograph recordings shows that leak rates below approximately 0.11 cc/sec can be placed in the fifth freezing mode category. This value was not affected by injector port area. See Section 3.0 for explanation.

Flow delays were experienced for all the freezing modes described above except the fifth mode. This was expected since in the fifth freezing mode there is no accumulation of frozen propellant to cause blockage. Flow delays were determined by measuring the elapsed time from the instant the leak valve was opened to the instant at which the downstream thermocouple indicated a temperature increase. During this portion of the run the recording oscillograph paper speed was set at one inch per second which permitted a time resolution of approximately 10 milliseconds. Flow delay

measurements were made on 66 of the 85 total tests conducted. No flow delay was seen on 25 of the 66 tests; however, on the other 41 tests, delays from 10 milliseconds to eight minutes were recorded.

Generally, the delays occurred as the result of propellant freezing within the valve. However, the eight-minute delay was observed when a plug was in the glass tube. The formation of this plug involved more than the mechanism referred to earlier in the discussion of the second freezing regime. During the run, several plugs formed according to that mechanism. After the pressure behind these had increased sufficiently, their centers were forced through the injector holes leaving a shell of frozen propellant in the tube at the injector end. Following one of these breakthroughs, the surface of the liquid remaining in the tube began solidifying in a manner similar to the third freezing regime. Since boiling of the propellant occurred during this freezing process, the resultant totally-frozen mass was very porous. Later, a solid-liquid slurry flowed into the glass section and filled the void spaces in the plug. The liquid near the tube wall proceeded to freeze as in the second regime. At the time the leak-valve was opened, the plug was at least as long as the glass section, and the vapor space between the plug and the tube wall appeared to be very thin and discontinuous. During the delay period, the solid formation melted from the upstream end, and the solid-liquid interface was observed to move toward the injector plate. After the plug broke, the remains indicated that the core of this plug was frozen for a considerable distance upstream from the plate, thereby explaining the strength of this formation. The propellant tank pressure was 150 psia during the leak period and during the eight-minute delay when the leak valve was open.

In some cases blockage was sufficient to permit only partial flow for a short period of time. When partial flow is achieved, N_2O_4 liquid is brought in contact with the frozen N_2O_4 remaining in some of the injector ports and glass tubes. This hastens the melting process, after which full flow is achieved. The time-lapse between initial flow and full flow can be significant and is dependent upon the type of blockage experienced.

Time-lapses as long as one second were noted. The decreased thrust resulting from the partial flow could adversely affect a mission. In the actual case where ignition is obtained, the heat generated by combustion would hasten the melting of frozen N_2O_4 in the injector ports and/or manifold. The strength of a frozen plug of N_2O_4 depends on the freezing mode experienced and is at a maximum immediately after a solid plug is formed. Because of sublimation, the plug strength gradually decreases, and consequently, the flow delay encountered after the leak valve is opened depends upon which part of the freezing cycle is in progress when flow is attempted.

As expected, the data show that leak rate and injector orifice area had far more effect on the freezing mode than any of the other variables investigated. Line size and initial temperature of the liquid and leak valve had little effect, although second-order effects were obscured to some degree by the fact that exact flow rates could not be reproduced, and, therefore, a direct comparison could not be made.

The temperature control system was designed to provide the initial desired temperature of the propellant and leak valve, but no attempt was made to compensate for the high heat fluxes encountered through evaporative cooling. Had such a compensation been made, an unrealistic condition would have been created. The result was that the heat flux from the temperature control system was very rapidly overshadowed by the heat flux from evaporative cooling of the propellant; therefore, shortly after the run began very little difference in temperature could be noted between the cases where the initial temperature was controlled (40° and 135°F) and the case where ambient initial conditions were used (approximately 85°F)

An exact relationship between the leak-rate limits of the freezing phenomena and the injector port area could not be measured; however, the data show sufficient evidence to corroborate the theoretical prediction that the maximum leak rate for propellant freezing in the injector manifold increases in direct proportion to the area of the injector

ports. This will allow reasonably accurate scaling of effects from the test model to the full-size SPS engine (see Section 3.0).

There are two reasons why an exact relationship could not be established experimentally. First, in order to establish a common basis for comparisons among tests and among test and analytical results, it is desirable that each test be characteristically distinguishable by a specific leak rate value. In the theoretical analysis, leak rate is an idealized concept which assumes the flow to be steady and independent of any evaporation, boiling, change in geometry, or freezing that might occur. Experimentally, this idealized flow would be realized in the absence of vacuum effects and geometric changes; but freezing and geometric changes cause reductions of the flow rates to levels significantly below the idealized rate. The obvious procedure for determining the ideal leak rate is to measure the rate in a normal atmosphere before or after performing the vacuum test; however, a given leak geometry is difficult to reproduce because of the cold-flow properties of teflon (the valve-seal material). Accordingly, this procedure could not be incorporated easily into the experiments in a manner such that overall test results would continue to meet the principal experimental objectives. Instead, another procedure which gives sufficiently accurate results was used, determination of the initial leak rate before substantial freezing of the liquid has developed. This procedure does involve some uncertainty since, at the start of each test, there is a void space in the line between the cut-off and leak valve (see Figure 4-6). When the cut-off valve is opened to start an experiment, the void space fills just before and during the moment that flow starts through the leak. Of course, while the void fills, an unrealistically high leak rate is recorded by the balance system (see Figure 4-7); but usually there is a sufficiently sharp change in the rate to indicate when the void has filled. This moment occurs a few seconds after the cut-off valve has been opened, and the indicated leak rate at this moment is assumed to be the ideal rate. Second, shortly

after liquid leaked into the glass pipe, the ports near the bottom of the injector plate became covered with liquid and consequently were plugged with frozen N_2O_4. When the liquid level rose in the glass pipe, more of the holes similarly were plugged. This resulted in a variable injector port area and precluded an accurate determination of the effects of port area upon freezing of N_2O_4 within the simulated manifold. Several tests were conducted with the glass pipe and valve assembly tilted up at a 45-degree angle, in an effort to prevent the liquid from covering the injector ports. However, this was not very successful since boiling caused the liquid to slosh against the injector and plug some of the ports.

Subsequently, a more successful design was used, in which all the ports were located above the centerline of the glass tube, and the tube was remounted in a horizontal position. This allowed the ports to remain open until after the glass pipe was approximately half full of liquid.

Because of the many fluctuations of the various parameters that were recorded as functions of time, it became necessary to present the data graphically to show the interdependence of some of the variables. Accordingly, leak-rate, downstream pressure, downstream temperature, injector temperature and leak valve temperature have been plotted versus time and are presented in Appendix A.

For exemplary purposes, data for a typical test are presented graphically in Figure 4-17. This example test utilized a one-inch inside-diameter glass pipe, a one-inch leak-valve and an injector plate containing forty 0.040-inch-diameter ports. The leak-valve was cooled to approximately 40°F and the liquid was heated to a temperature of approximately 135°F. During the run, the injector ports plugged and unplugged four times in a cyclic manner. The pressure in the region between the leak-valve and injector plate increased sharply each time plugging occurred, and exceeded the maximum recordable pressure (6.4 psia) of the transducer used. The plugging phenomena also were reflected by the temperature measured in the same region. During most of the run the leak-rate was too high to allow complete freezing; therefore, a two-phase mixture of liquid and frozen

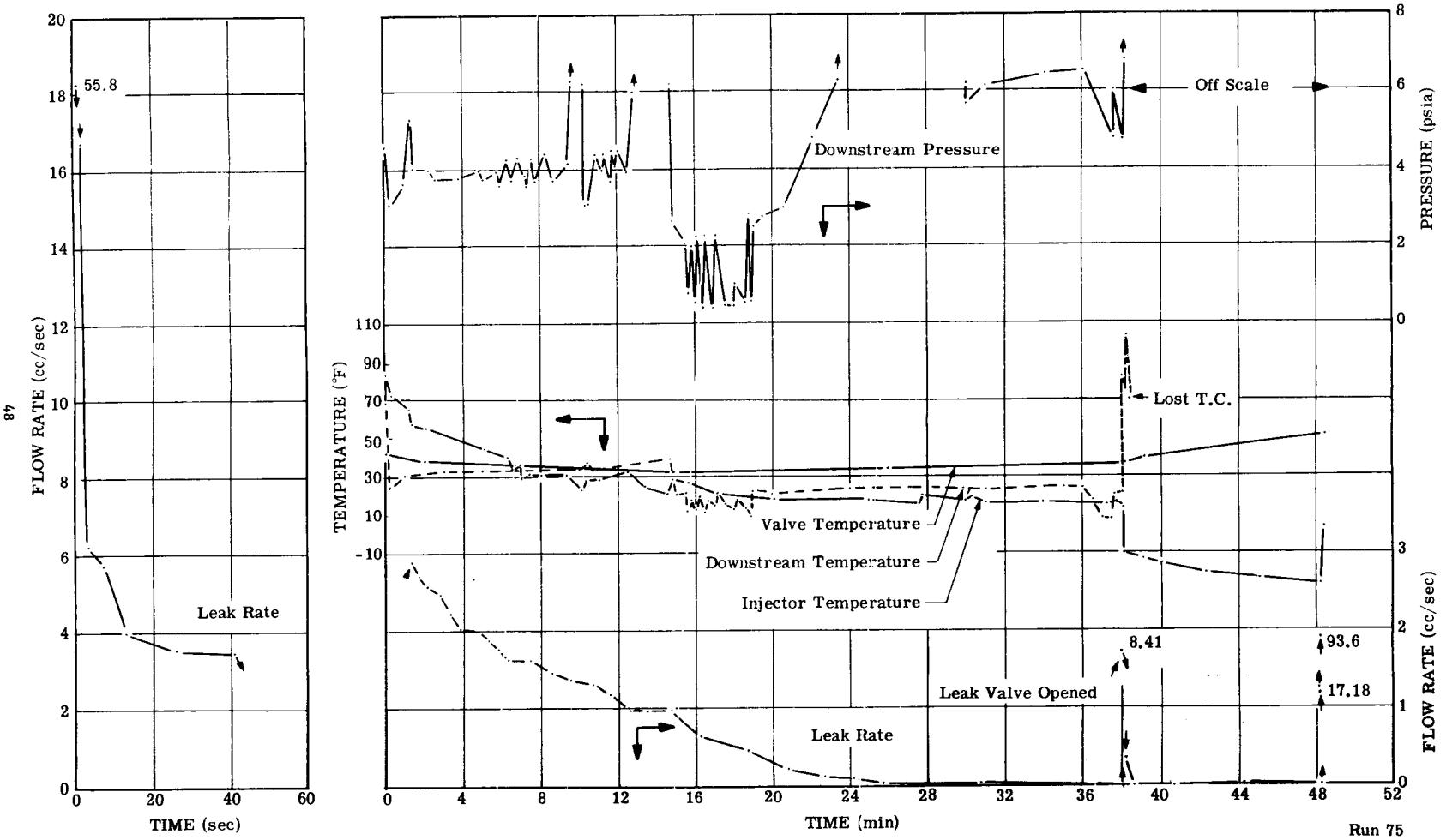

Figure 4-17 TEST D/ 7/

N_2O_4 was observed in the glass pipe. The characteristic decline in leak rate occurred throughout the run. About 38 minutes after the run began the flow rate had reduced to zero and the liquid rapidly cooled and solidified. A minute later the leak-valve was opened and a small amount of liquid flow was recorded for about one second. The frozen plug then prevented flow for a period of eight minutes after which sufficient sublimation and melting had taken place to allow the plug to become dislodged. A more detailed description of the freezing mechanism for this particular run is presented above in the discussion of the third type of freezing mode. The liquid temperature measurement was lost on this run shortly after the leak-valve was opened. The failure occurred in the thermocouple plug connection and was caused by repeated exposure to the N_2O_4 environment in the tunnel.

4.5 SAFETY

As is always the case when working with high energy propellants, there is a certain element of danger involved. The personnel who are working on this program have had extensive experience with all the propellants concerned. Adequate safety precautions are being taken to insure protection from explosions and the toxicity of the propellants. A safety shower and eye-wash system are located in the test area. Precautions are also taken to assure compatibility of materials with the various propellants involved.

5.0 REMEDIAL TECHNIQUES

Tests conducted in Phase I and those planned for Phase II were designed to define and characterize the evaporative freezing phenomena resulting from propellant valve leakage in a vacuum environment. Remedial techniques to solve the problems created by leaky valves will be evaluated in the Phase III series of tests. Specific emphasis will be given to the flow system used by the Apollo SPS engine. Some of the techniques that will be considered are

1. Heating
2. Propellant additives
3. Gas purging.

While no remedial techniques were evaluated experimentally during Phase I, some preliminary analysis of these techniques has been performed based upon experimental and theoretical results obtained to date. The application of heaters might seem to be an obvious convenient approach to alleviate evaporative freezing problems; however, as pointed out in the theoretical discussion (Section 3.0), the evaporative heat-fluxes that result when liquids are exposed to a vacuum are very high. For the case of liquid N_2O_4, this value is about 4.75×10^6 Btu/hr.-ft.^{2} (356 cal/cm^2-sec). Consequently, heater output (and associated size) requirements, to compensate for this high evaporative heat flux, appear to be prohibitive. Further, theoretical as well as experimental investigations on heater requirements, and, in addition, propellant additives, gas purging, and others will be conducted in Phase III. A tradeoff-analysis will then be made to permit selection of the best remedial techniques of those examined.

6.0 PROGRAM STATUS

6.1 PROGRAM SCHEDULE AND MANPOWER EXPENDITURE

The program schedule, showing accomplishments to date and work remaining, is presented in Figure 6.1. Work has progressed as originally scheduled, and no major areas are apparent or anticipated which might affect a successful conclusion of the program.

Approximately 5,150 man-hours were expended to complete the scheduled work through Phase I. This expenditure represents about 54 per cent of the total program.

6.2 FUTURE WORK

The apparatus for conducting the Phase II tests has been completed, and Phase II testing, using Aerozine-50, will be underway within a few days. Beased upon the theoretical analysis of propellant freezing, estimates were made of the maximum leak-rates for the accumulation of frozen Aerozine-50 within propellant manifolds. The results indicated that little or no accumulation of frozen propellant will be observed with the injector plates used for the N_2O_4 tests, because the total port areas are too small. Accordingly, injectors with total port areas of at least 0.1 sq. in., twice that of the largest used for the N_2O_4 tests, will be used for the Aerozine-50 tests.

Phase III tests will be conducted as scheduled and outlined in the proposal (Reference 2) for this effort. Effects of propellant freezing on hypergolic ignition will be determined, and investigations of remedial techniques will be made.

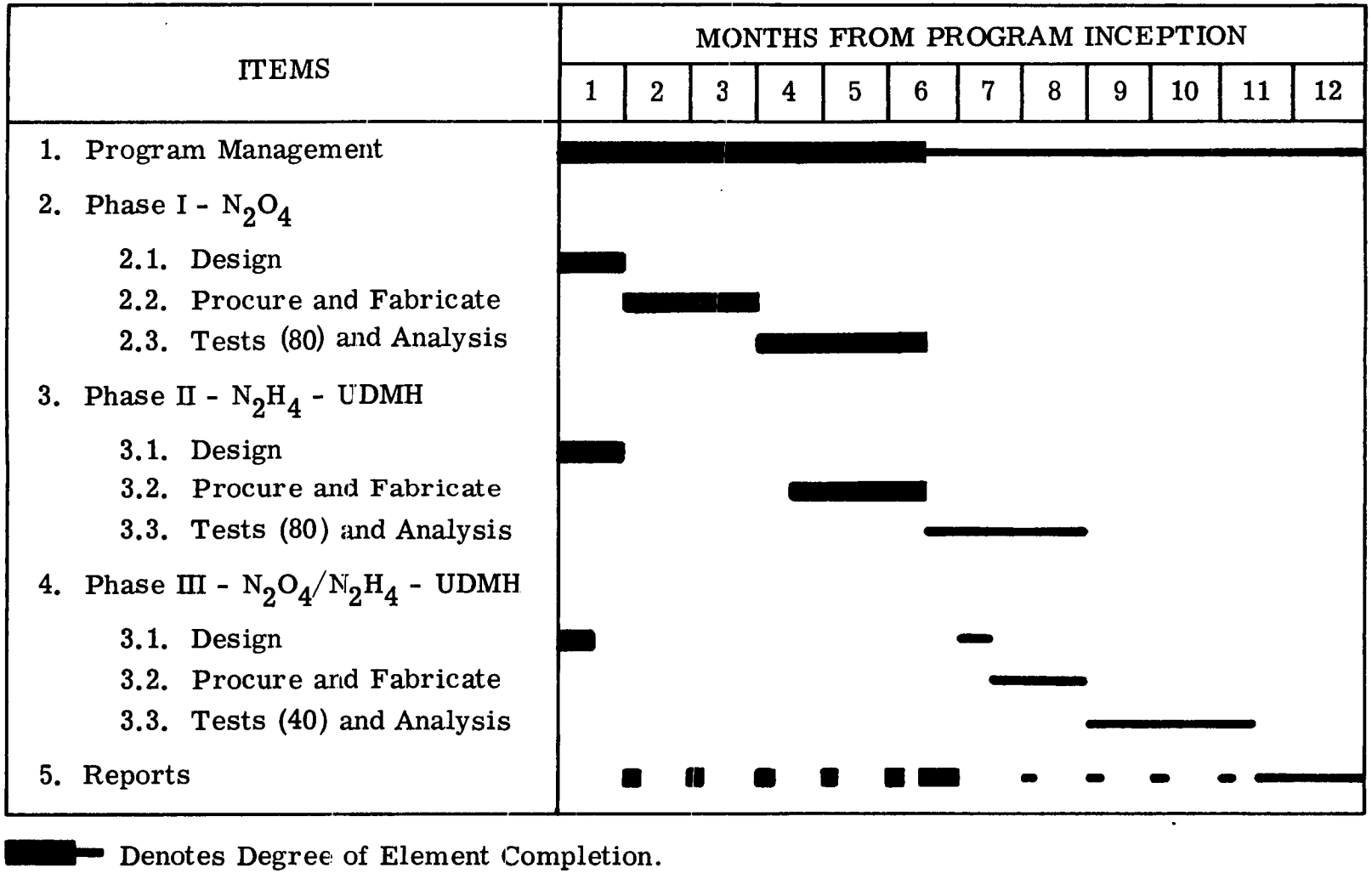

Figure 6-1. Program Schedule.

LITERATURE CITATIONS

1. Atlantic Research Corporation, "Investigation of the Effects of Vacuum on Liquid Hydrogen and Other Cryogens Used on Launch Vehicles," Final Summary Report by J. A. Simmons, R. D. Gift and M. Markels, Jr. for Contract NAS8-11044, December 18, 1964.

2. Atlantic Research Corporation, "Study of Propellant Valve Leakage in a Vacuum," Technical Proposal ARC No. 43-2579, February 24, 1965.

APPENDIX A
TEST DATA

This appendix contains the pertinent run data obtained during the 85 tests conducted in Phase I. Because of the many fluctuations of the various parameters that were recorded versus time, it is necessary to present the data graphically to show the interdependence of some of the variables. The runs of major interest are those during which propellant freezing was achieved and during which no experimental difficulties were experienced. Accordingly, graphs for 45 tests are presented. Data for the other 39 tests have been analyzed but have not been plotted for one of the following reasons: (1) leak rate too slow, (2) leak rate too fast or (3) experimental difficulties.

Five of the variables recorded were plotted versus time for the runs during which these variables were measured.

1. Leak-rate, cc/sec
2. Downstream pressure, psia
3. Downstream temperature, °F
4. Injector temperature, °F
5. Leak valve surface temperature, °F.

Other measured quantities which were recorded but were not plotted are

1. Tank pressure, psia
2. Upstream pressure, psia
3. Upstream temperature, °F
4. Tunnel pressure.

The test configurations used for the 85 runs involved five variables: glass pipe size, leak-valve size, injector port area, liquid temperature, and leak-valve temperature. The schedule of tests, in terms of combinations of these variables, is shown in Table A-1. These variables are discussed in detail in Section 4.2.2.

TABLE A-1

SCHEDULE OF TESTS

Run No.	Glass Pipe I. D.	Leak-Valve Size	No. of .04 I. D. Inj. Ports	Liquid Temp	Leak-Valve Temp
1-30	1/2"	1"	4	ambient	ambient
31-47	1/2"	1"	37	ambient	ambient
48-53	1/2"	1"	37	cooled	cooled
54	1/2"	1"	37	ambient	ambient
55-58	1/2"	1"	37	cooled	cooled
59	1/2"	1"	37	ambient	ambient
60	1/2"	1"	37	cooled	cooled
61-63	1"	1"	4	cooled	cooled
64	1"	1"	4	ambient	ambient
65-66	1"	1"	4	cooled	cooled
67-72	1"	1"	40	cooled	cooled
73	1"	1"	40	ambient	ambient
74-78	1"	1"	40	cooled	cooled
79-85	1"	2"	40	ambient	ambient

Notes:

1. "Ambient" temperatures ranged from 85°F to 95°F.
2. "Cooled" temperatures were approximately 40°F.
3. "Heated" temperatures were approximately 135°F.

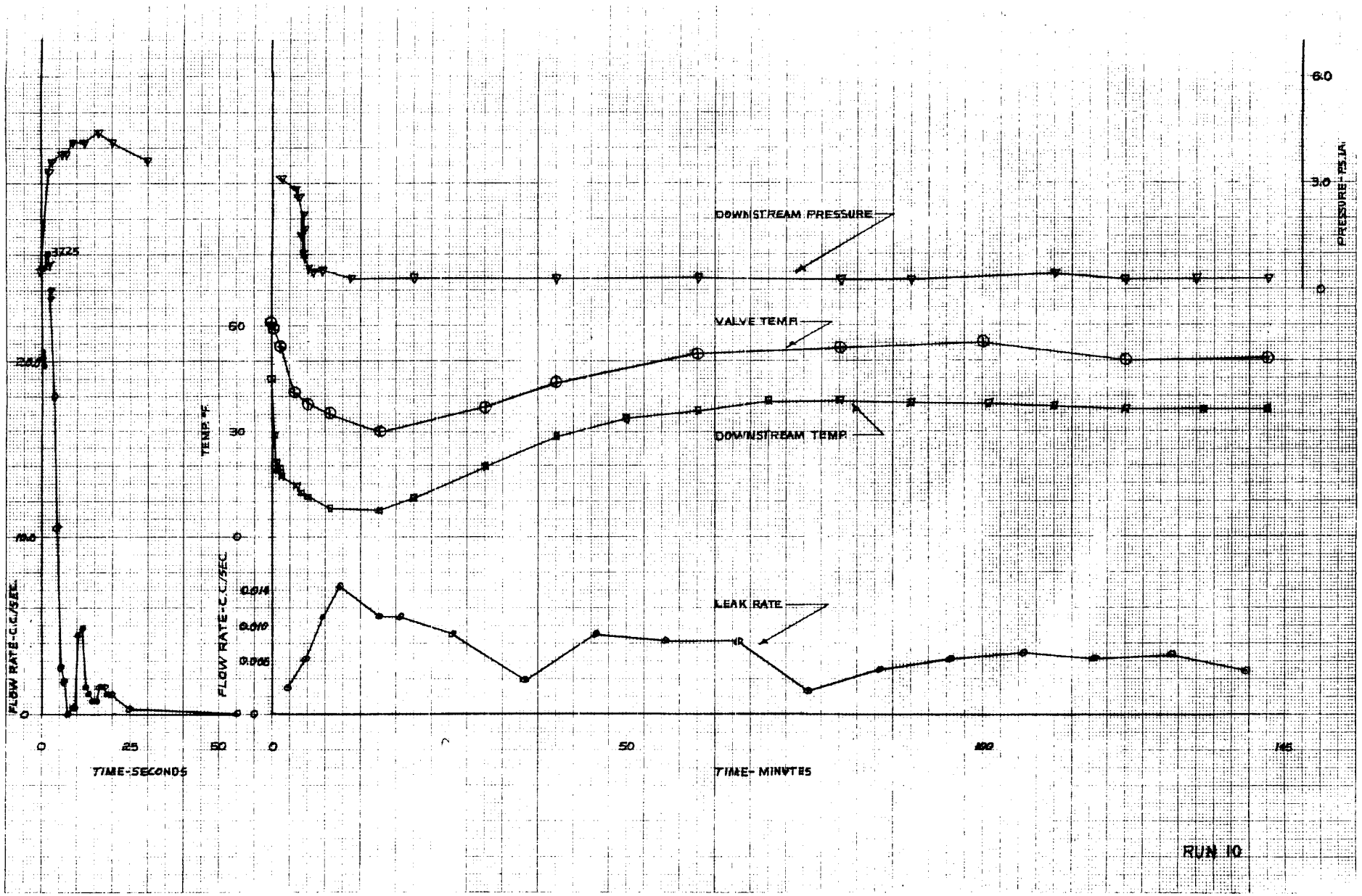
FLOW RATE-C.C./SEC.
0.3725
0.2485
0.124
0
0
25
50
TIME-SECONDS
TEMP °F
60
30
0
FLOW RATE-C.C./SEC
0.014
0.010
0.005
0
0
50
100
145
TIME- MINUTES
DOWNSTREAM PRESSURE
VALVE TEMP
DOWNSTREAM TEMP
LEAK RATE
6.0
3.0
0
PRESSURE-PS.I.A.
RUN 10

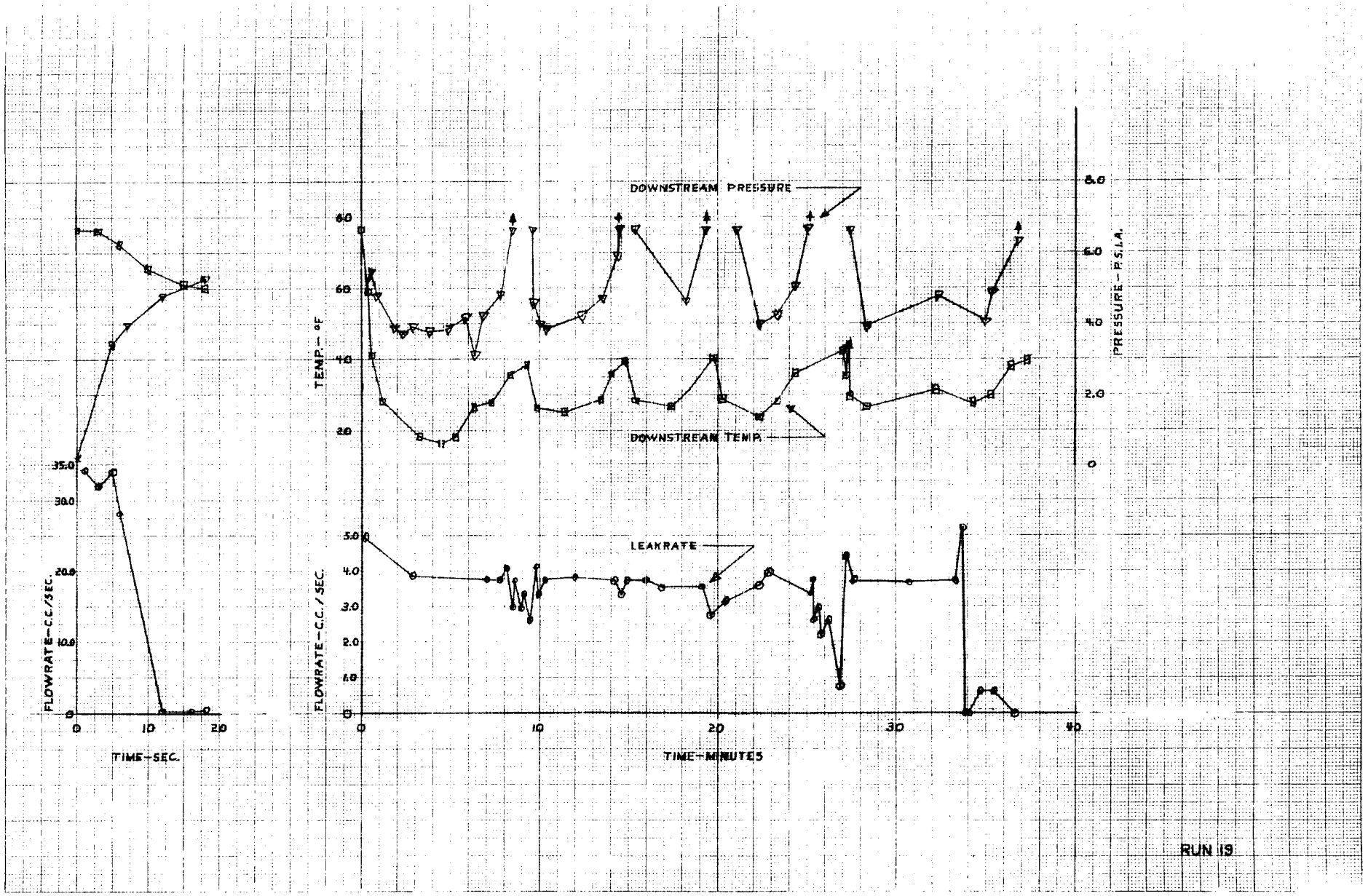
DOWNSTREAM PRESSURE
DOWNSTREAM TEMP.
LEAKRATE
TEMP. - °F
PRESSURE - P.S.I.A.
FLOWRATE - C.C./SEC.
TIME - MINUTES
FLOWRATE - C.C./SEC.
TIME - SEC.
RUN 19

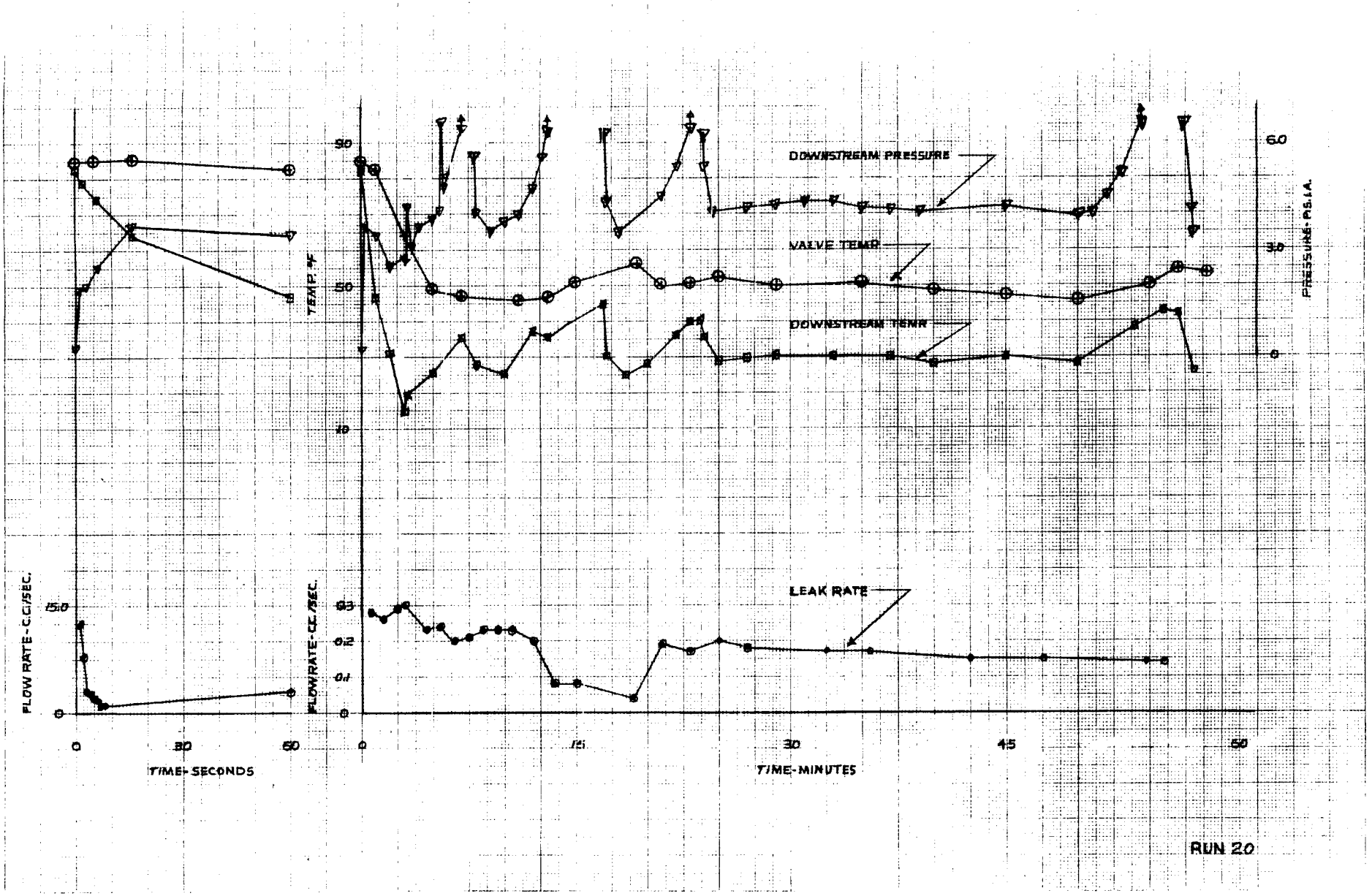
DOWNSTREAM PRESSURE
VALVE TEMP
DOWNSTREAM TEMP
LEAK RATE
TEMP °F
PRESSURE - P.S.I.A.
FLOW RATE - C.C./SEC.
FLOW RATE - CC./SEC.
TIME - SECONDS
TIME - MINUTES
RUN 20

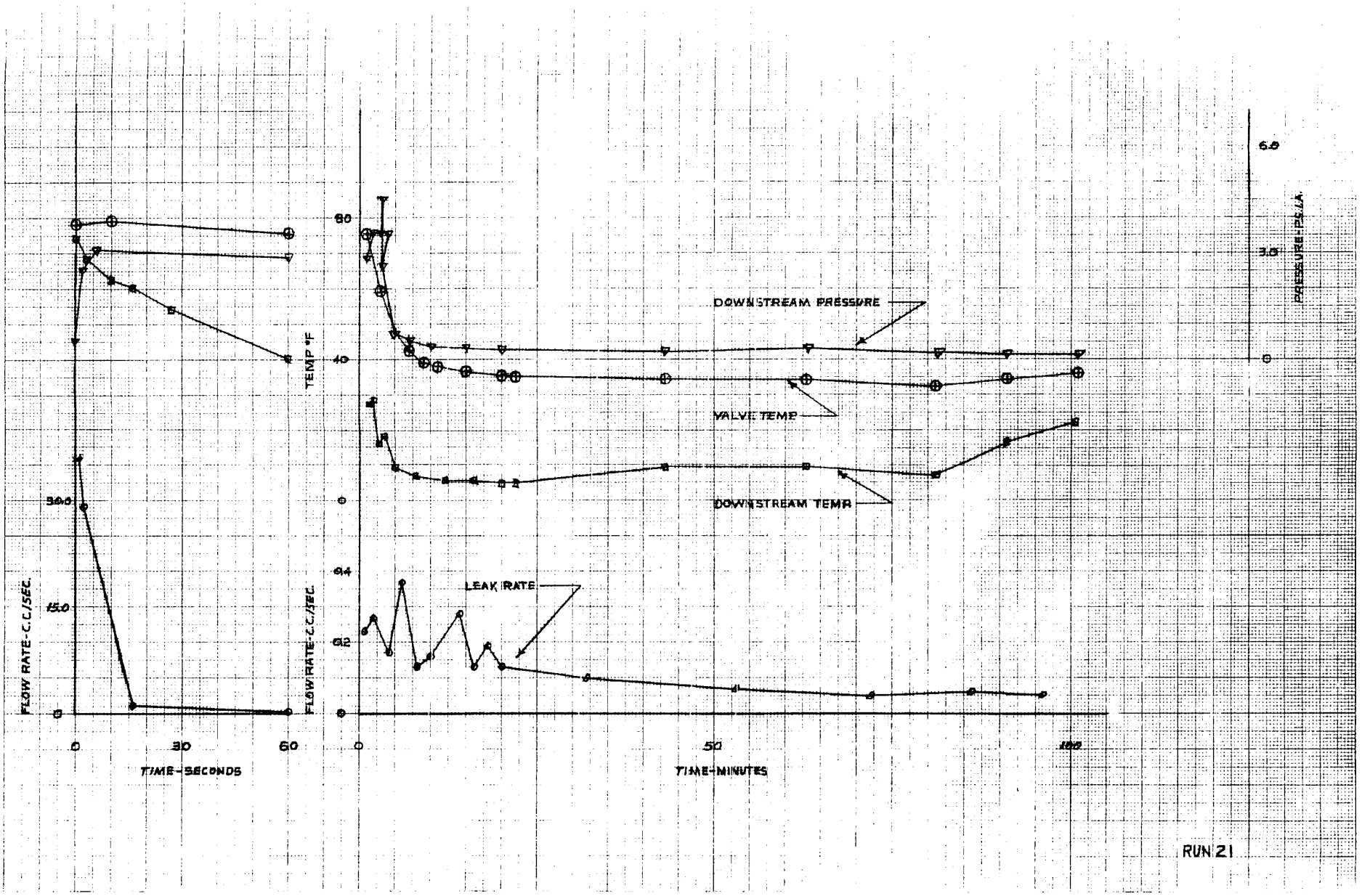
FLOW RATE-C.C./SEC.
30.0
15.0
0
0
30
60
TIME-SECONDS
TEMP °F
60
40
0
FLOW RATE-C.C./SEC.
0.4
0.2
0
0
50
100
TIME-MINUTES
DOWNSTREAM PRESSURE
VALVE TEMP
DOWNSTREAM TEMP
LEAK RATE
6.0
3.0
0
PRESSURE-PS.I.A.

RUN 21

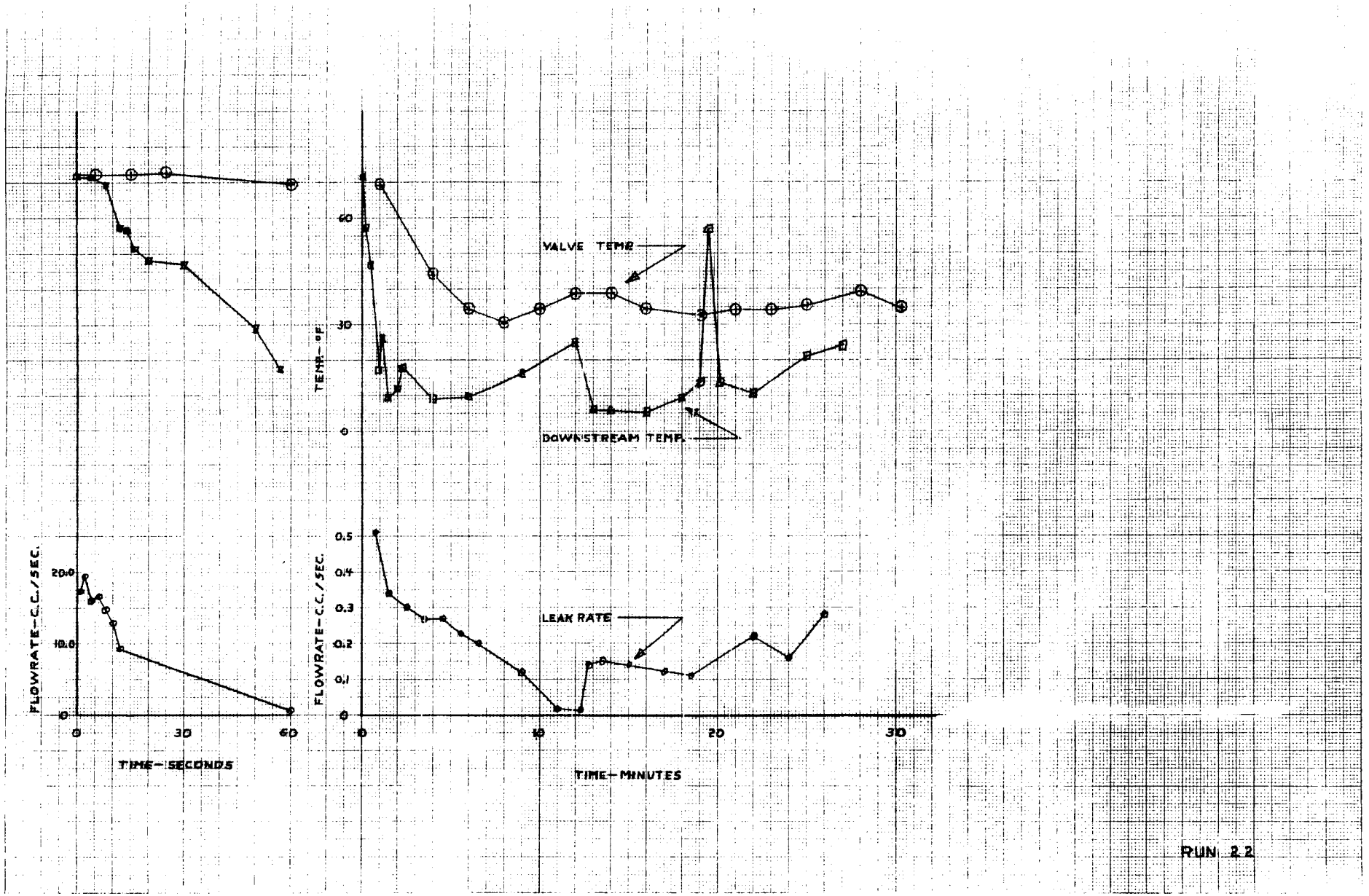
FLOWRATE - C.C./SEC.
20.0
10.0
0
0
30
60
TIME - SECONDS
TEMP. - °F.
60
30
0
VALVE TEMP.
DOWNSTREAM TEMP.
FLOWRATE - C.C./SEC.
0.5
0.4
0.3
0.2
0.1
0
LEAK RATE
0
10
20
30
TIME - MINUTES

RUN 22

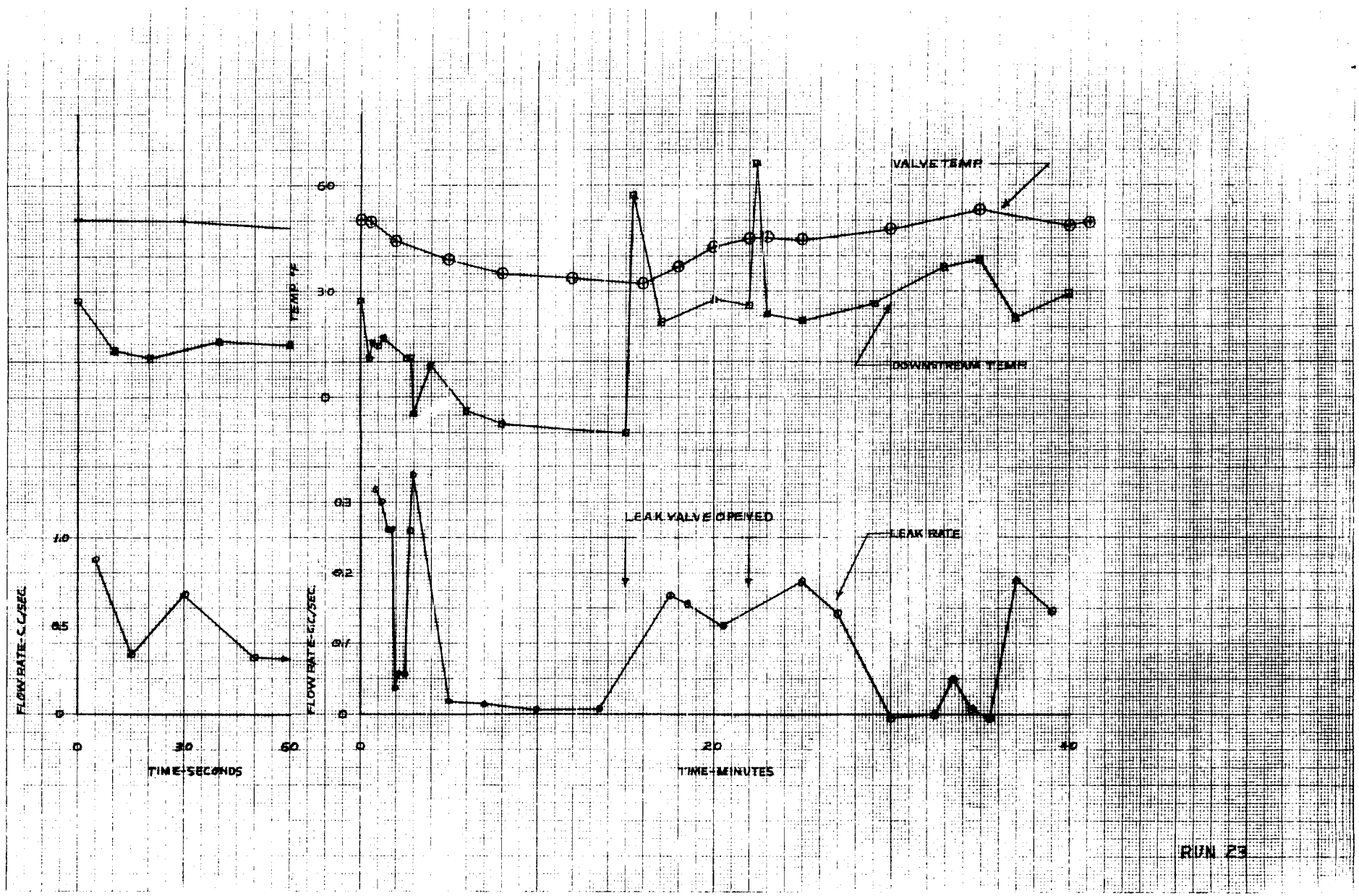
VALVE TEMP
DOWNSTREAM TEMP
TEMP °F
60
30
0
LEAK VALVE OPENED
LEAK RATE
FLOW RATE-C.C./SEC.
1.0
0.5
0
0.3
0.2
0.1
0
FLOW RATE-C.C./SEC.
0
30
60
TIME-SECONDS
0
20
40
TIME-MINUTES
RUN 23

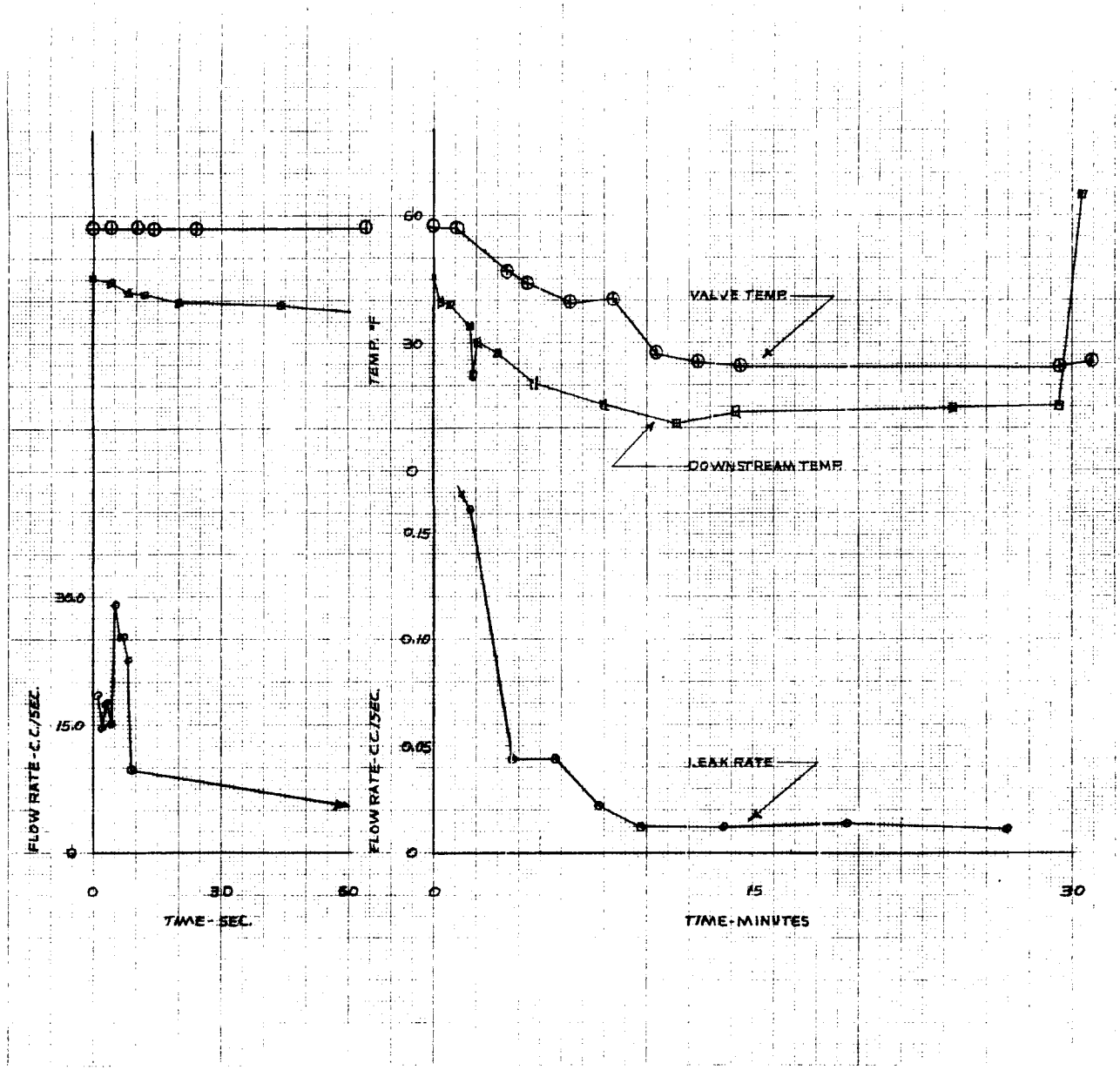
60
30
0
TEMP. °F
VALVE TEMP.
DOWNSTREAM TEMP.
0.15
0.10
0.05
0
LEAK RATE
FLOW RATE - C.C./SEC.
30.0
15.0
0
0
30
60
TIME - SEC.
0
15
30
TIME - MINUTES

RUN 24

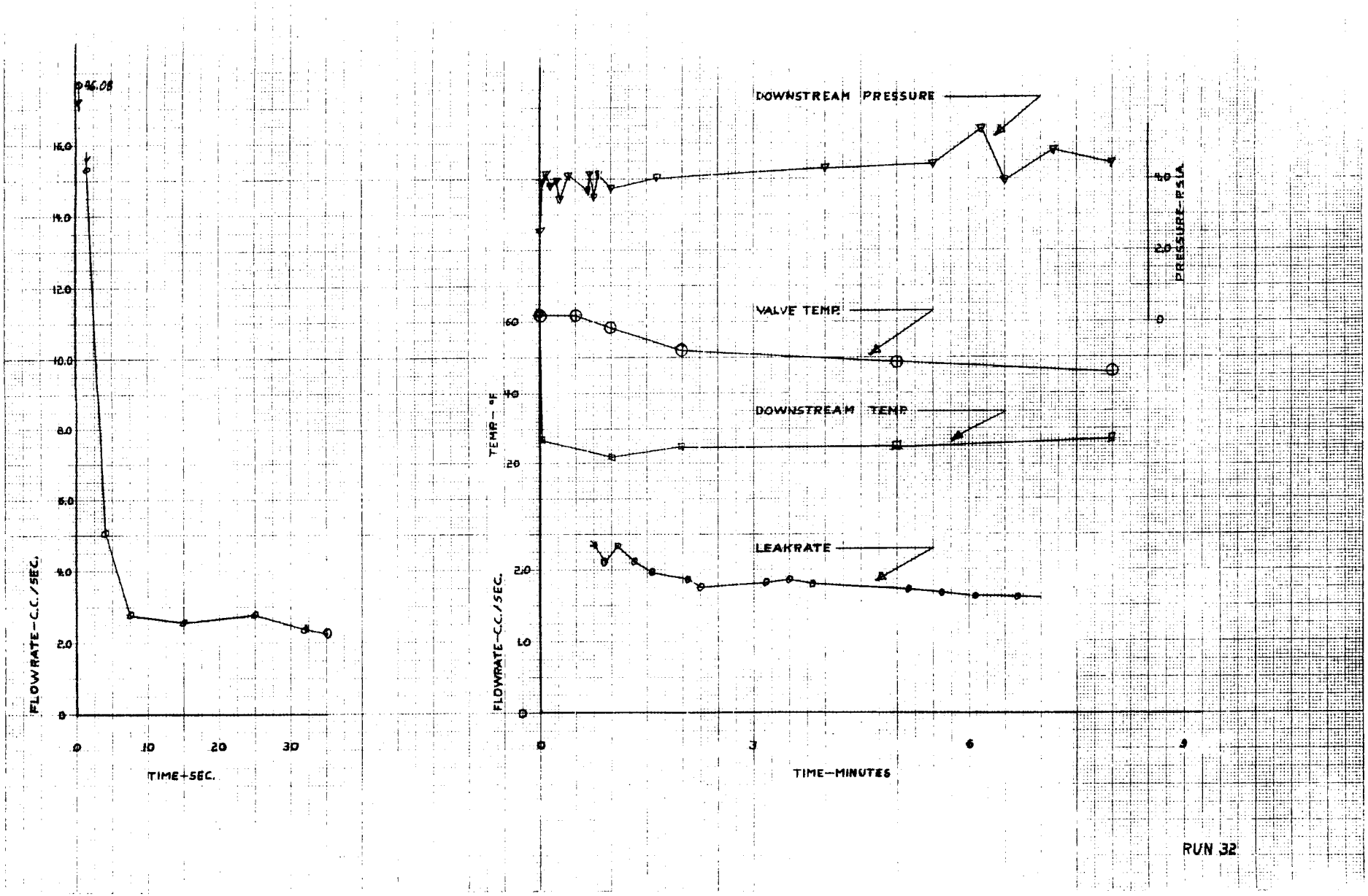
46.08
16.0
14.0
12.0
10.0
8.0
6.0
4.0
2.0
0
FLOWRATE-C.C./SEC.
0
10
20
30
TIME-SEC.
DOWNSTREAM PRESSURE
VALVE TEMP
DOWNSTREAM TEMP
LEAKRATE
TEMP - °F
60
40
20
2.0
1.0
0
FLOWRATE-C.C./SEC.
3
6
9
TIME-MINUTES
4.0
2.0
0
PRESSURE-PSIA
RUN 32

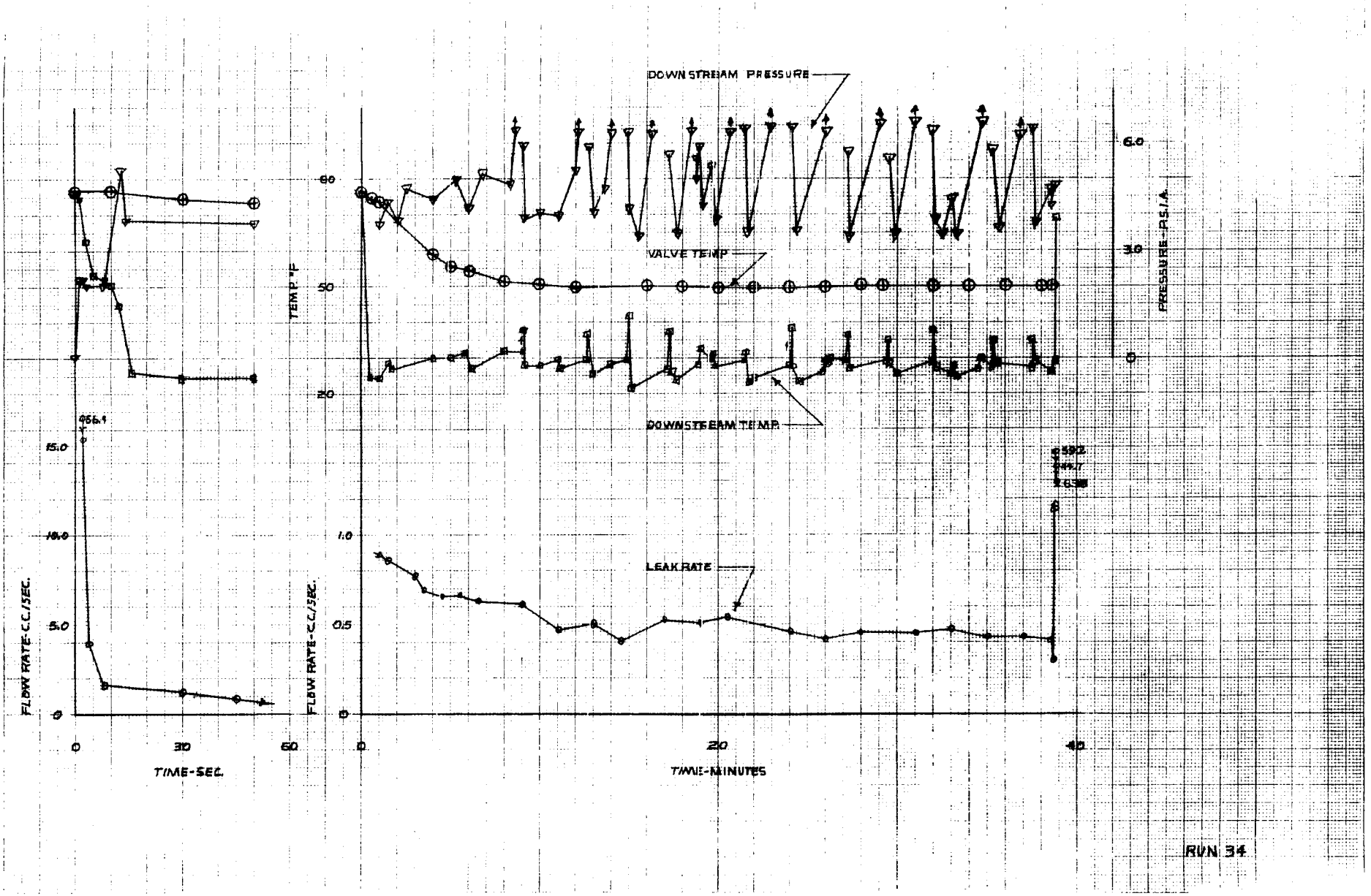
DOWNSTREAM PRESSURE
VALVE TEMP
DOWNSTREAM TEMP
LEAK RATE
TEMP °F
PRESSURE-P.S.I.A.
FLOW RATE-C.C./SEC.
TIME-SEC.
TIME-MINUTES
RUN 34

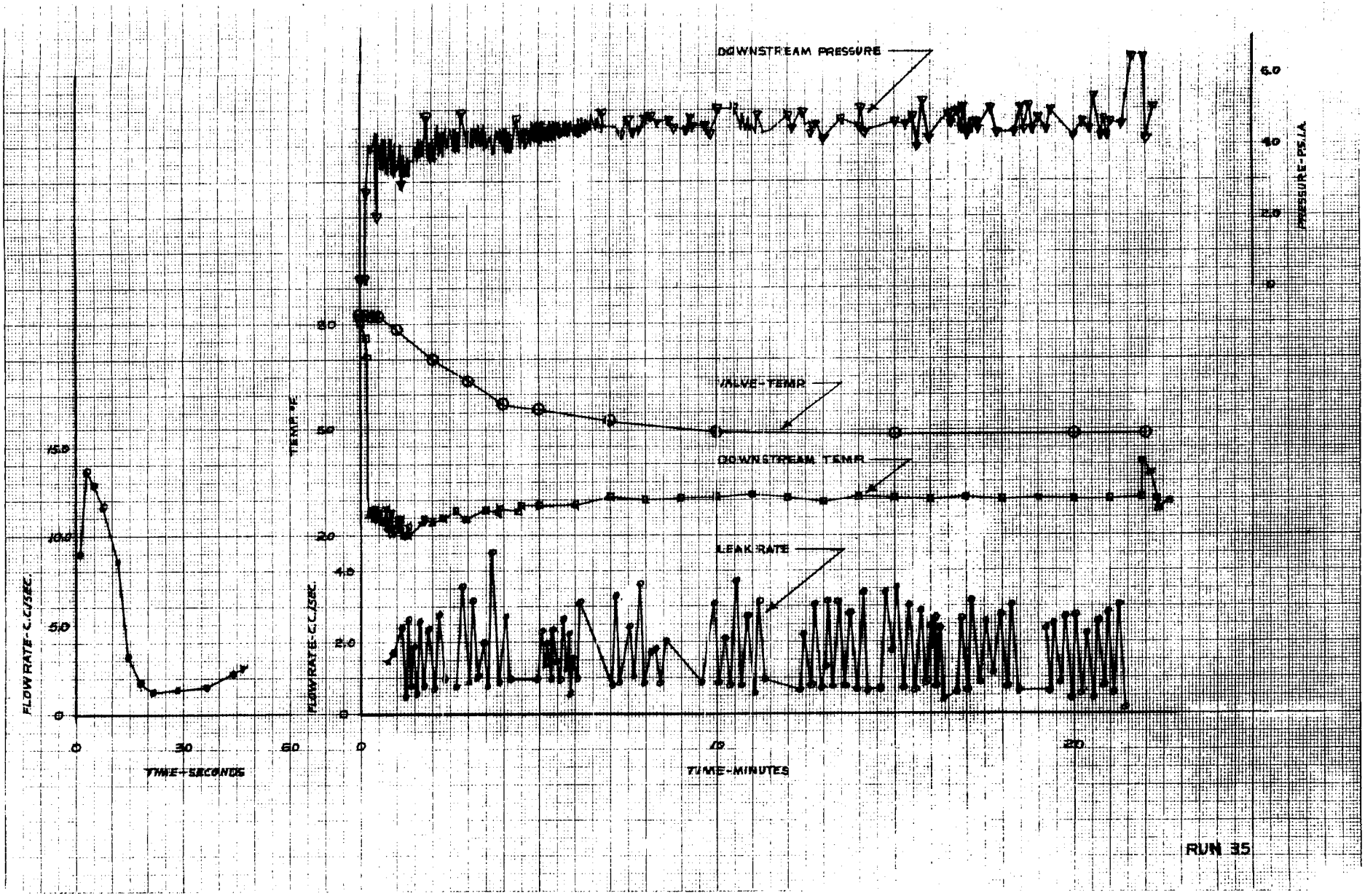
DOWNSTREAM PRESSURE
VALVE-TEMP
DOWNSTREAM TEMP
LEAK RATE
FLOW RATE-C.C./SEC.
TEMP °F
PERM RATE-C.C./SEC.
PRESSURE-PSI.A.
TIME-SECONDS
TIME-MINUTES
RUN 35

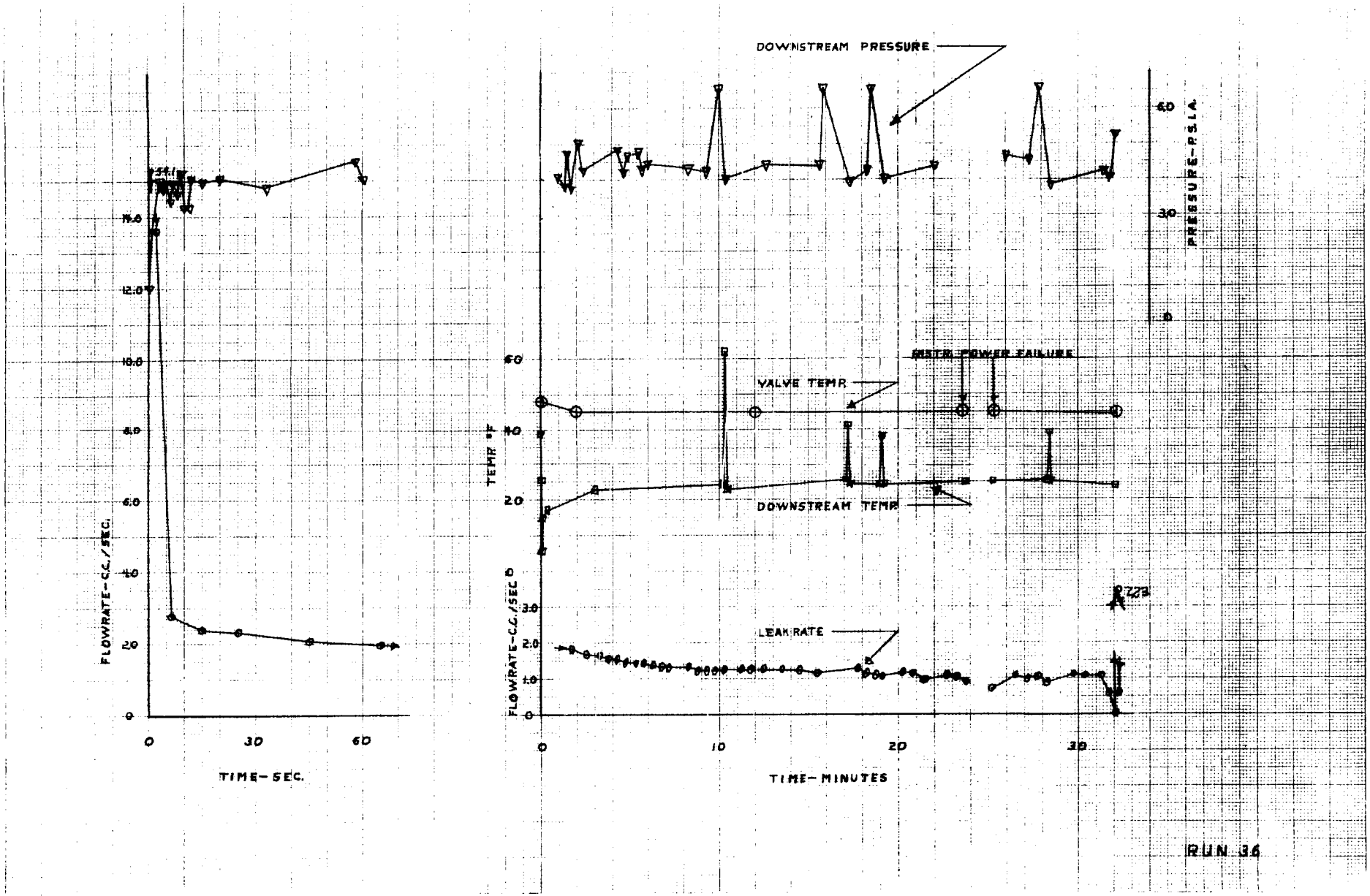
DOWNSTREAM PRESSURE
PRESSURE-P.S.I.A.
60
30
0
MASTER POWER FAILURE
VALVE TEMP
DOWNSTREAM TEMP
TEMP °F
60
40
20
A223
LEAK RATE
FLOWRATE-C.C./SEC.
3.0
2.0
1.0
0
0
10
20
30
TIME-MINUTES
FLOWRATE-C.C./SEC.
14.0
12.0
10.0
8.0
6.0
4.0
2.0
0
0
30
60
TIME-SEC.
RUN 36

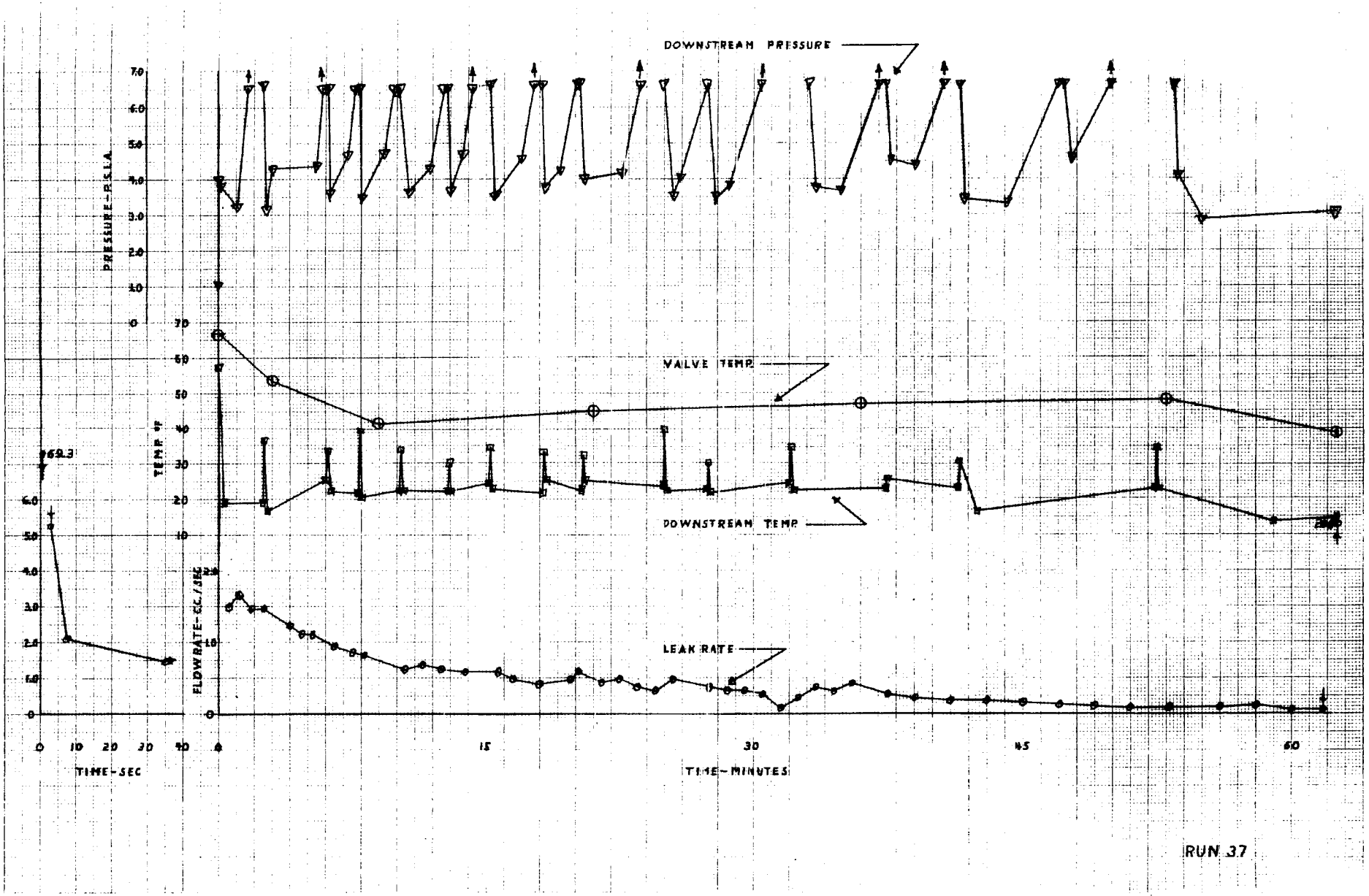
DOWNSTREAM PRESSURE
PRESSURE - P.S.I.A.
7.0
6.0
5.0
4.0
3.0
2.0
1.0
0
VALVE TEMP.
DOWNSTREAM TEMP.
TEMP °F
70
60
50
40
30
20
10
969.3
LEAK RATE
FLOW RATE - CC. / SEC
0 10 20 30 40
TIME - SEC
0 15 30 45 60
TIME - MINUTES
RUN 37

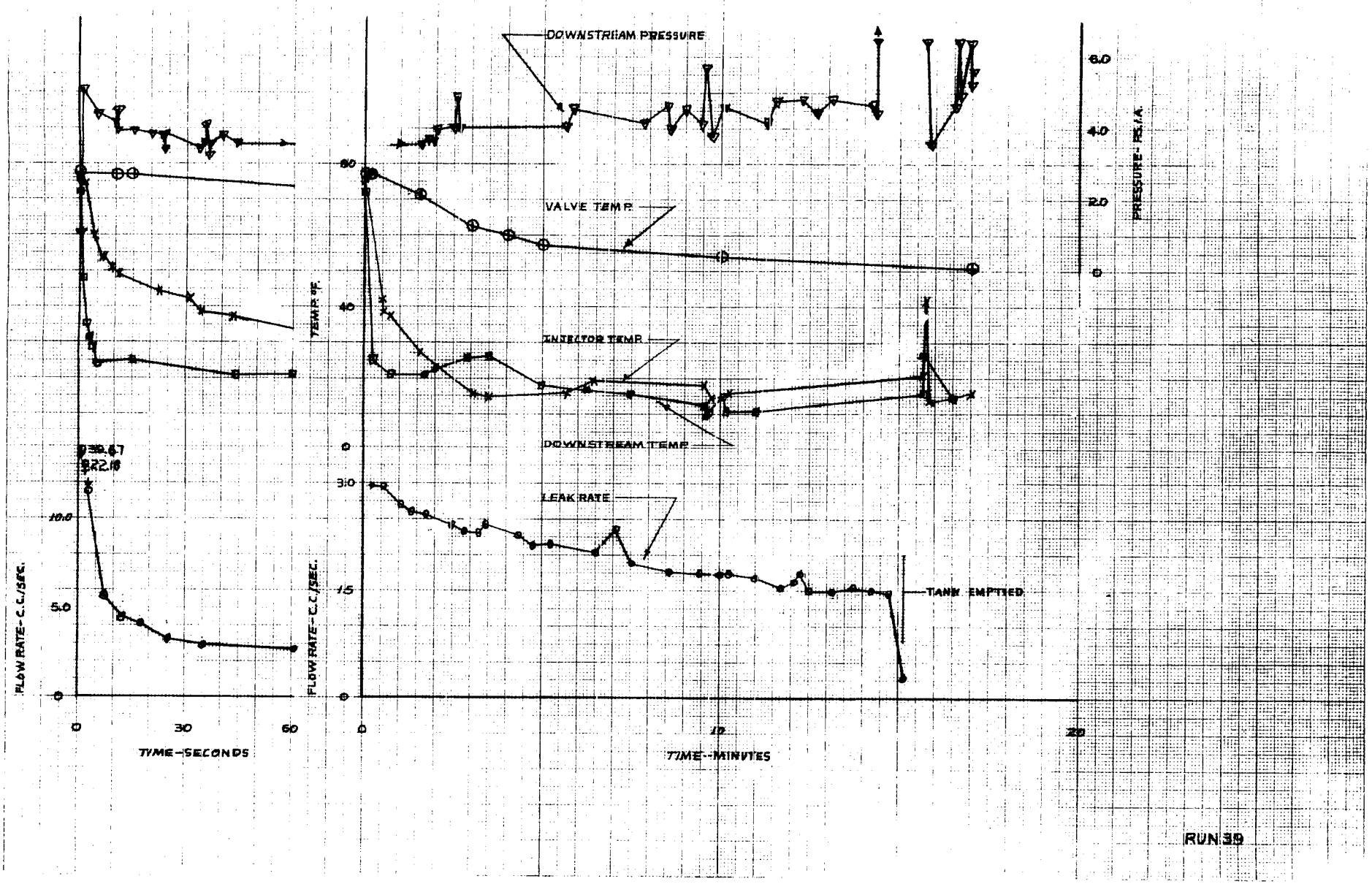
DOWNSTREAM PRESSURE
VALVE TEMP.
INJECTOR TEMP.
DOWNSTREAM TEMP.
LEAK RATE
TANK EMPTIED
TEMP °F.
PRESSURE - PS.I.A.
6.0
4.0
2.0
0
60
40
0
30
10
FLOW RATE - C.C./SEC.
10.0
5.0
0
30.67
22.18
0
30
60
TYME - SECONDS
0
10
20
TIME - MINUTES
RUN 39

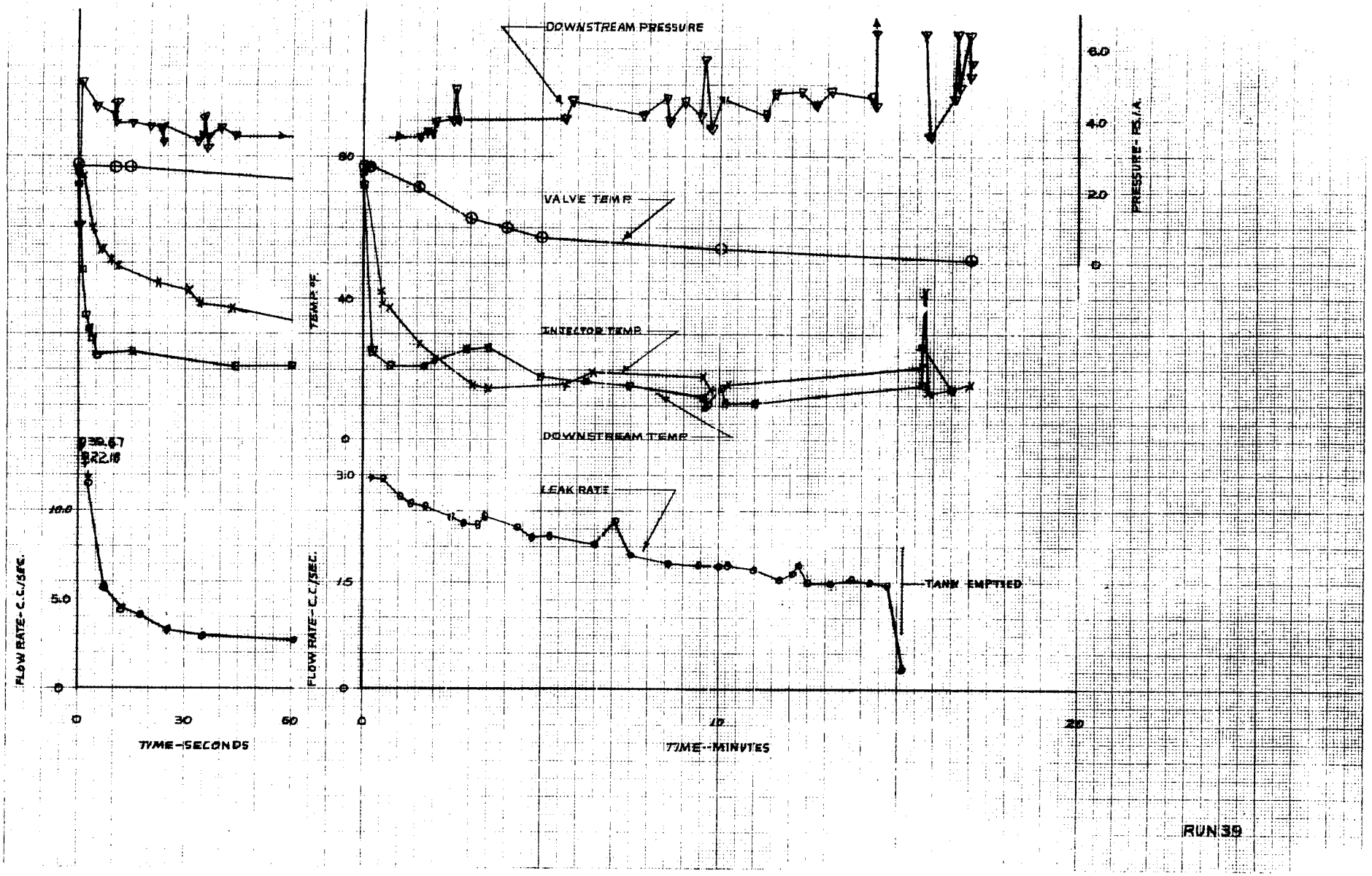
DOWNSTREAM PRESSURE
VALVE TEMP.
INJECTOR TEMP.
DOWNSTREAM TEMP.
LEAK RATE
TANK EMPTIED
FLOW RATE - C.C./SEC.
TEMP. °F.
PRESSURE - P.S.I.A.
TIME - SECONDS
TIME - MINUTES
RUN 39

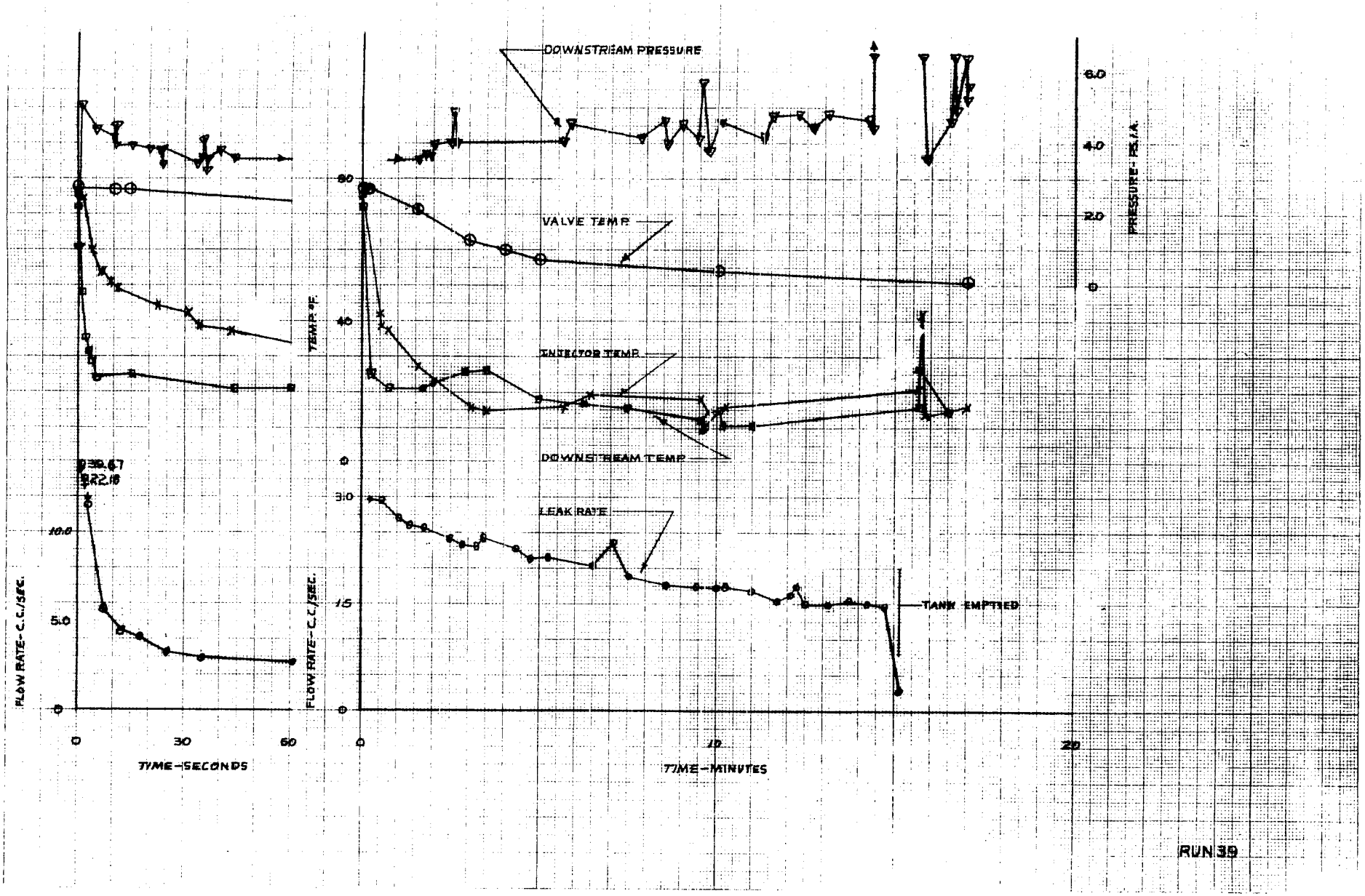
DOWNSTREAM PRESSURE
VALVE TEMP.
INJECTOR TEMP.
DOWNSTREAM TEMP.
LEAK RATE
TANK EMPTIED
TEMP °F.
PRESSURE - P.S.I.A.
FLOW RATE - C.C./SEC.
TIME - SECONDS
TIME - MINUTES
RUN 39

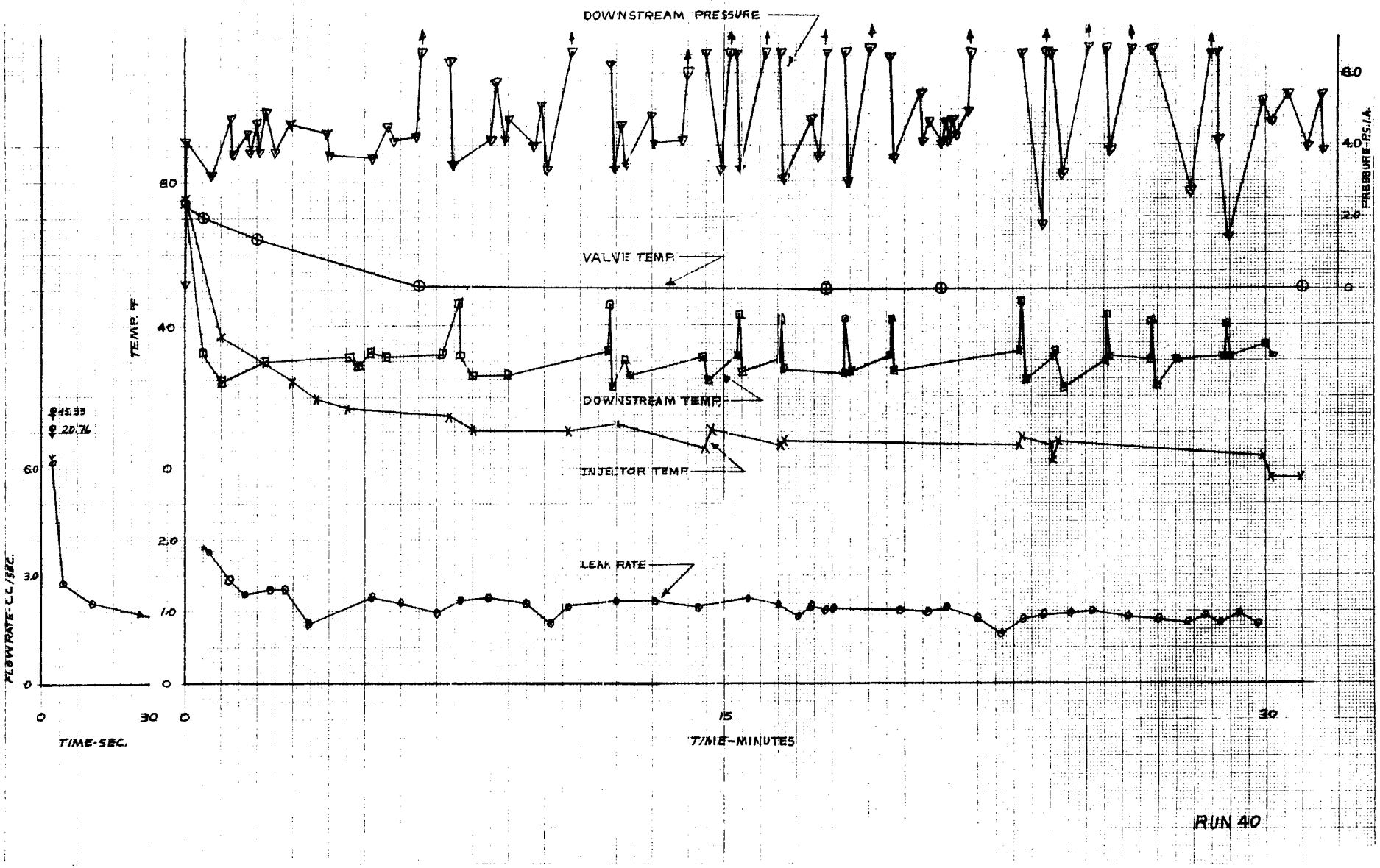
DOWNSTREAM PRESSURE
VALVE TEMP
DOWNSTREAM TEMP
INJECTOR TEMP
LEAK RATE
TEMP. °F
PRESSURE-P.S.I.A.
FLOW RATE-C.C./SEC.
TIME-SEC.
TIME-MINUTES
RUN 40

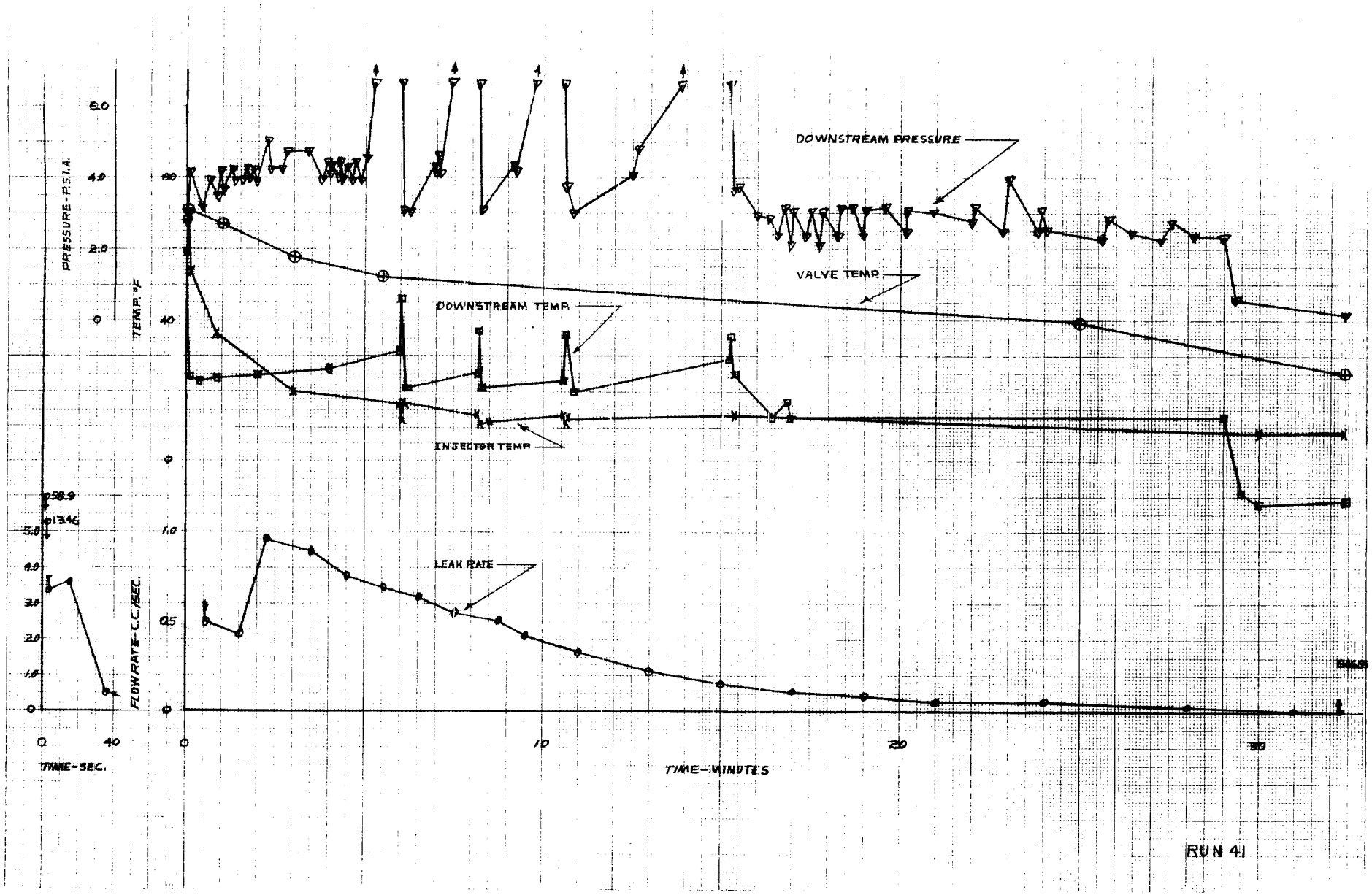
PRESSURE - P.S.I.A.
6.0
4.0
2.0
0
TEMP. °F
80
40
0
DOWNSTREAM PRESSURE
VALVE TEMP.
DOWNSTREAM TEMP.
INJECTOR TEMP.
LEAK RATE
FLOW RATE - C.C./SEC.
5.0
4.0
3.0
2.0
1.0
0
1.0
0.5
0
0
40
TIME - SEC.
0
10
20
30
TIME - MINUTES
RUN 41

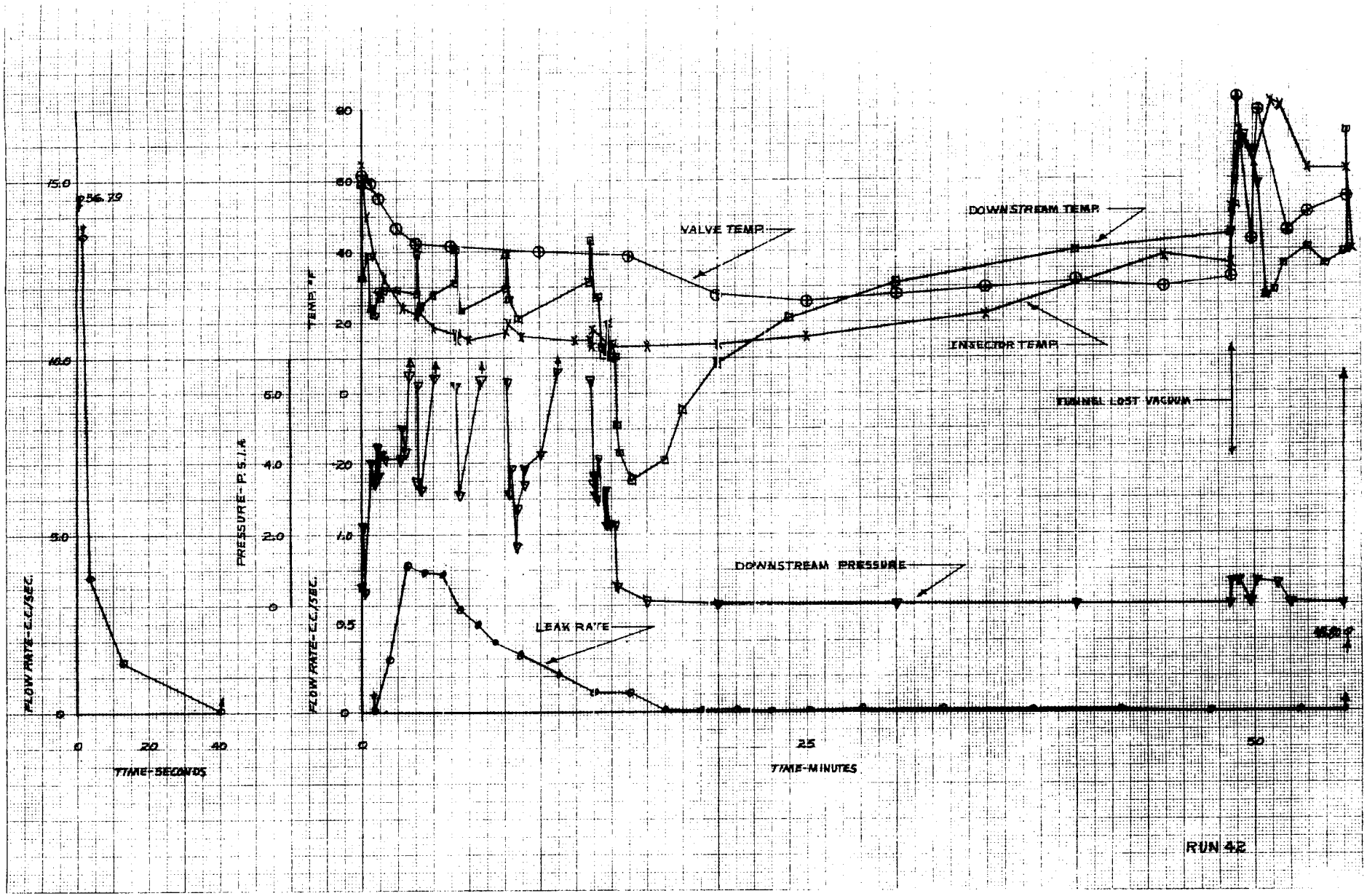
15.0
10.0
5.0
0
FLOW RATE-C.C./SEC.
0
20
40
TIME-SECONDS
PRESSURE-P.S.I.A.
6.0
4.0
2.0
0
TEMP °F
80
60
40
20
0
-20
1.0
0.5
0
FLOW RATE-C.C./SEC.
0
25
50
TIME-MINUTES
VALVE TEMP
DOWNSTREAM TEMP
INJECTOR TEMP
FUNNEL LOST VACUUM
DOWNSTREAM PRESSURE
LEAK RATE
RUN 42

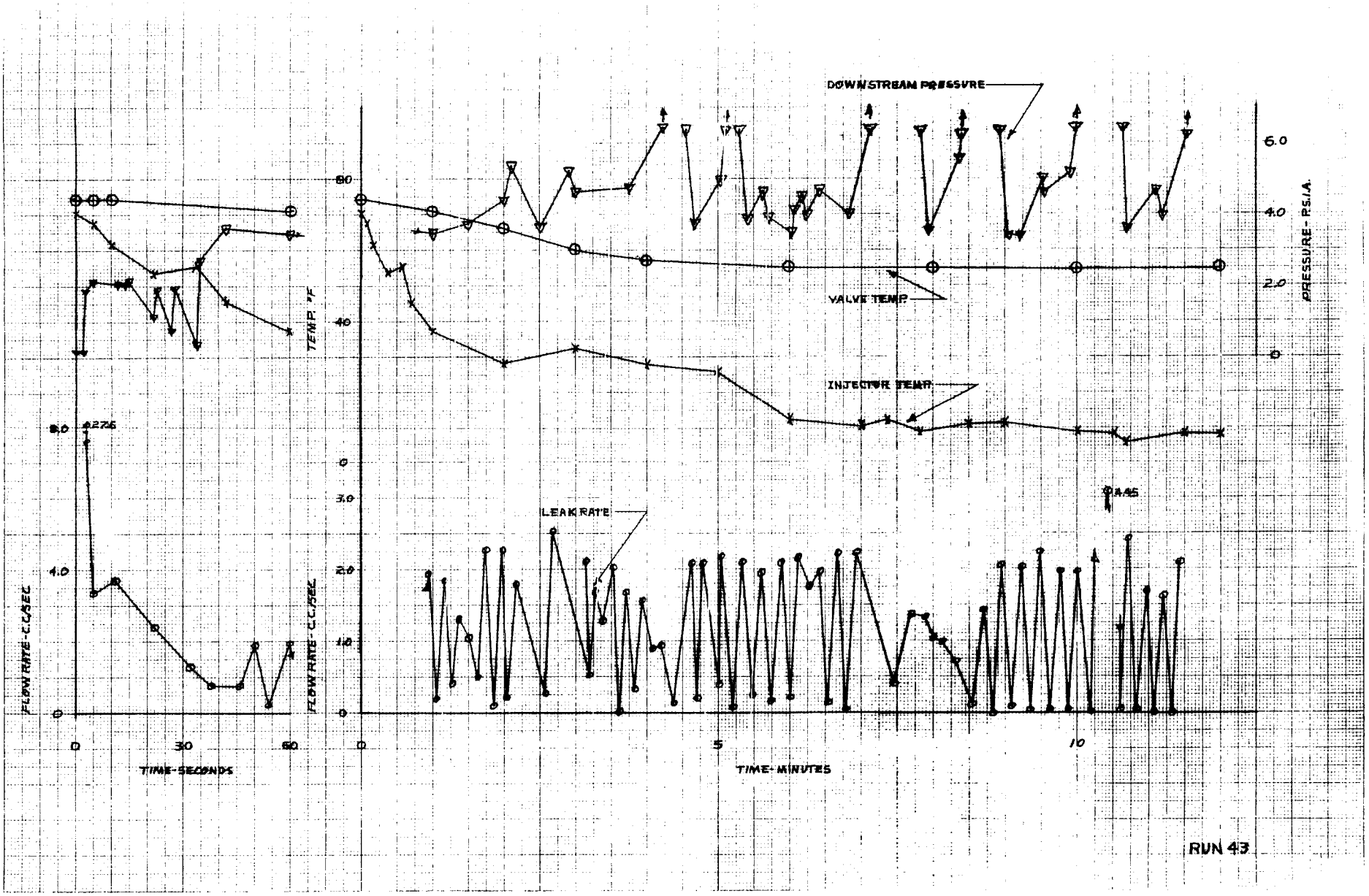
DOWNSTREAM PRESSURE
VALVE TEMP
INJECTOR TEMP
LEAK RATE
.2726
.445
TEMP °F
PRESSURE - P.S.I.A.
FLOW RATE - C.C./SEC
FLOW RATE - C.C./SEC
TIME - SECONDS
TIME - MINUTES
RUN 43

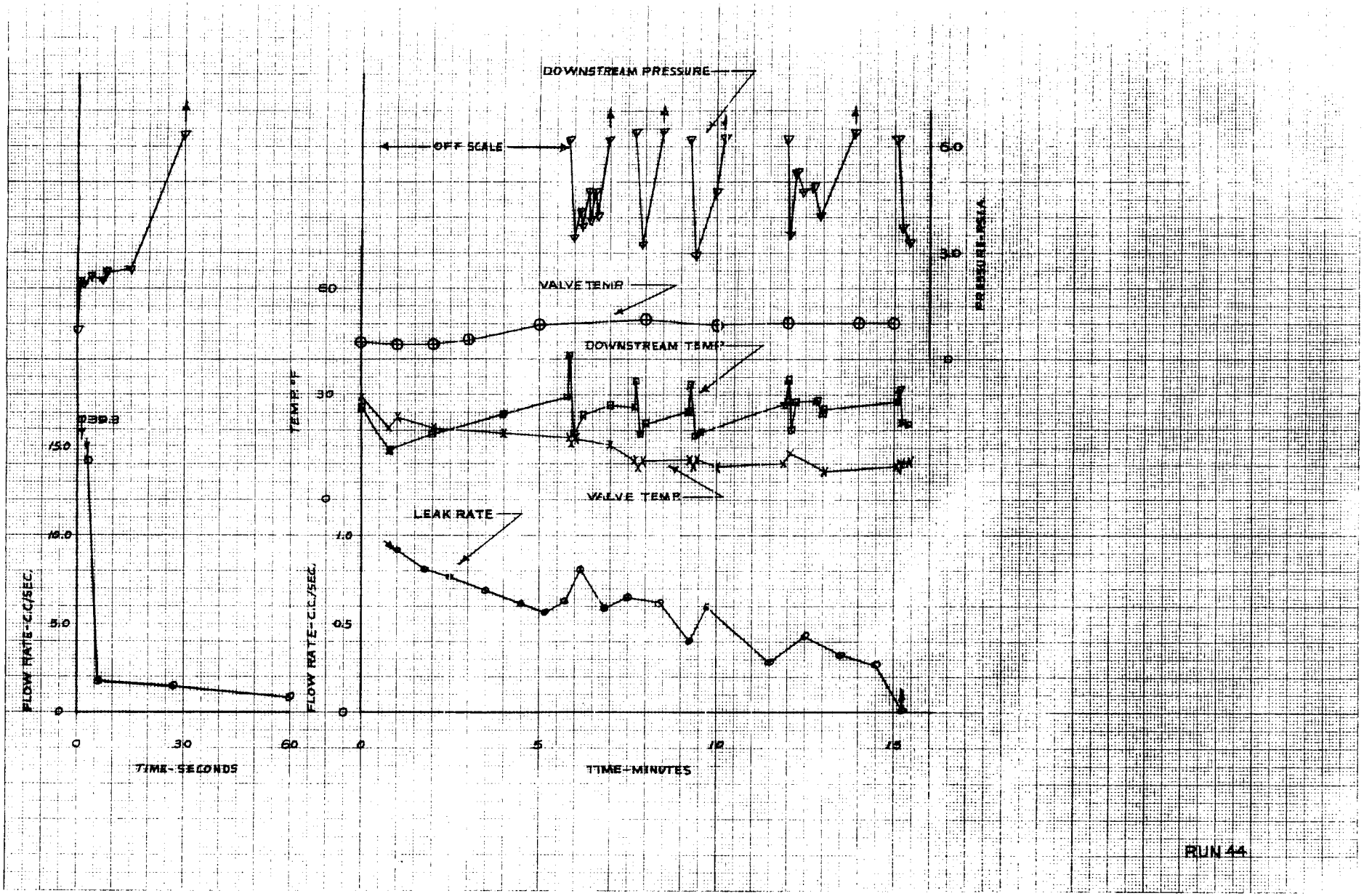
DOWNSTREAM PRESSURE
OFF SCALE
6.0
3.0
0
PRESSURE-PSIA
VALVE TEMP
60
30
0
TEMP °F
DOWNSTREAM TEMP
VALVE TEMP
LEAK RATE
1.0
0.5
0
FLOW RATE-C.C./SEC.
239.2
15.0
10.0
5.0
0
FLOW RATE-C.C./SEC.
0
30
60
TIME-SECONDS
0
5
10
15
TIME-MINUTES
RUN 44

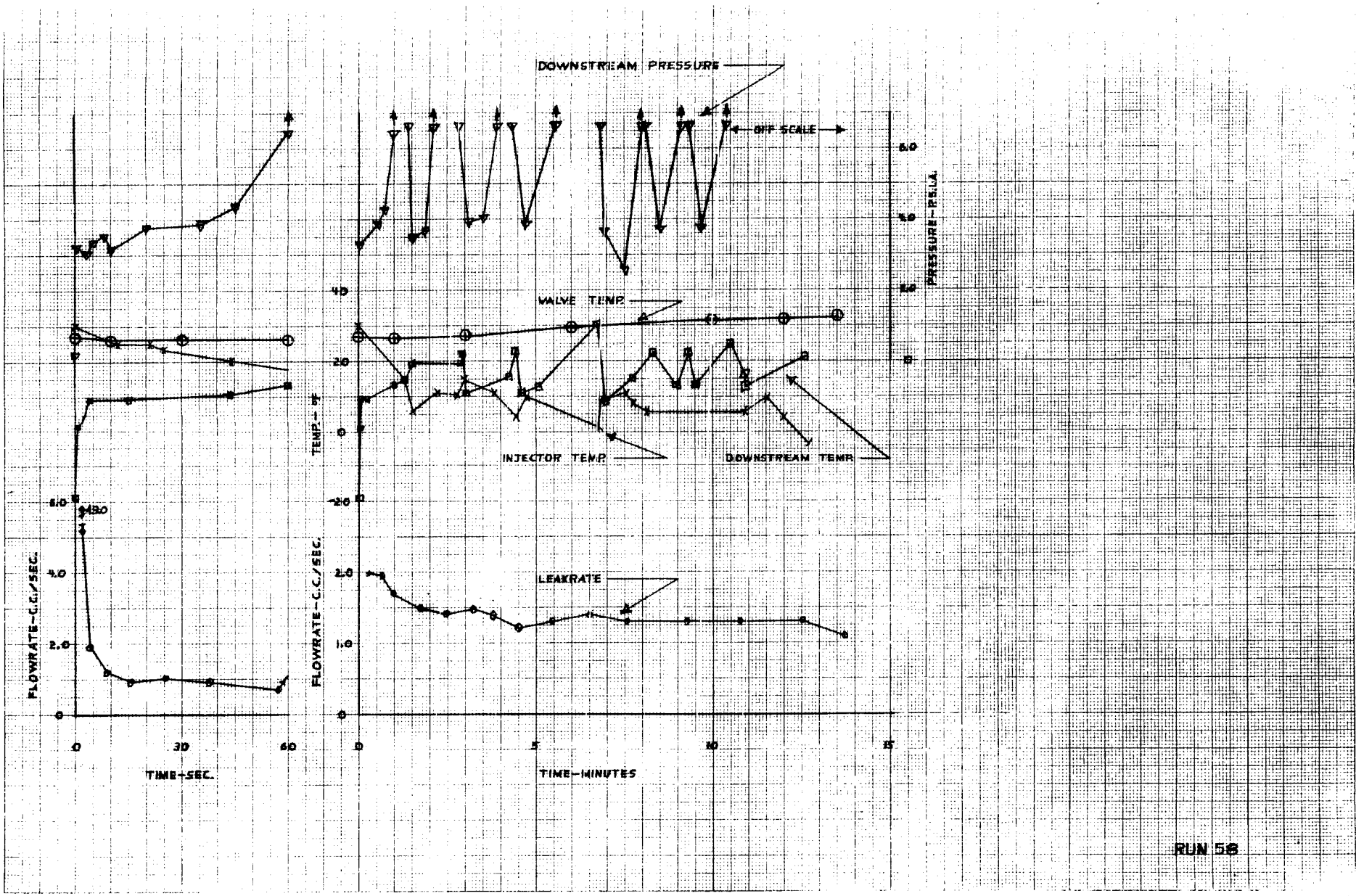
DOWNSTREAM PRESSURE
OFF SCALE
VALVE TEMP.
INJECTOR TEMP.
DOWNSTREAM TEMP.
LEAKRATE
PRESSURE-P.S.I.A.
TEMP.-°F
FLOWRATE-C.C./SEC.
TIME-SEC.
TIME-MINUTES
$49.0
RUN 58

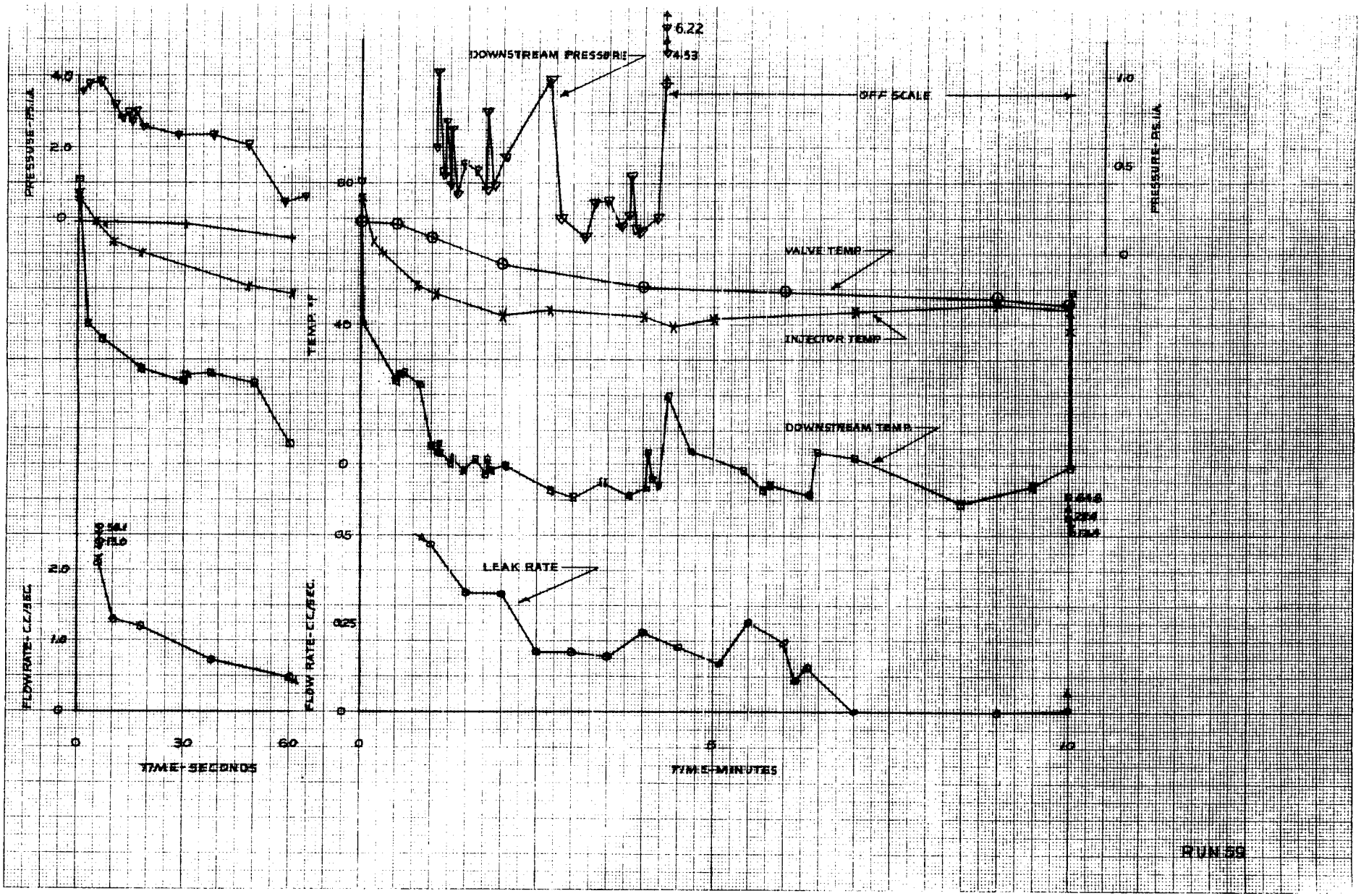
PRESSURE-PSIA
4.0
2.0
0
TEMP.°F
80
40
0
FLOW RATE-C.C./SEC.
2.0
1.0
0
30
60
TIME-SECONDS
6.22
4.53
DOWNSTREAM PRESSURE
OFF SCALE
1.0
.5
0
PRESSURE-PSIA
VALVE TEMP
INJECTOR TEMP
DOWNSTREAM TEMP
.95
.925
LEAK RATE
0
5
10
TIME-MINUTES
RUN 59

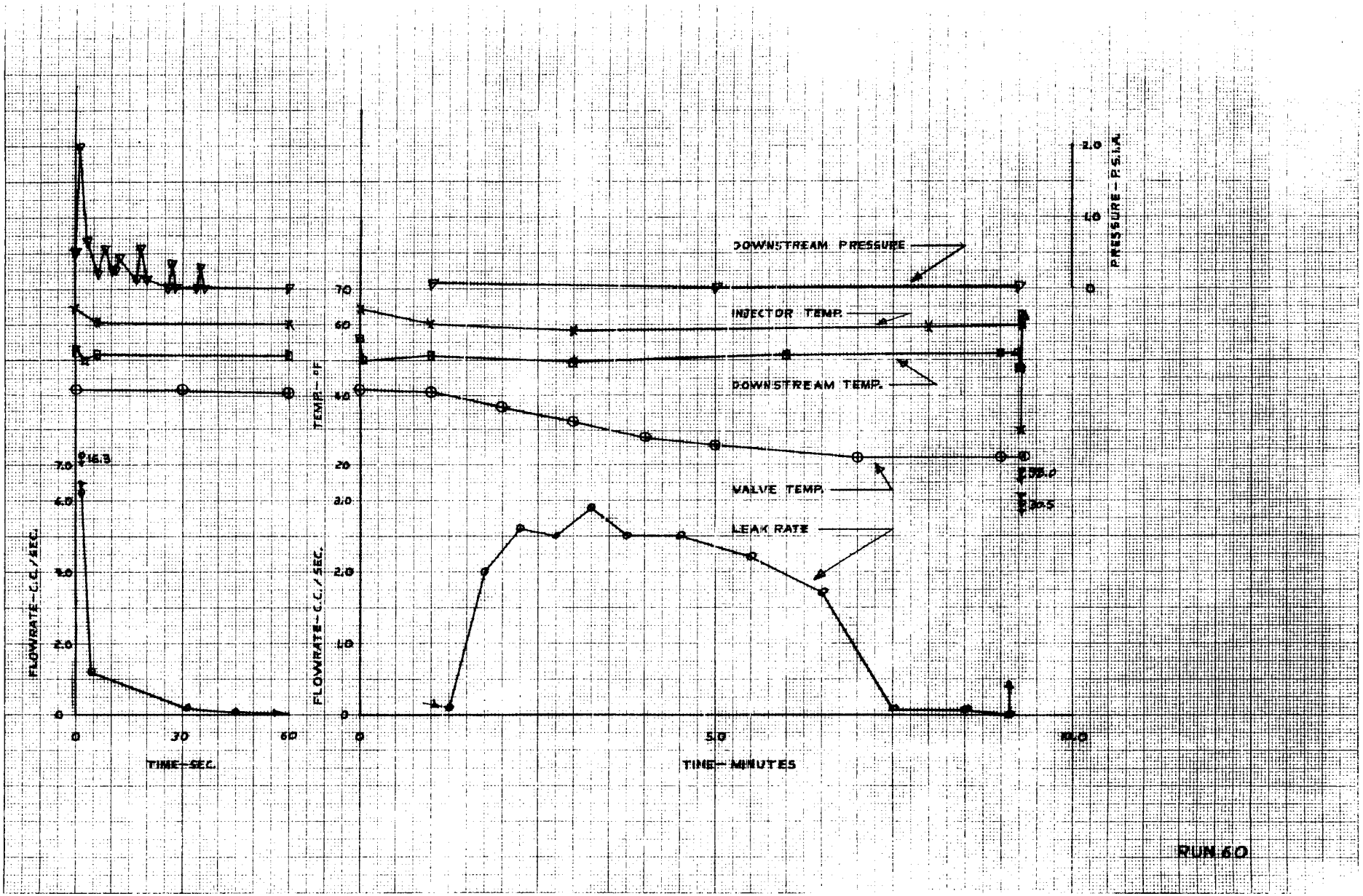
FLOWRATE-C.C./SEC.
TIME-SEC.
0
30
60
7.0
6.0
5.0
4.0
3.0
2.0
1.0
0
16.3
TEMP.-°F
70
60
50
40
30
20
10
0
FLOWRATE-C.C./SEC.
TIME-MINUTES
5.0
10.0
DOWNSTREAM PRESSURE
INJECTOR TEMP.
DOWNSTREAM TEMP.
VALVE TEMP.
LEAK RATE
PRESSURE-P.S.I.A.
2.0
1.0
0
58.0
30.5
RUN 60

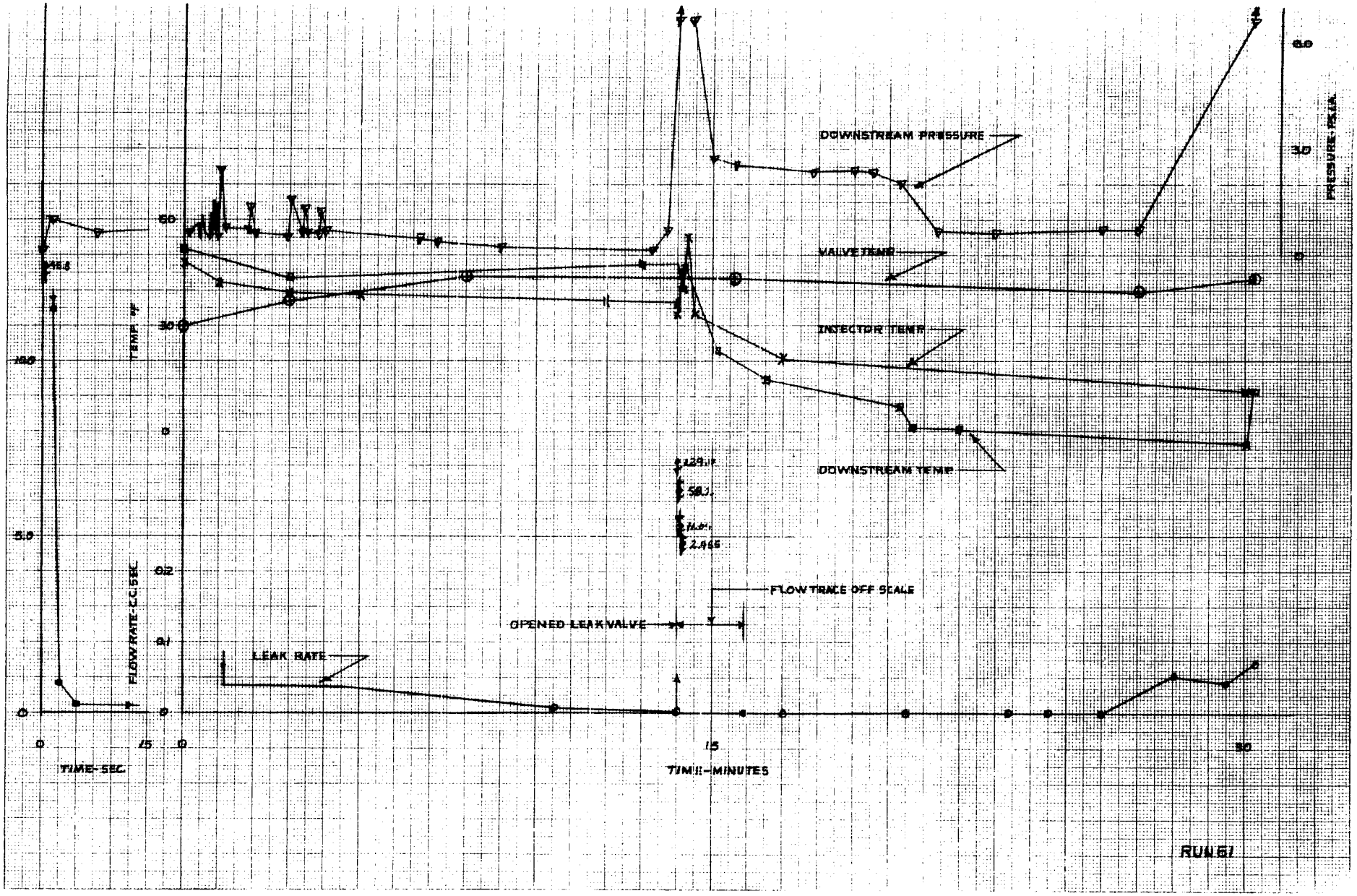
DOWNSTREAM PRESSURE
VALVE TEMP
INJECTOR TEMP
DOWNSTREAM TEMP
FLOW TRACE OFF SCALE
OPENED LEAK VALVE
LEAK RATE
TEMP °F
FLOW RATE-CC/SEC
PRESSURE-PS.I.A.
TIME-SEC.
TIME-MINUTES
RUN 61

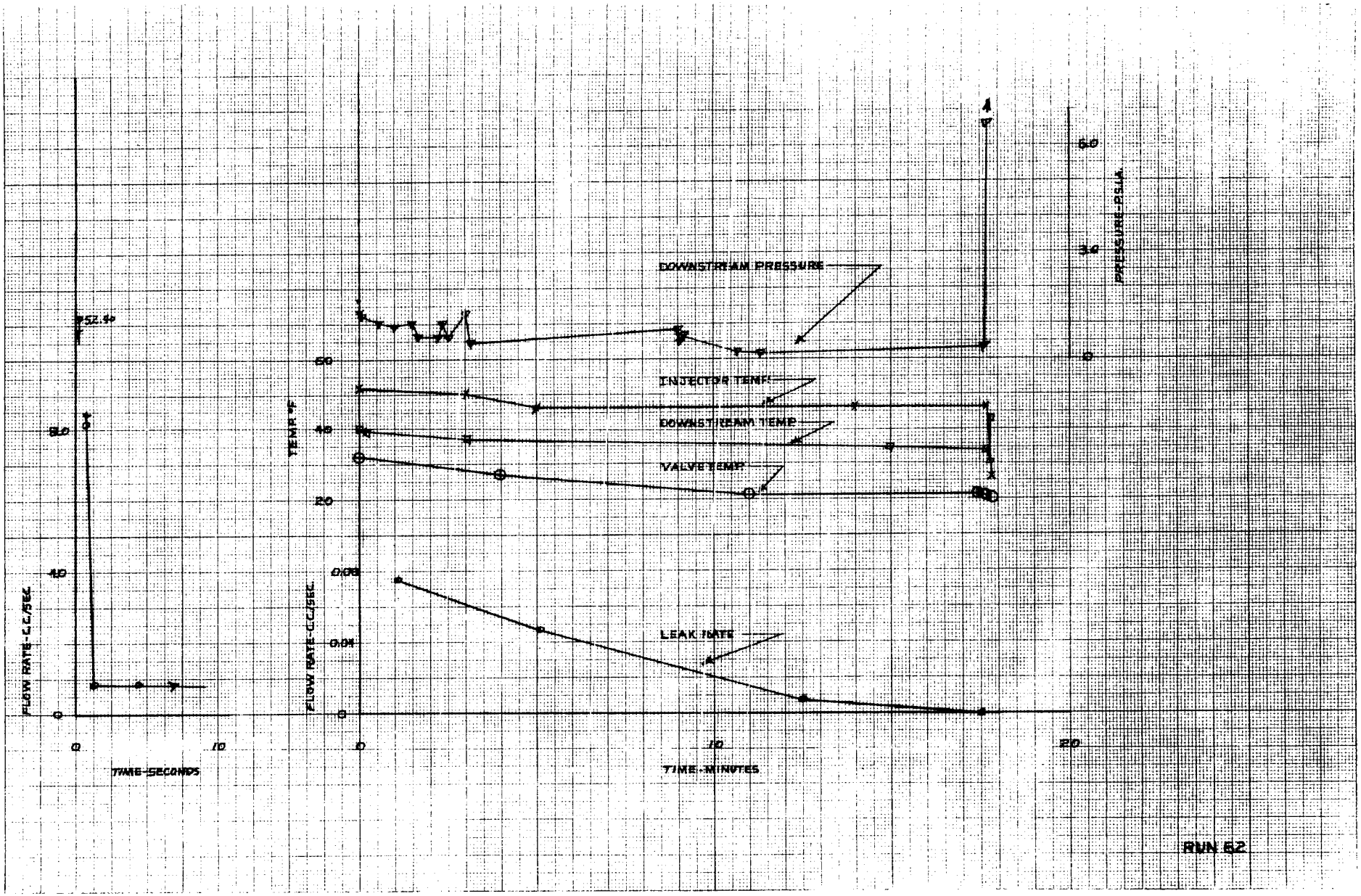
DOWNSTREAM PRESSURE
INJECTOR TEMP
DOWNSTREAM TEMP
VALVE TEMP
LEAK RATE
FLOW RATE-C.C./SEC.
TEMP °F
PRESSURE-PS.I.A.
TIME-SECONDS
TIME-MINUTES
RUN 62

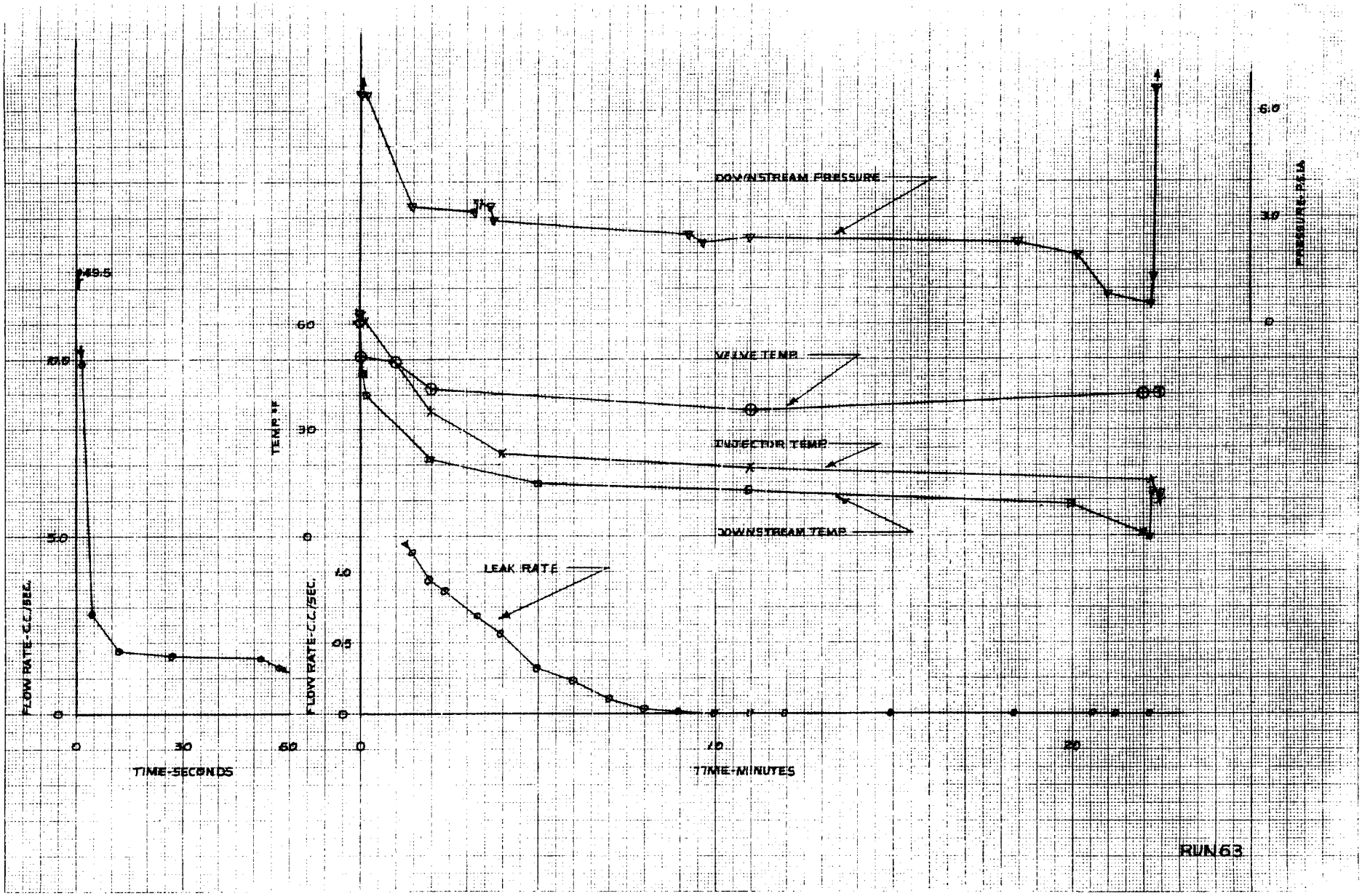
FLOW RATE-C.C./SEC.
49.5
33.0
5.0
0
0
30
60
TIME-SECONDS
TEMP °F
60
30
0
FLOW RATE-C.C./SEC.
1.0
0.5
0
0
10
20
TIME-MINUTES
DOWNSTREAM PRESSURE
VALVE TEMP
INJECTOR TEMP
DOWNSTREAM TEMP
LEAK RATE
6.0
3.0
0
PRESSURE-P.S.I.A
RUN 63

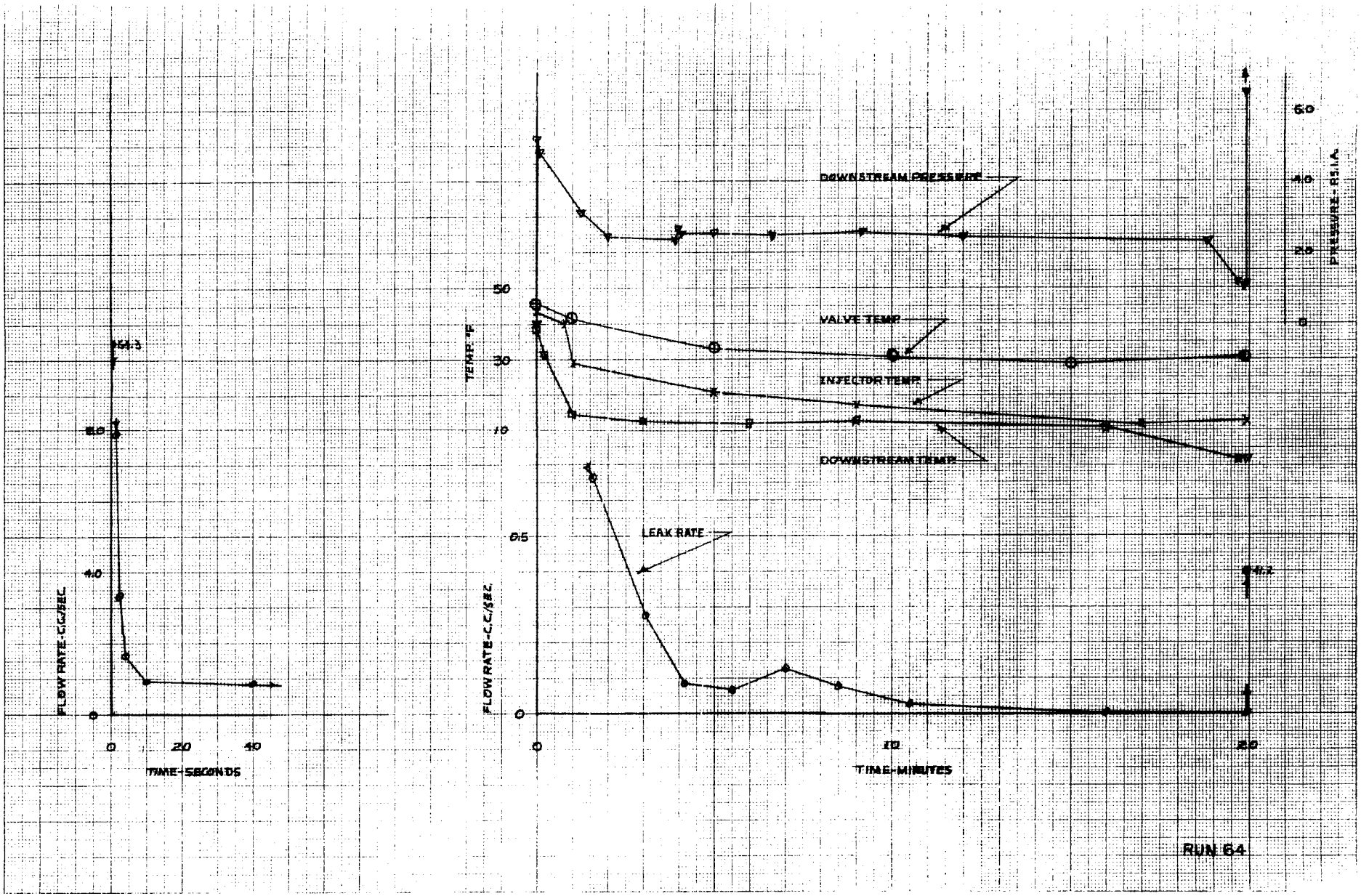
FLOW RATE-CC/SEC.
8.0
4.0
0
0
20
40
TIME-SECONDS
TEMP. °F
50
30
10
FLOW RATE-C.C./SEC.
0.5
0
0
10
20
TIME-MINUTES
DOWNSTREAM PRESSURE
VALVE TEMP.
INJECTOR TEMP.
DOWNSTREAM TEMP.
LEAK RATE
PRESSURE-P.S.I.A.
6.0
4.0
2.0
0
RUN 64

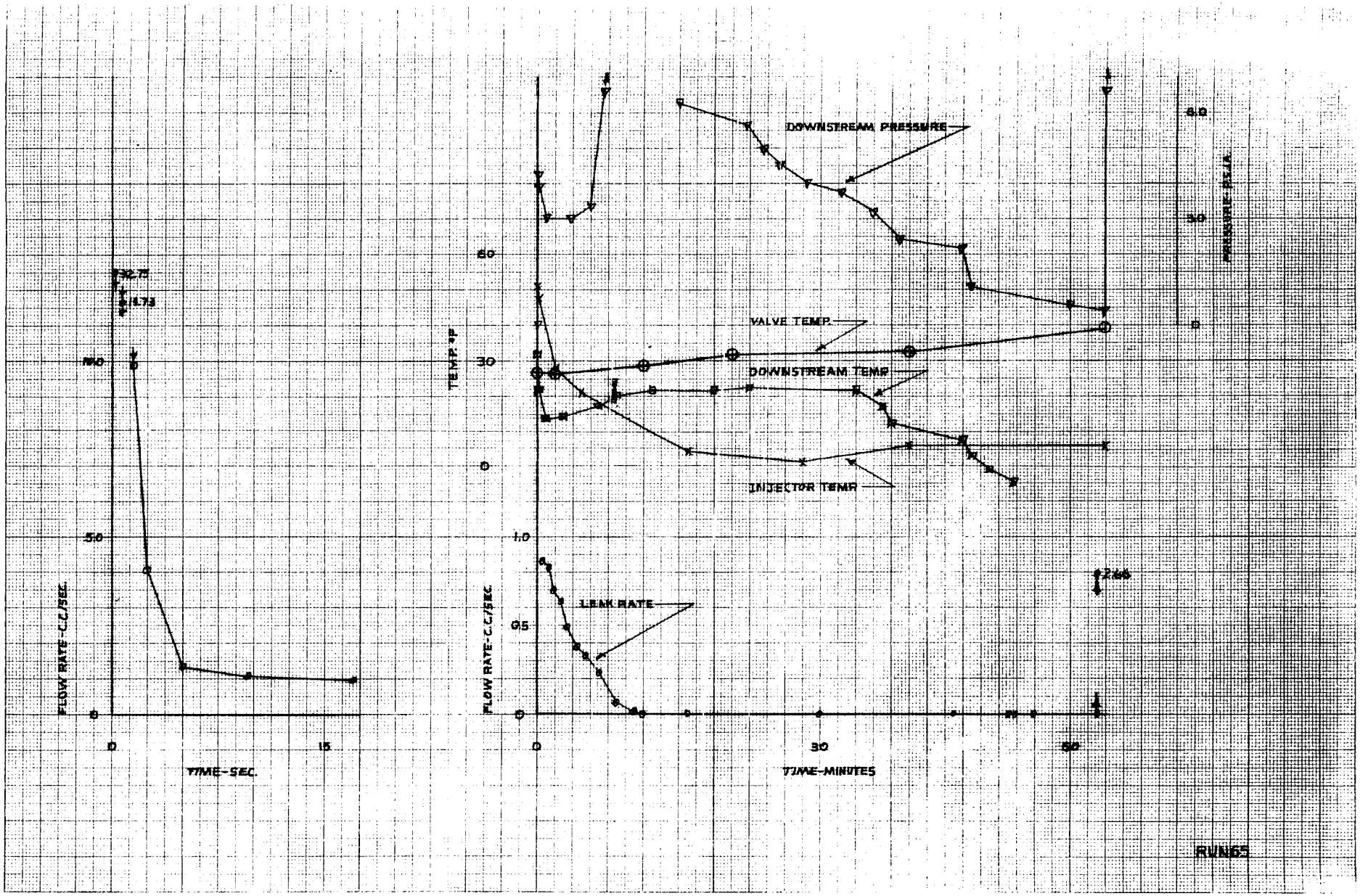
FLOW RATE-C.C./SEC.
1.0
.5
0
0
15
TIME-SEC.
32.7
4.73
TEMP. °F
60
30
0
1.0
.5
0
FLOW RATE-C.C./SEC.
LEAK RATE
DOWNSTREAM PRESSURE
VALVE TEMP.
DOWNSTREAM TEMP.
INJECTOR TEMP.
6.0
3.0
0
PRESSURE-P.S.I.A.
2.65
0
30
50
TIME-MINUTES
RUN 65

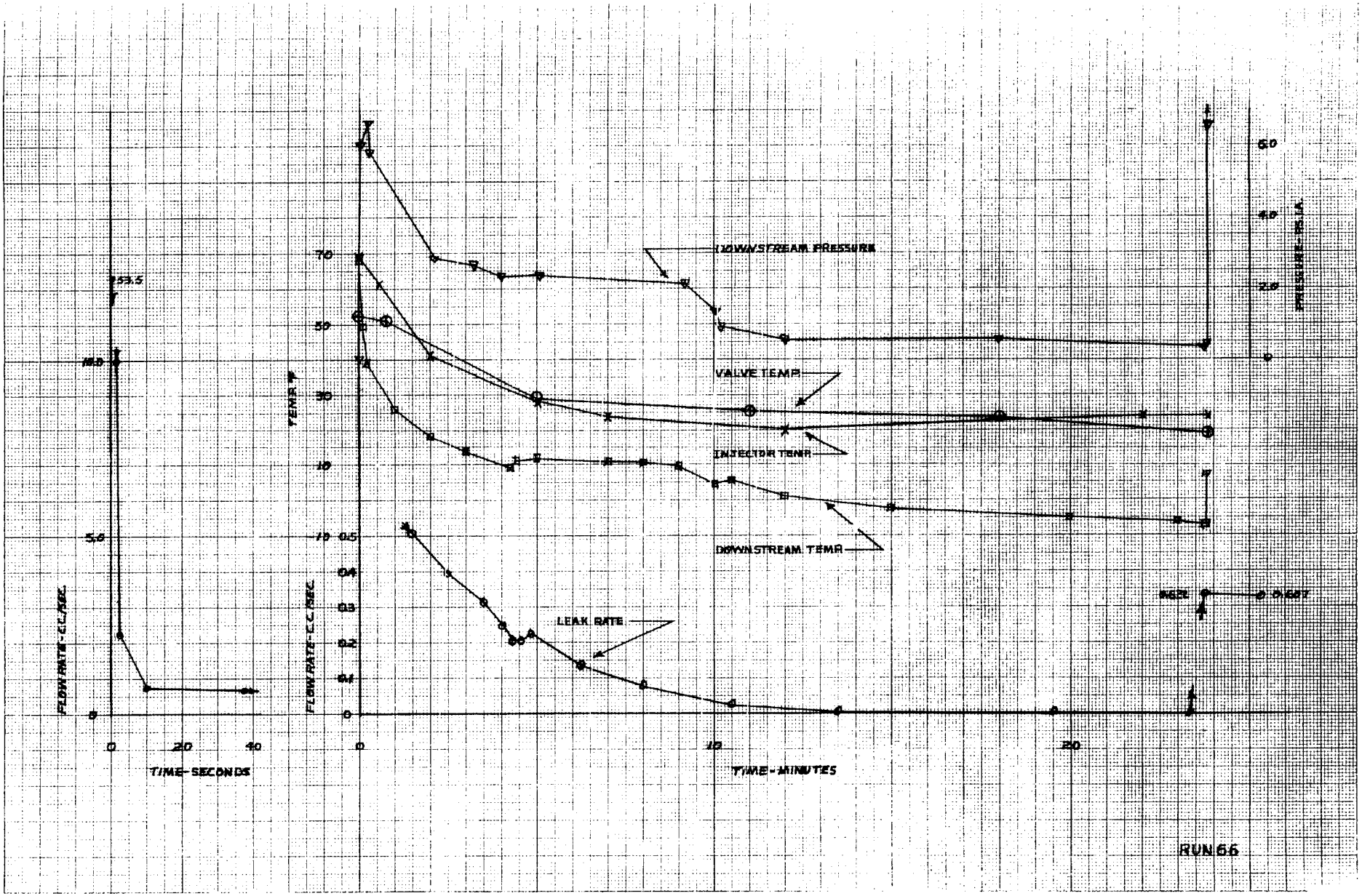
153.5
16.0
5.0
0
FLOW RATE - C.C./SEC.
0
20
40
TIME - SECONDS
70
50
30
10
TEMP.
0.5
0.4
0.3
0.2
0.1
0
FLOW RATE - C.C./SEC.
0
10
20
TIME - MINUTES
DOWNSTREAM PRESSURE
VALVE TEMP.
INJECTOR TEMP.
DOWN STREAM TEMP.
LEAK RATE
6.0
4.0
2.0
0
PRESSURE - P.S.I.
0.627
RUN 66

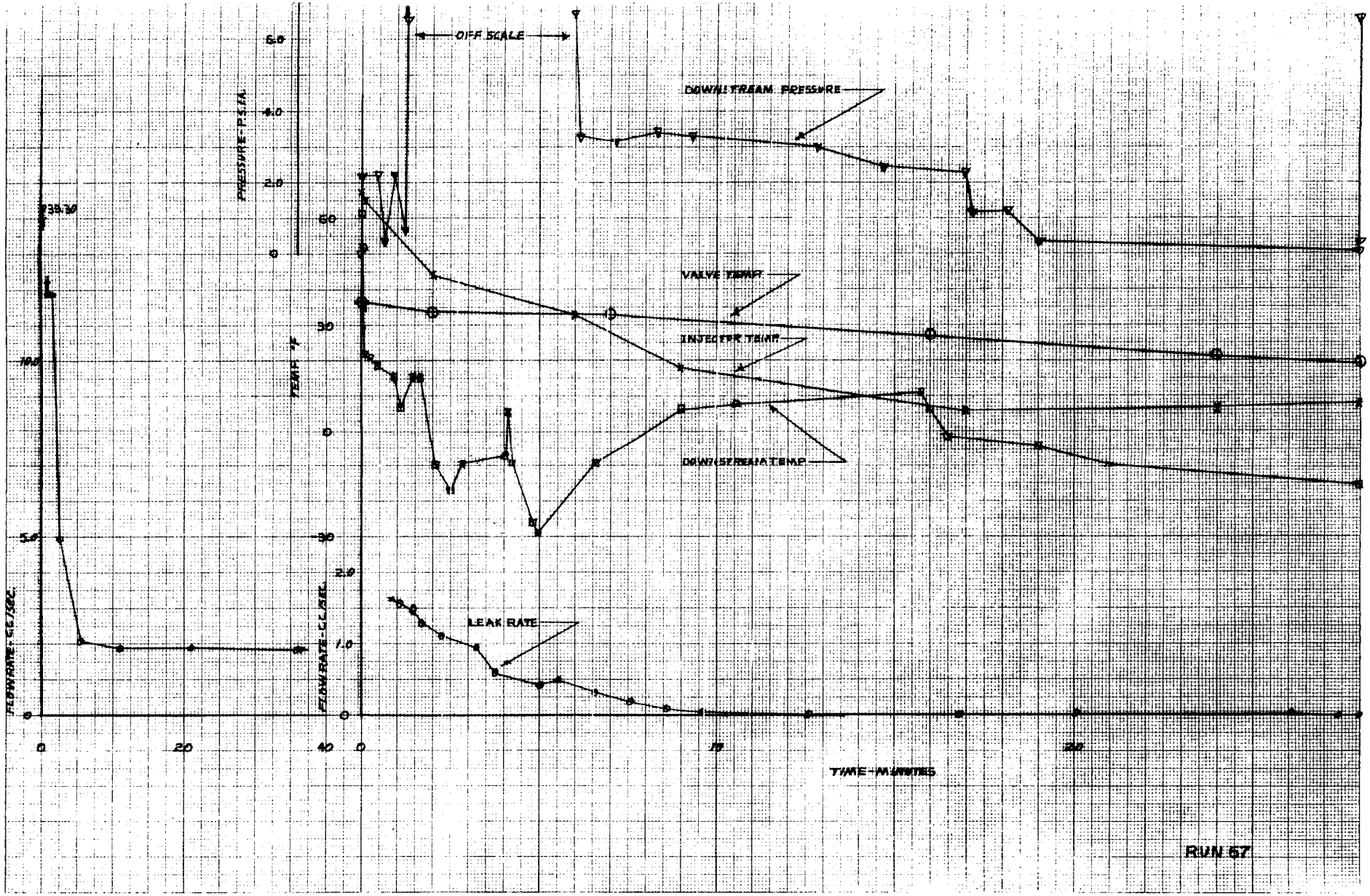
DIFF SCALE
DOWNSTREAM PRESSURE
VALVE TEMP
INJECTOR TEMP
DOWNSTREAM TEMP
LEAK RATE
PRESSURE-P.S.I.A.
TEMP °F
FLOW RATE-LBS/SEC.
FLOW RATE-C.C./SEC.
TIME-MINUTES
RUN 67

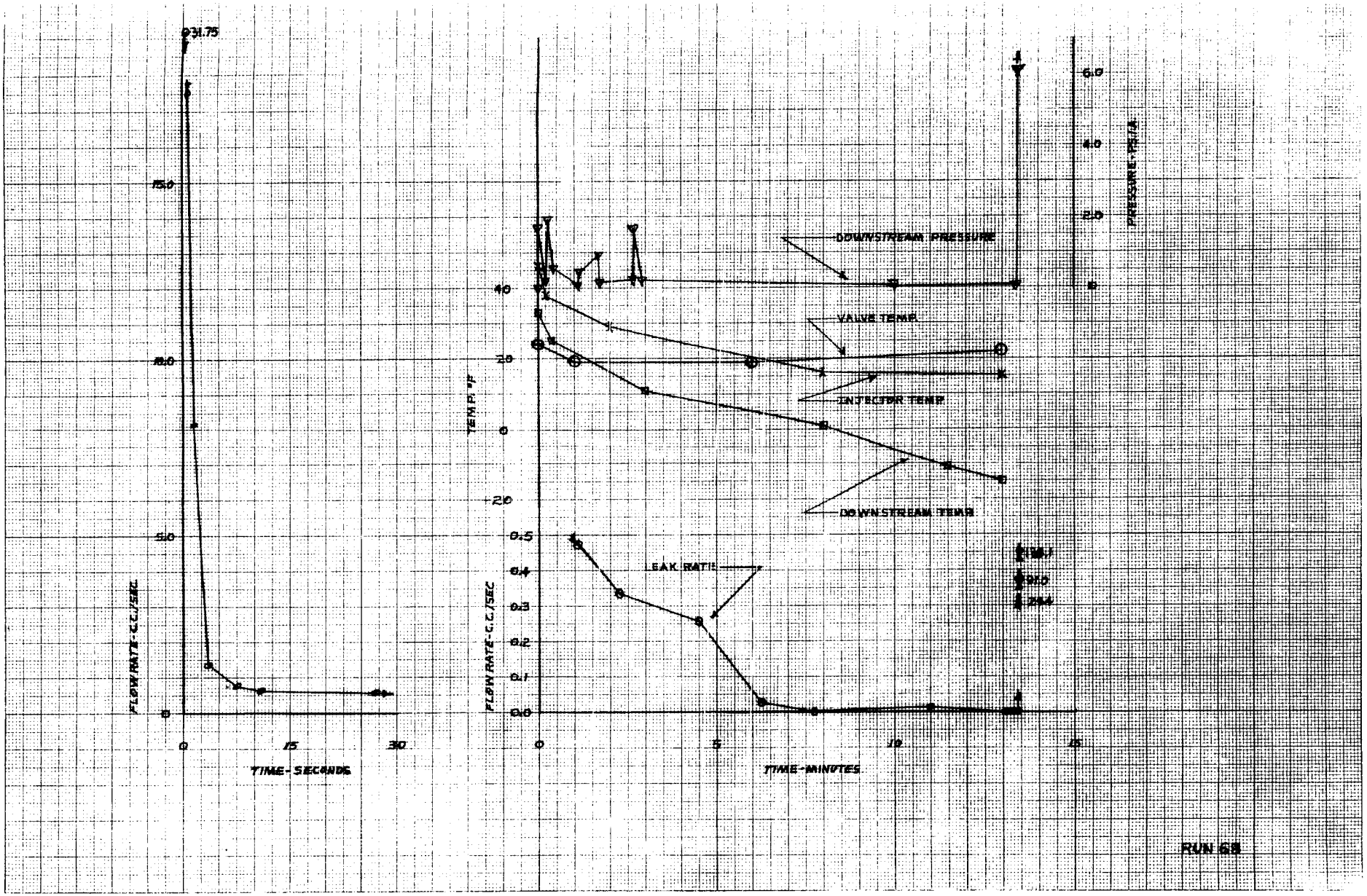
231.75
15.0
10.0
5.0
0
FLOW RATE-C.C./SEC.
0
15
30
TIME-SECONDS
TEMP. °F
40
20
0
-20
DOWNSTREAM PRESSURE
VALVE TEMP.
INJECTOR TEMP.
DOWN STREAM TEMP.
0.5
0.4
0.3
0.2
0.1
0.0
LEAK RATE
FLOW RATE-C.C./SEC
0
5
10
15
TIME-MINUTES
6.0
4.0
2.0
0
PRESSURE-PSIA
RUN 68

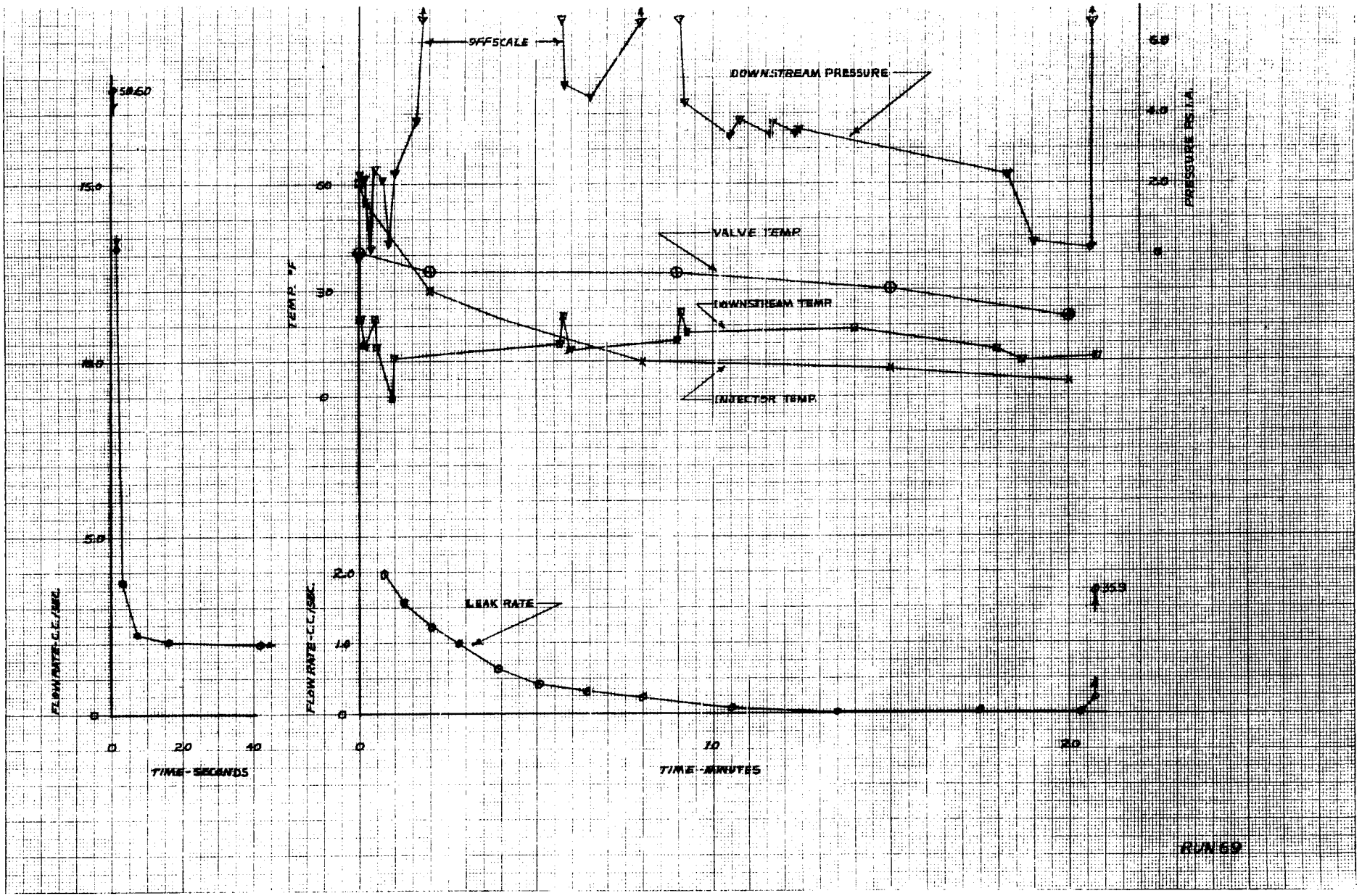
OFF SCALE
DOWNSTREAM PRESSURE
VALVE TEMP.
DOWNSTREAM TEMP.
INJECTOR TEMP.
LEAK RATE
FLOW RATE-C.C./SEC.
TEMP. °F
PRESSURE PSIA
TIME-SECONDS
TIME-MINUTES
RUN 69

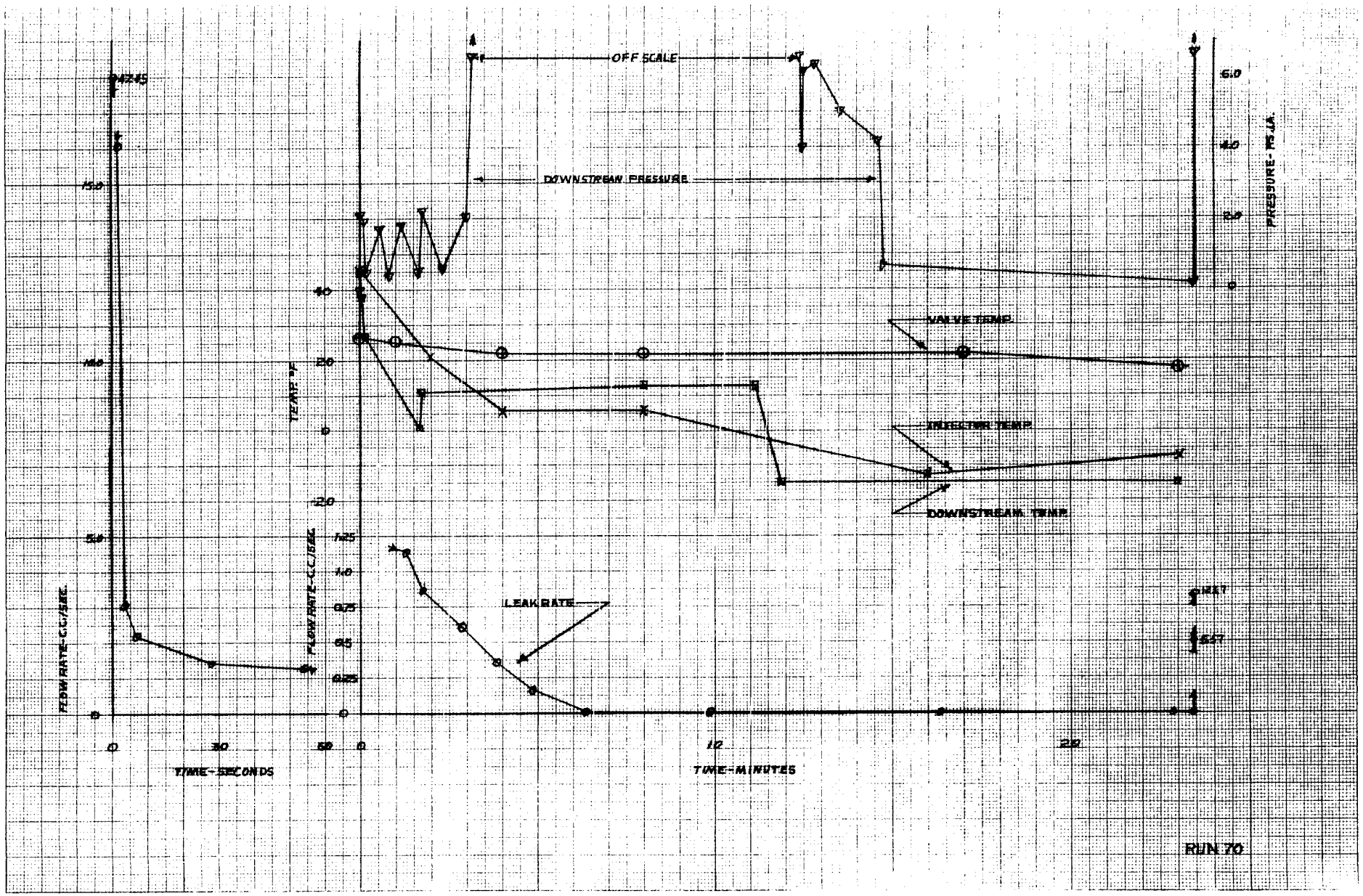
OFF SCALE
DOWNSTREAM PRESSURE
VALVE TEMP.
INJECTOR TEMP.
DOWNSTREAM TEMP.
LEAK RATE
FLOW RATE-C.C./SEC.
TEMP. °F
PRESSURE-P.S.I.A.
TIME-SECONDS
TIME-MINUTES
RUN 70

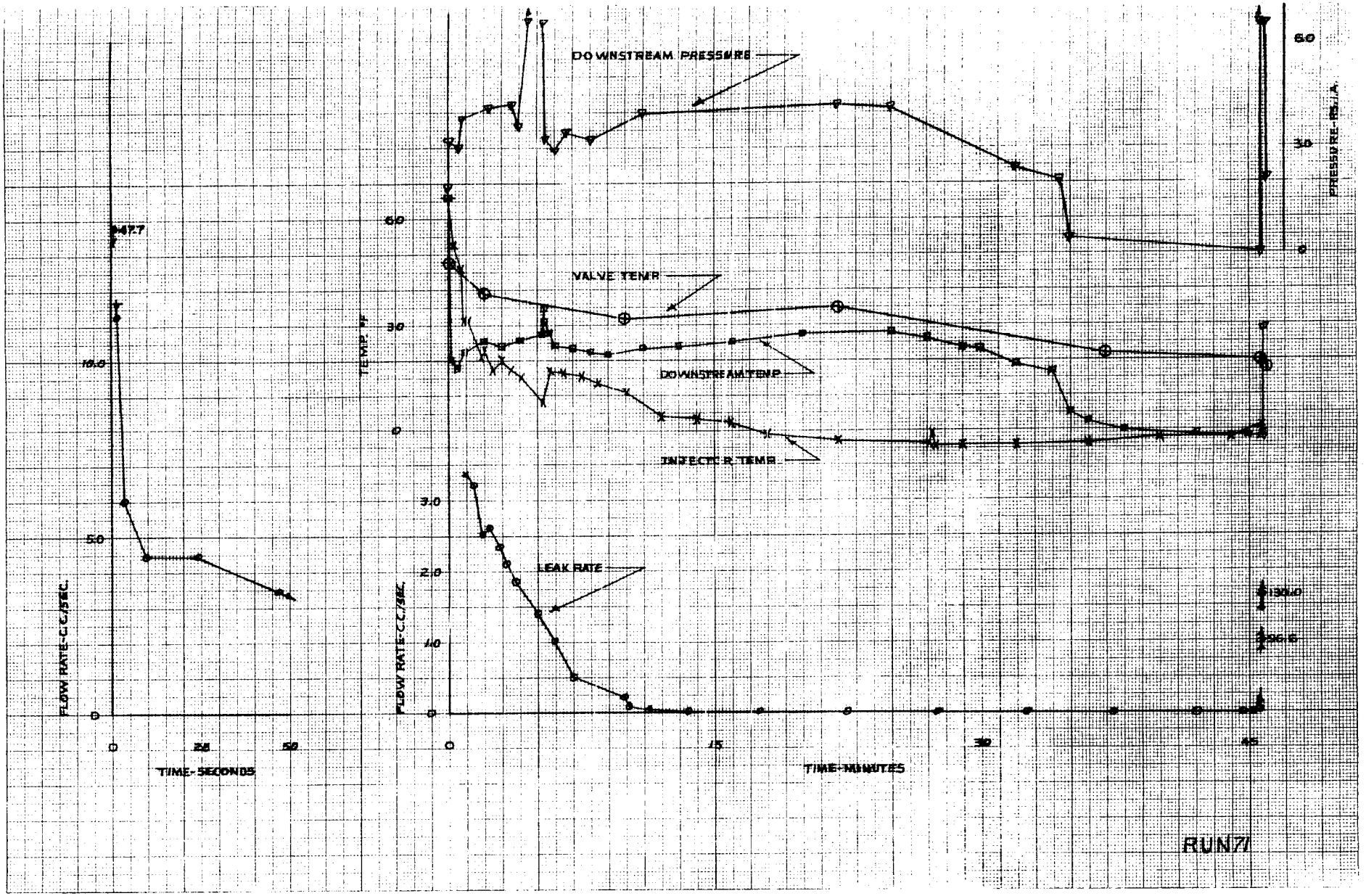
DOWNSTREAM PRESSURE
VALVE TEMP
DOWNSTREAM TEMP
INJECTOR TEMP
LEAK RATE
TEMP °F
PRESSURE-LBS./I.A.
FLOW RATE-C.C./SEC.
FLOW RATE-C.C./SEC.
TIME-SECONDS
TIME-MINUTES
RUN 71

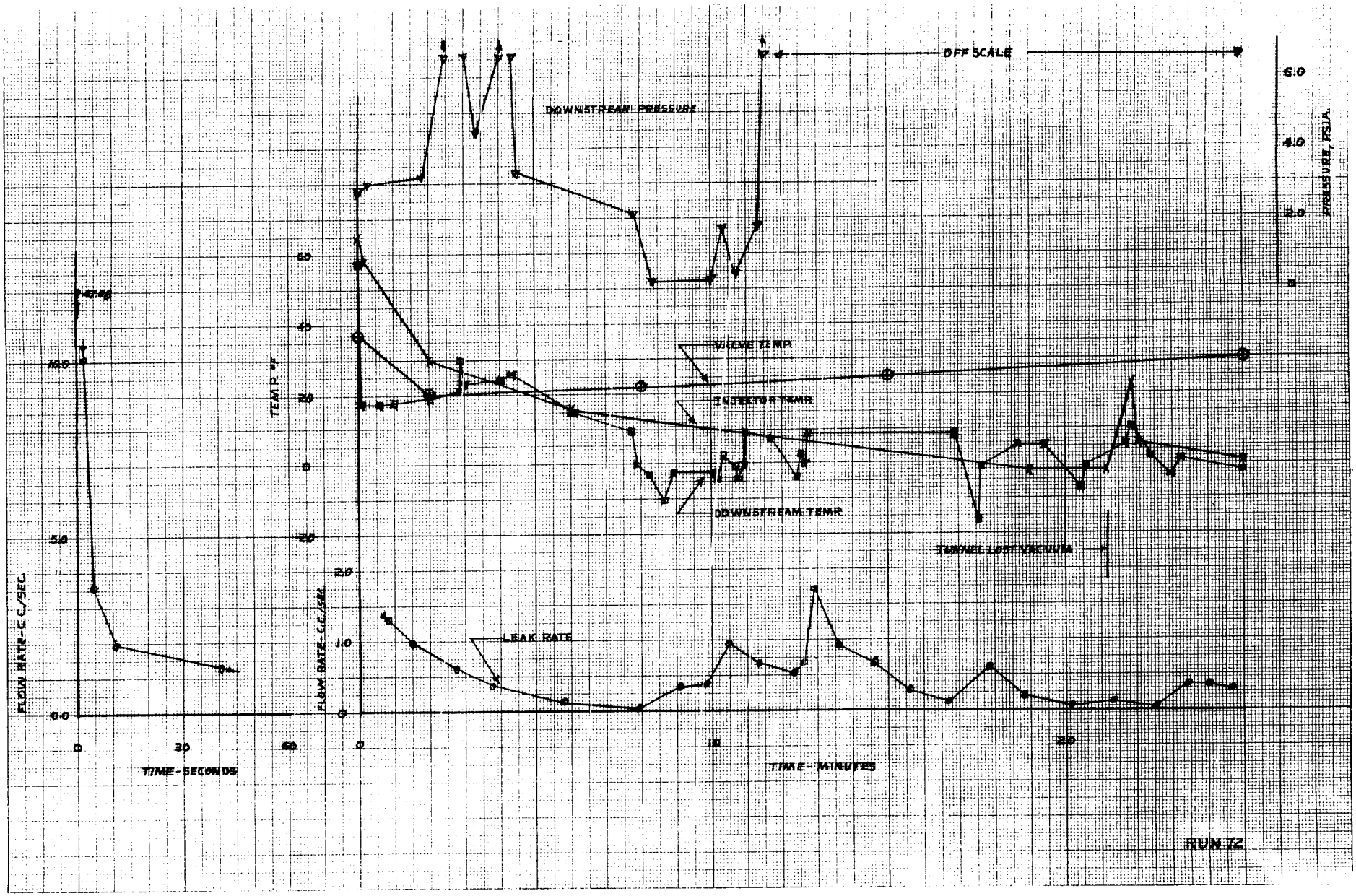
OFF SCALE
DOWNSTREAM PRESSURE
PRESSURE PSIA
5.0
4.0
3.0
2.0
1.0
0
VALVE TEMP
INJECTOR TEMP
DOWNSTREAM TEMP
TUNNEL LOST VACUUM
TEMP °F
60
40
20
0
FLOW RATE-C.C./SEC.
16.0
12.0
8.0
4.0
0.0
LEAK RATE
FLOW RATE-C.C./SEC.
2.0
1.0
0
0
30
60
TIME-SECONDS
0
10
20
TIME-MINUTES
RUN 72

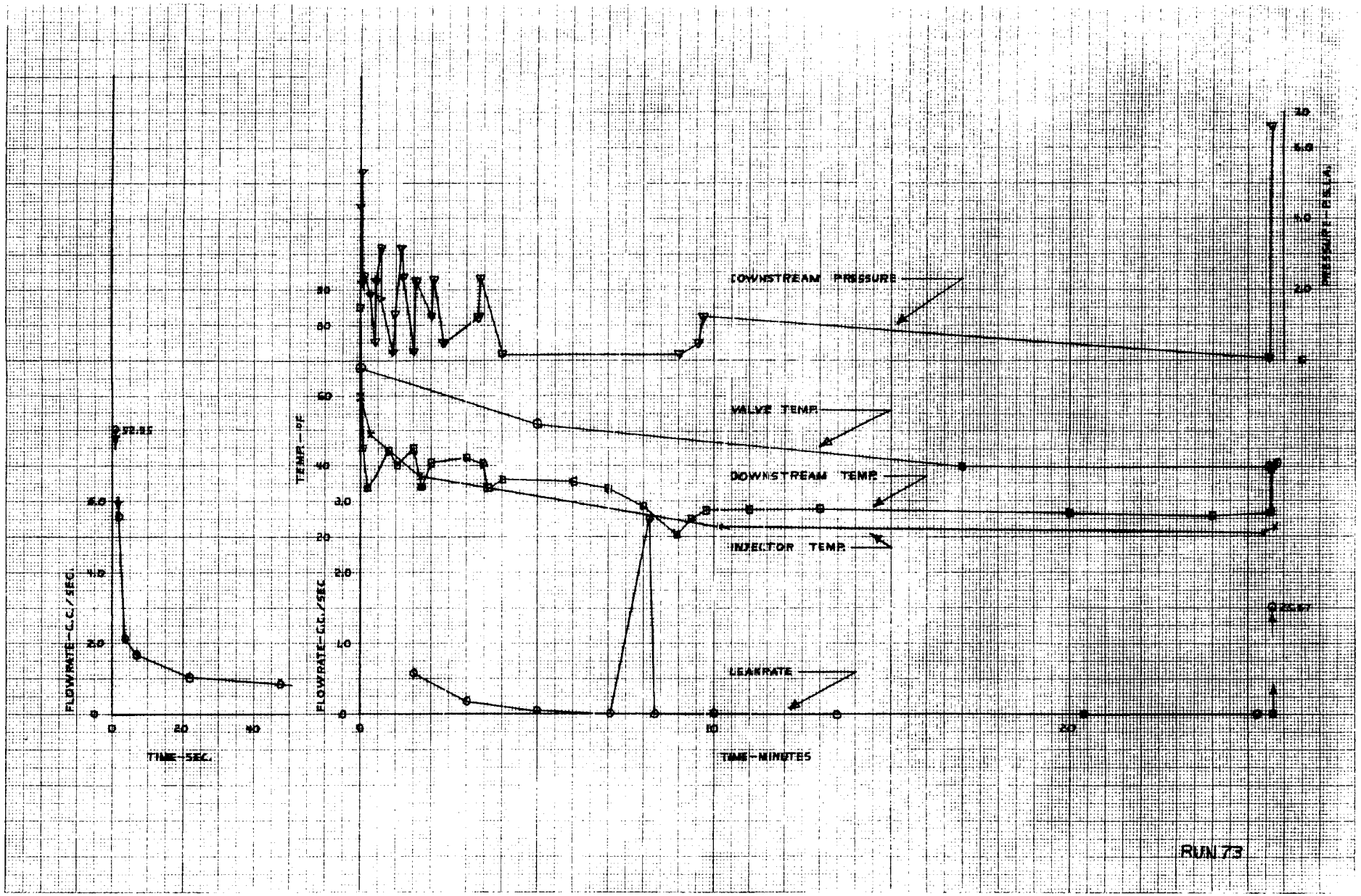
DOWNSTREAM PRESSURE
VALVE TEMP.
DOWNSTREAM TEMP.
INJECTOR TEMP.
LEAKRATE
TEMP. - °F
PRESSURE - PSIA
FLOWRATE - C.C./SEC.
FLOWRATE - G.M./SEC.
TIME - SEC.
TIME - MINUTES
32.85
25.67
RUN 73

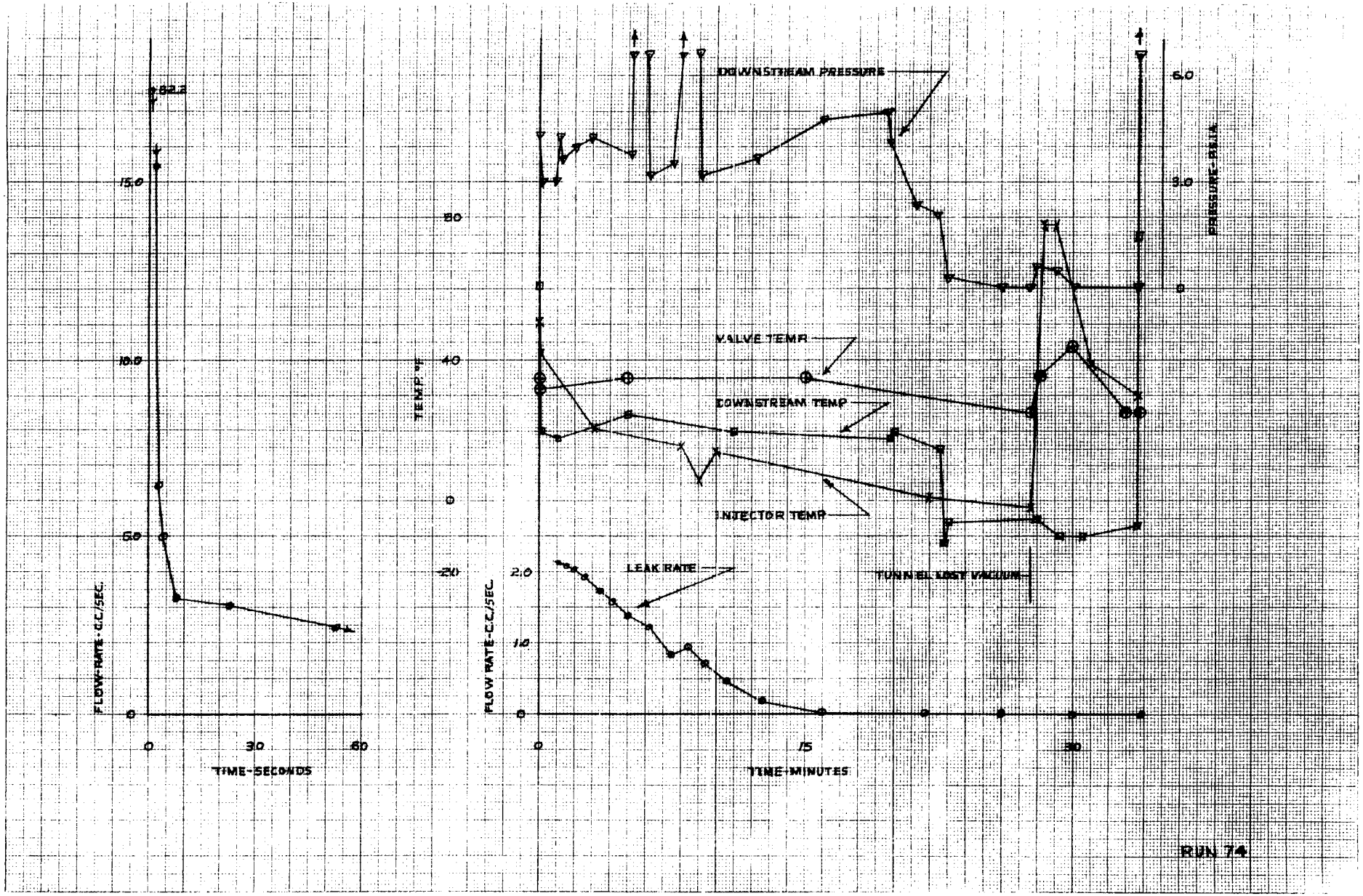
FLOW-RATE - C.C./SEC.
15.0
10.0
5.0
0
62.2
0
30
60
TIME-SECONDS
TEMP °F
80
40
0
-20
DOWNSTREAM PRESSURE
VALVE TEMP
DOWNSTREAM TEMP
INJECTOR TEMP
LEAK RATE
TUNNEL LOST VACUUM
FLOW RATE-C.C./SEC.
2.0
1.0
0
0
15
30
TIME-MINUTES
PRESSURE-P.S.I.A.
6.0
3.0
0
RUN 74

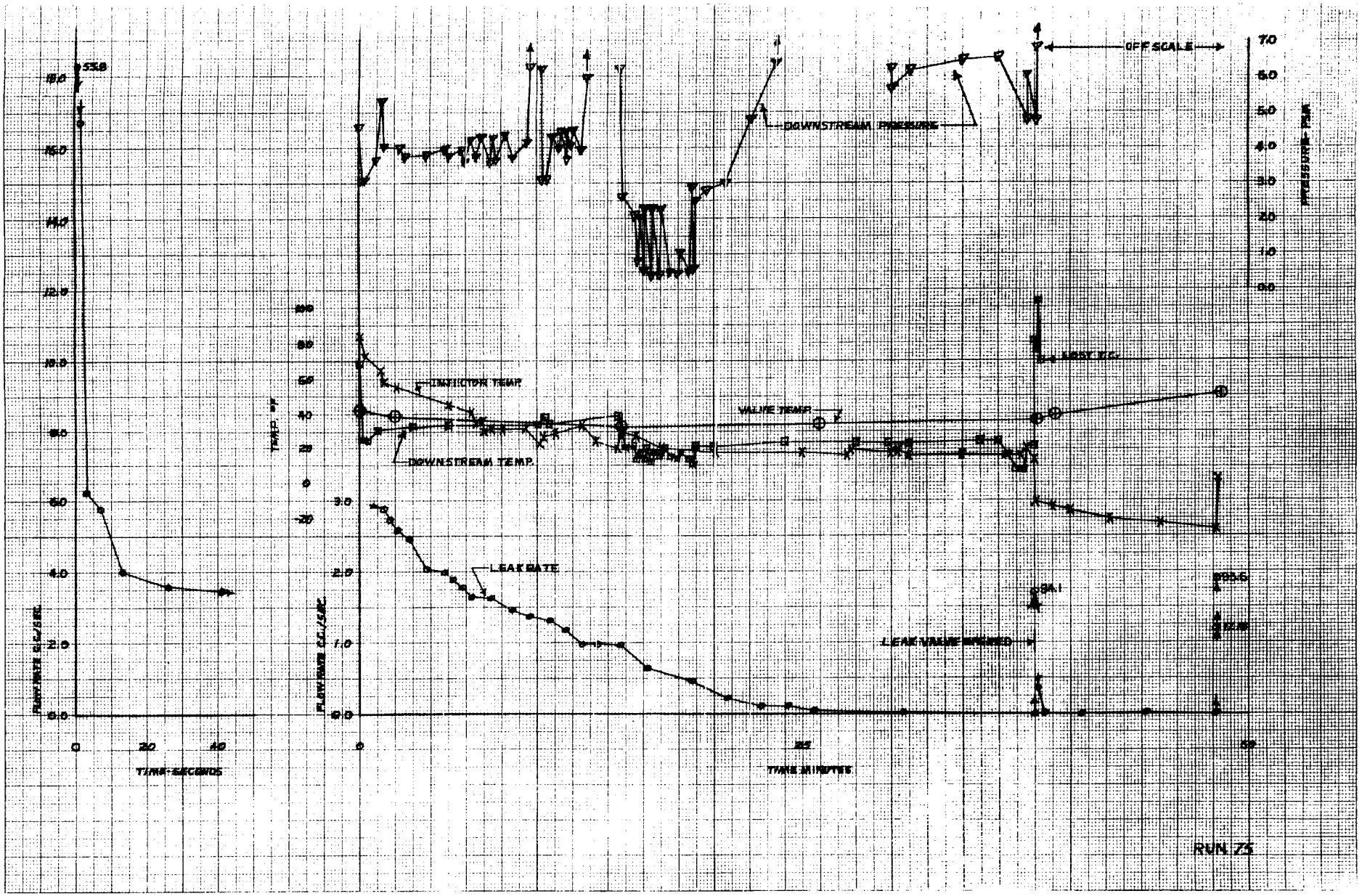
OFF SCALE
DOWNSTREAM PRESSURE
PRESSURE PSIA
INJECTOR TEMP
VALVE TEMP
DOWNSTREAM TEMP.
TEMP °F
LEAK RATE
LEAK VALUE CLOSED
TIME SECONDS
TIME MINUTES
RUN 75

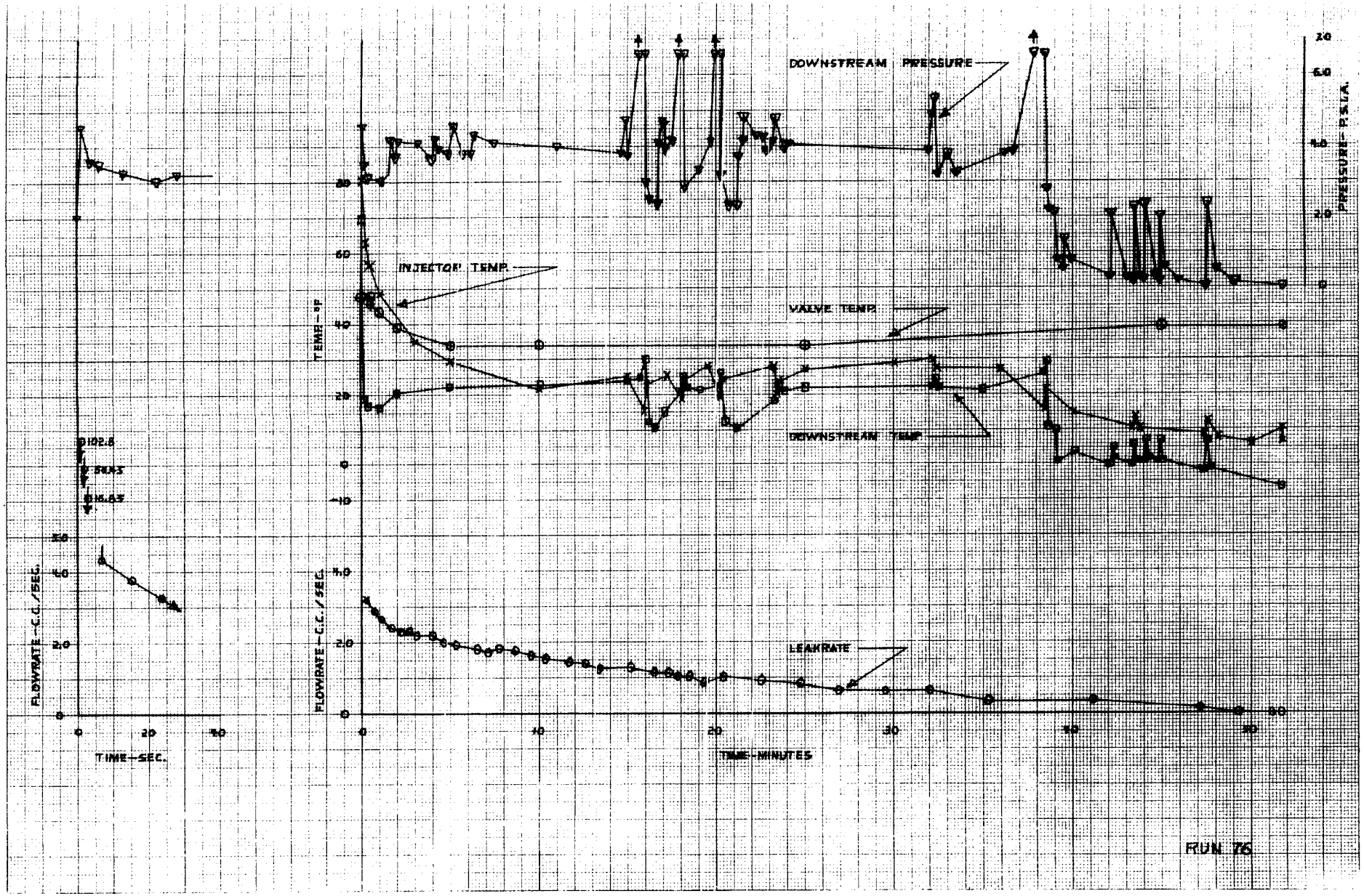
DOWNSTREAM PRESSURE
INJECTOR TEMP.
VALVE TEMP.
DOWNSTREAM TEMP.
LEAK RATE
TEMP - °F
PRESSURE - P.S.I.A.
FLOWRATE - C.C./SEC.
TIME - SEC.
TIME - MINUTES
RUN 76

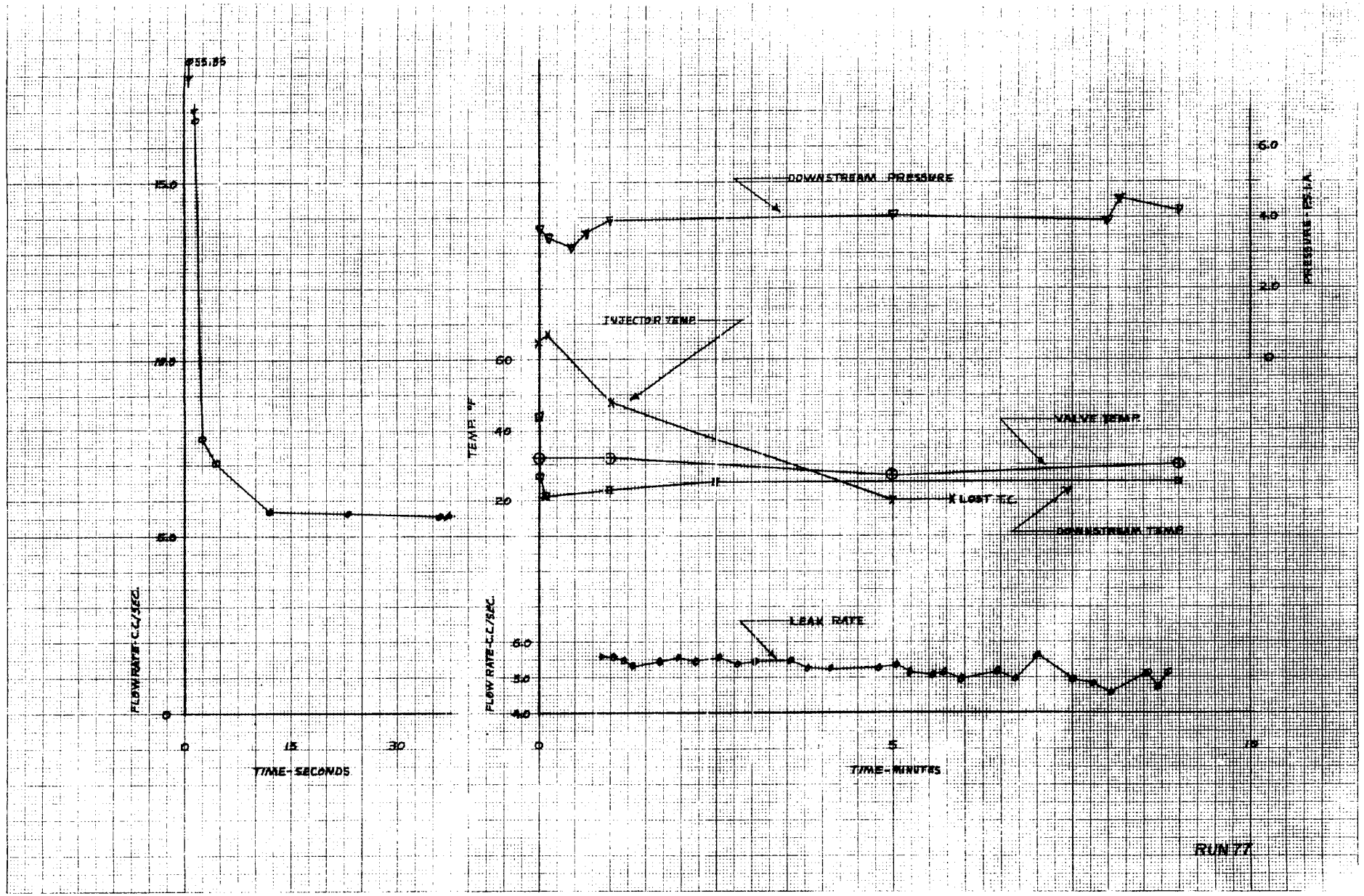
@55.85
15.0
10.0
5.0
0
FLOW RATE-C.C./SEC.
0
15
30
TIME-SECONDS
DOWNSTREAM PRESSURE
INJECTOR TEMP
VALVE TEMP.
LOST T.C.
DOWNSTREAM TEMP
60
40
20
TEMP. °F
6.0
4.0
2.0
0
PRESSURE P.S.I.A.
LEAK RATE
6.0
5.0
4.0
FLOW RATE-C.C./SEC.
0
5
10
TIME-MINUTES
RUN 77

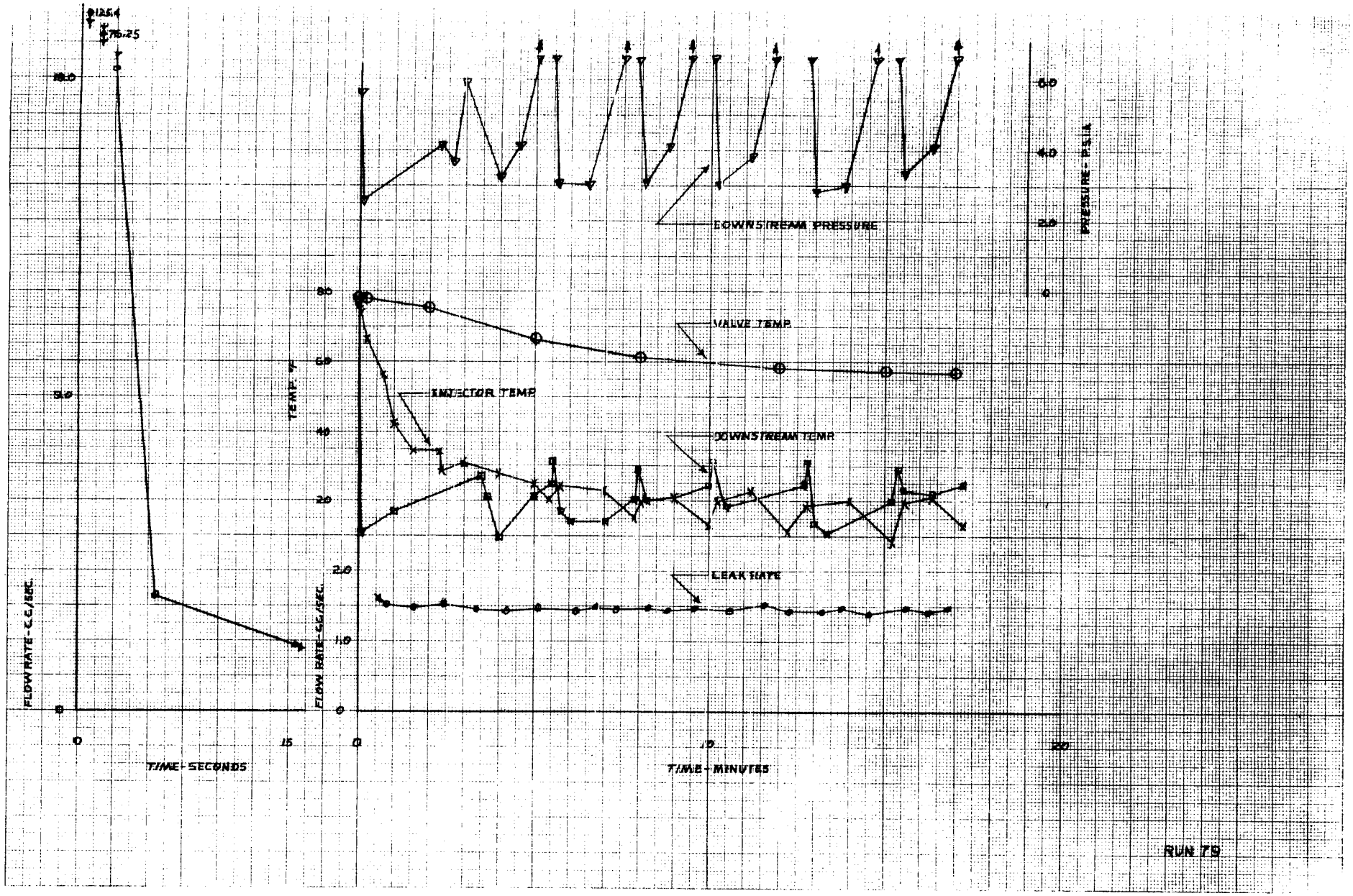
FLOW RATE - C.C./SEC.
TIME - SECONDS
FLOW RATE - LBS./SEC.
TEMP. °F
TIME - MINUTES
PRESSURE - P.S.I.A.
DOWNSTREAM PRESSURE
VALVE TEMP.
INJECTOR TEMP.
DOWNSTREAM TEMP.
LEAK RATE
RUN 79

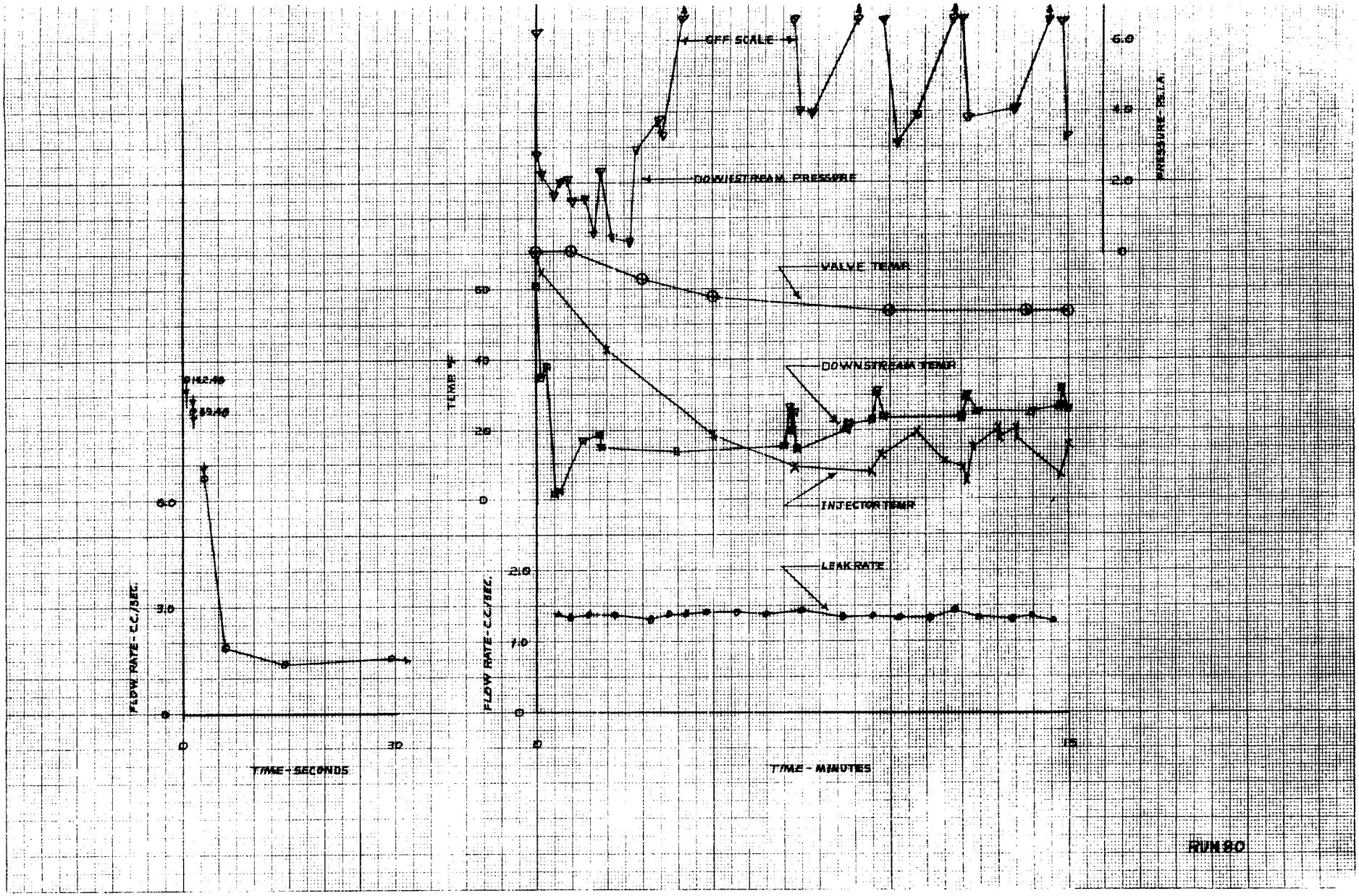
OFF SCALE
DOWNSTREAM PRESSURE
VALVE TEMP
DOWNSTREAM TEMP
INJECTOR TEMP
LEAK RATE
PRESSURE - P.S.I.A.
TEMP
FLOW RATE - C.C./SEC.
TIME - SECONDS
TIME - MINUTES
RUN 90

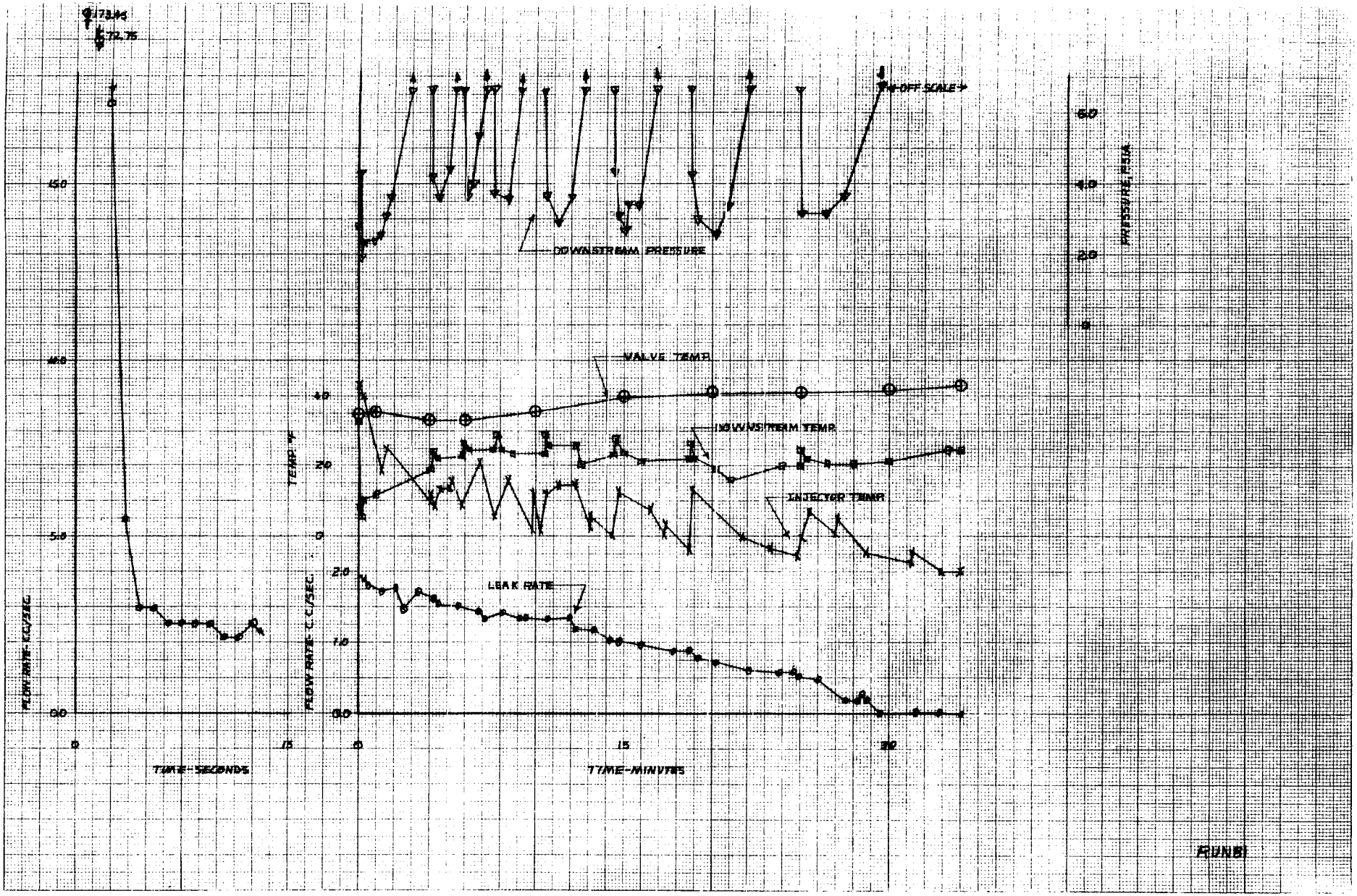
172.45
172.75
150
100
50
0
FLOW RATE-CU/SEC
0
15
TIME-SECONDS
OFF SCALE
DOWNSTREAM PRESSURE
VALVE TEMP
DOWNSTREAM TEMP
INJECTOR TEMP
LEAK RATE
TEMP °F
40
20
0
FLOW RATE-C.C./SEC.
2.0
1.0
0.0
0
15
20
TIME-MINUTES
6.0
4.0
2.0
0
PRESSURE-PSIA
RUN 8

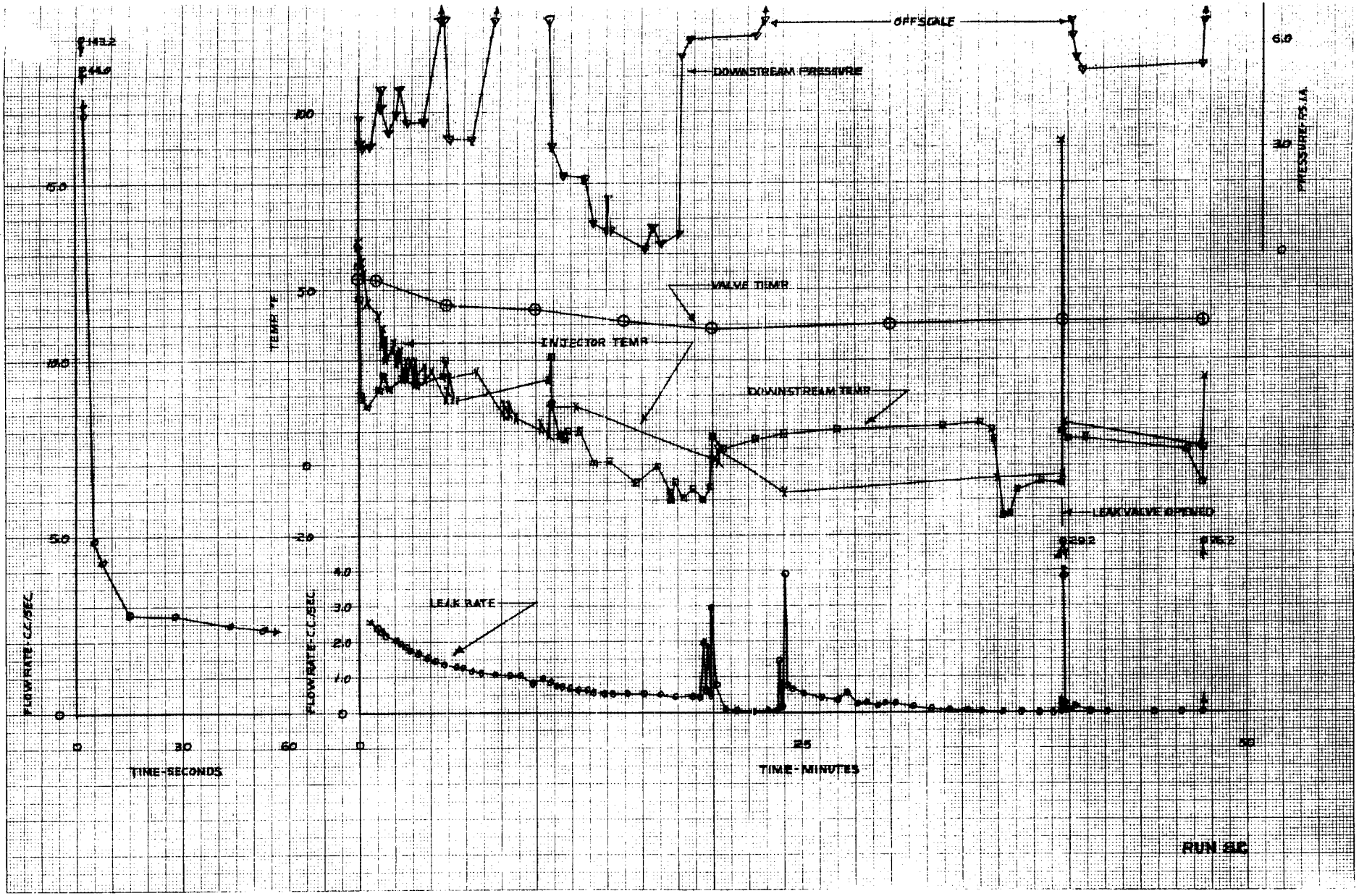
OFFSCALE
DOWNSTREAM PRESSURE
6.0
PRESSURE-PS.I.A.
VALVE TEMP
INJECTOR TEMP
DOWNSTREAM TEMP
TEMP °F
LEAK VALVE OPENED
@ 29.2
@ 35.2
LEAK RATE
FLOW RATE C.C./SEC.
FLOW RATE C.C./SEC.
TIME-SECONDS
TIME-MINUTES
RUN 58

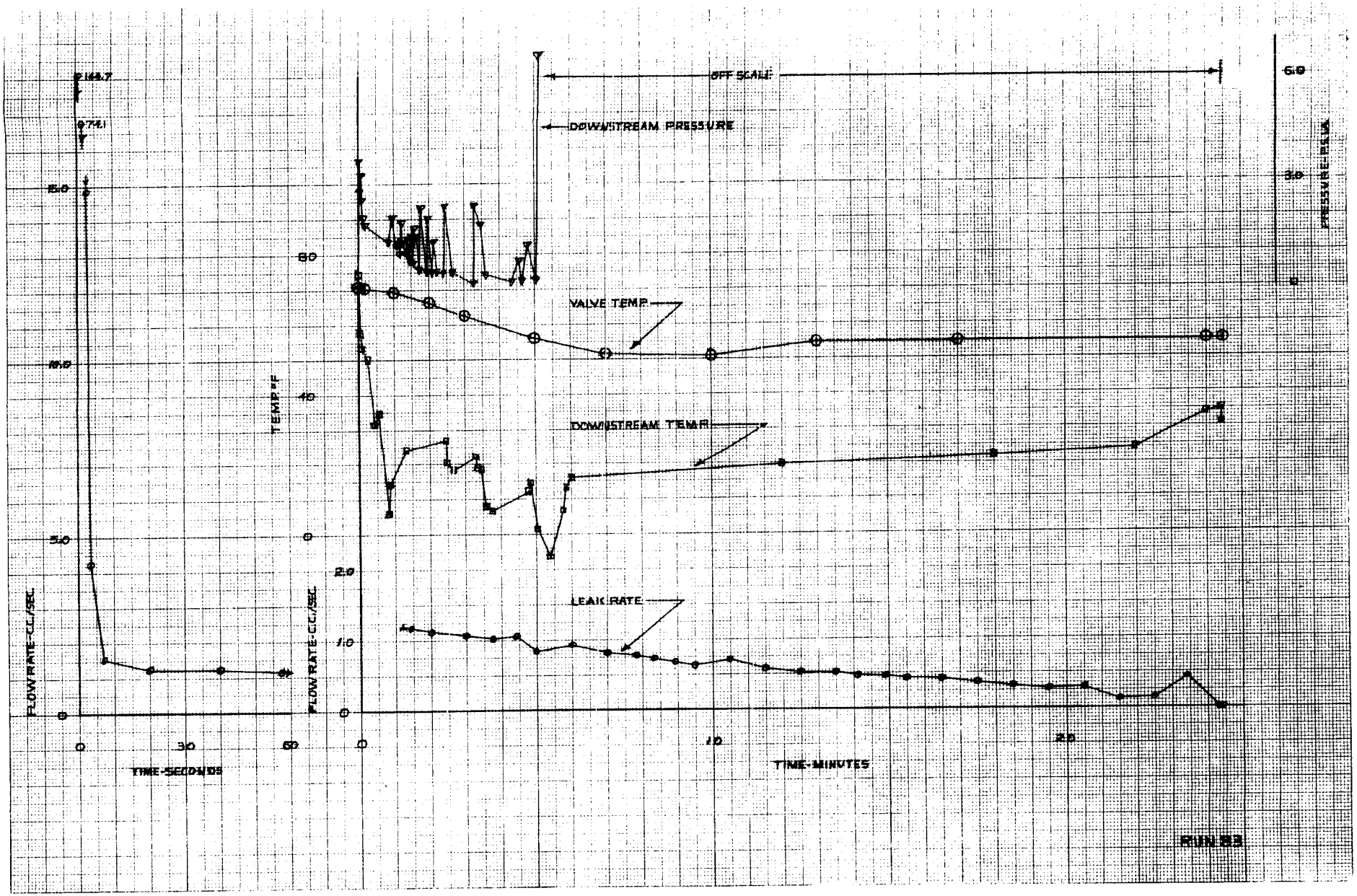
OFF SCALE
DOWNSTREAM PRESSURE
VALVE TEMP
DOWNSTREAM TEMP
LEAK RATE
TEMP °F
PRESSURE-PSIA
FLOW RATE-C.C./SEC.
TIME-SECONDS
TIME-MINUTES
RUN 23

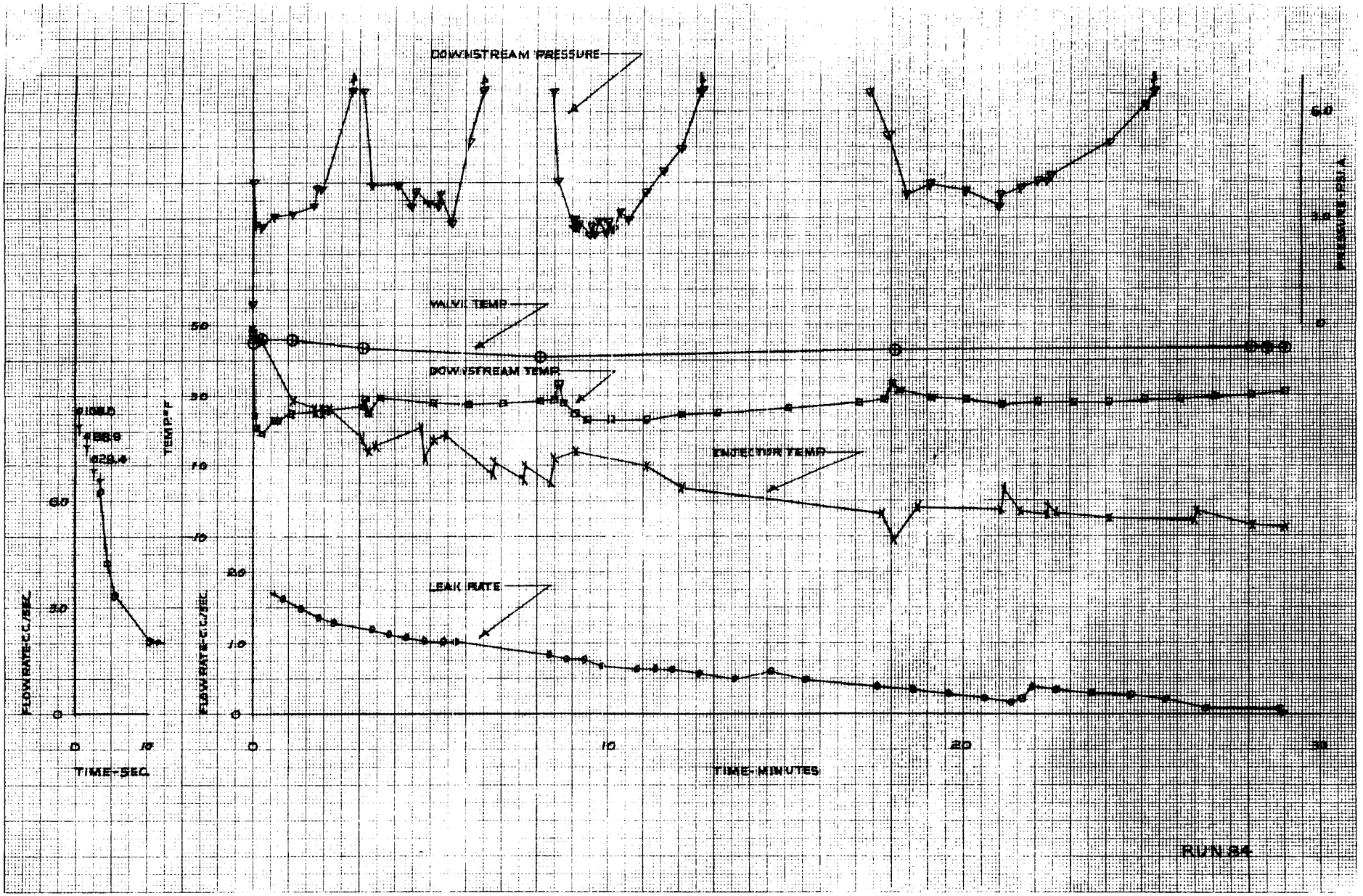
DOWNSTREAM PRESSURE
VALVE TEMP
DOWNSTREAM TEMP
INJECTION TEMP
LEAK RATE
FLOW RATE-C.C./SEC.
TEMP.°F
FLOW RATE-C.C./SEC.
PRESSURE-PSI A
TIME-SEC.
TIME-MINUTES
RUN 84

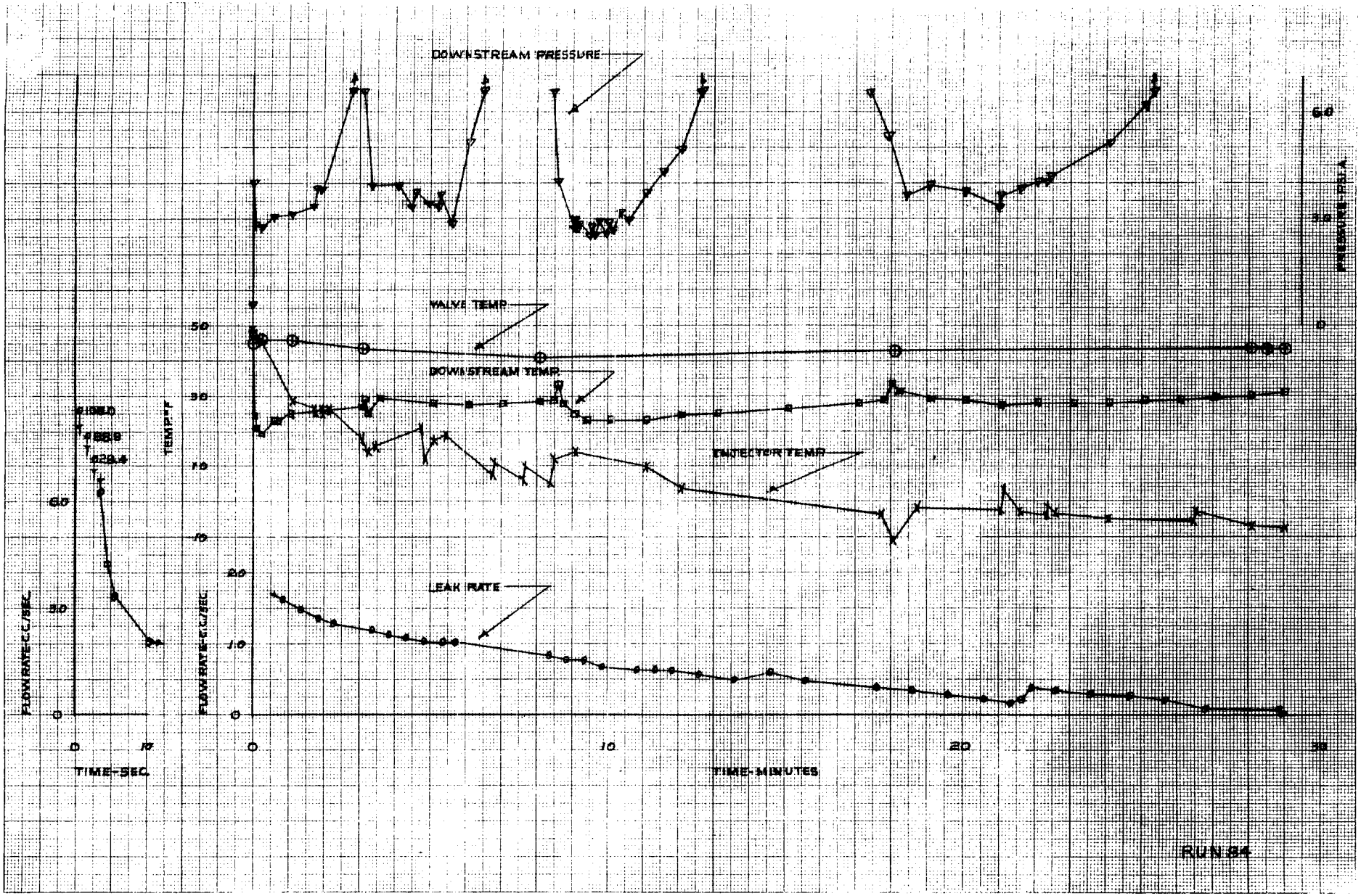
DOWNSTREAM PRESSURE
VALVE TEMP
DOWNSTREAM TEMP
INJECTOR TEMP
LEAK RATE
TEMP°F
FLOW RATE-CC/SEC.
FLOW RATE-G.C./SEC.
PRESSURE-PSIA
TIME-SEC.
TIME-MINUTES
RUN 84

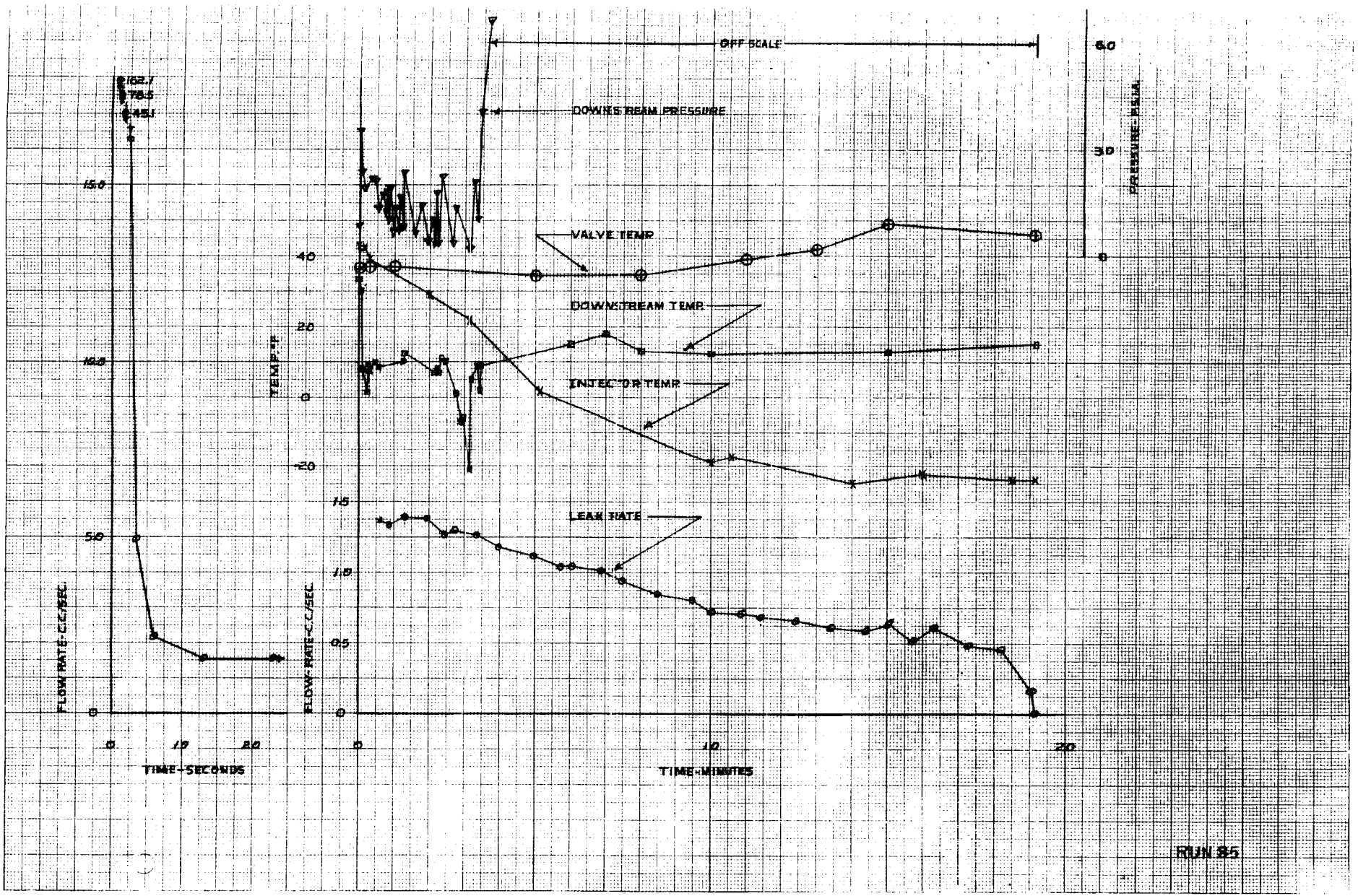
OFF SCALE
DOWNSTREAM PRESSURE
VALVE TEMP
DOWNSTREAM TEMP
INJECTOR TEMP
LEAK RATE
FLOW RATE-CC/SEC.
TEMP-°F
FLOW RATE-C.C/SEC.
PRESSURE-PSIA
TIME-SECONDS
TIME-MINUTES
RUN 85